IMPROVING THE DEVIRO PANEL

TECHNICAL ENHANCEMENTS OF A WOOD FIBRE – CEMENT COMPOSITE FROM PAPER MILL DE-INKING SLUDGE

by

F. MOSTERT

Thesis presented in partial fulfillment of the requirements for the degree of

Master of Wood Science

at

The University of Stellenbosch

Stellenbosch, April 2004

Study Leader: **Prof. G.F.R. Gerischer**

Internal Examinator: **Prof. T.Rypstra**

External Examinator: **Dr. R.E. Ysbrandy**

DECLARATION

I, the undersigned, hereby declare that the work contained in this thesis is my own original work and has not previously in its entirety or in part been submitted at any university for a degree.

Signature / **Date**/

SUMMARY

This research focuses on the utilisation of de-inking sludge from a tissue mill to produce a wood-fibre inorganic composite called the Deviro panel. The study is based on the SA provisional patent 95/9594 by Ysbrandy and Gerischer[6] and the further research conducted by Crafford[1]. The patented Deviro panel contains up to 70% de-inking sludge. Cement and a cement extender serve to fortify the composite. The panel's fibre content of 25-30% is significantly greater than encountered in commercial fibre inorganic composites which contain 8-12% fibre by weight.

The physico-mechanical characteristics of the Deviro panel compare favourably with resin bonded wood-fibre composites, but less favourably compared to conventional wood and wood-fibre inorganic composites. These properties are strongly dependent on panel density. For instance flexural strength being directly proportional while dimensional stability and hygroscopicity being inversely proportional to density.

After confirming the results from the preceding work by Crafford, further improvements were investigated through chemical and curing enhancements. For instance, an autoclaving treatment during the curing period showed an increase in flexural strength. Addition of water glass could be associated with bulking of the panel, which resulted in increased flexural strength and a slight reduction of density. Panel density could be significantly reduced by the addition of Perlite, while inhibiting the concomitant reduction in strength.

In addition a pilot production process was developed to produce $1m^2$ panels, which exhibited similar curing characteristics as the smaller panel units.

OPSOMMING

Hierdie navorsing handel oor die gebruik van ontinkingsslyk van 'n sneespapier meule om die Deviro paneel, 'n houtvesel anorganiese saamgestelde produk, te produseer. Die studie volg uit die SA voorlopige patent 95/9594 deur Ysbrandy en Gerischer en verdere narvorsing deur Crafford[1]. Die gepatenteerde Deviro paneel bevat tot 70% ontinkingsslyk. Sement en sement-byvoegmiddels dien om die saamgestelde produk te versterk. Die paneel bevat 25-30% vesel wat aansienlik meer is as ander kommersiële anorganiese saamgestelde produkte wat 'n vesel inhoud van 8-12% het.

Die meganiese eienskappe van die Deviro paneel is vergelykbaar met houtvesel saamgestelde produkte waar hars as kleefmiddel dien, maar vergelyk minder gunstig teenoor konvensionele hout en houtvesel anorganiese saamgestelde produkte. Die paneel se eienskappe is afhanklik van sy digtheid. Buig sterkte is eweredig terwyl dimensionele stabiliteit en hygroskopisiteit omgekeerd eweredig aan die digtheid van die paneel is.

Die voorafgaande werk van Crafford is eers gestaaf voordat veranderinge aan die chemiese samestelling en drogingsmetodes van die paneel nagevors is. Daar is byvoorbeeld bevind dat, deur die paneel te outoklaveer gedurende die set periode, dit lei tot 'n toename in buig sterkte. Die byvoeging van water glas kan swelling laat plaasvind wat 'n afname in buig sterkte en 'n afname in digtheid tot gevolg het. Digtheid kan ook aansienlik verlaag word deur die byvoeging van Perlite terwyl 'n dienooreenkomstige verlaging in buig sterkte tot 'n mate voorkom word.

'n Loods produksie proses is ook ontwikkel om 'n $1m^2$ paneel te vervaardig wat dieselfde eienskappe toon as die kleiner paneel.

CONTENTS

LIST OF TABLES

TABLE OF FIGURES

INTRODUCTION

Solid waste called sludge is generated in the production of pulp and paper. The largest amount of solid waste generated at pulp and paper mills is the sludge from primary and secondary clarifiers, aeration basins, sludge lagoons and recycled fibre plants.[2] Mills with activated sludge treatment systems average 31kg dry primary sludge per air dry ton of pulp. Secondary sludge, that is sludge generated from paper mills, is reportedly produced at an approximate rate of 16 kg per ton of paper. De-inking sludge, which is sludge from waste paper plants, is produced at an average of 80 to 150 kg of dry sludge per ton of recycled paper.[4] This is significantly more per ton of paper than primary or secondary sludge.

The sludge produced by the pulp and paper industry is predominantly land filled or incinerated. The problems associated with waste disposal increases as landfill sites grow scarcer, recycled fibre plants increase and environmental regulations become more stringent.

A proactive strategy therefore needs to be developed. As early as the 1940s, alternatives have been sought for the management of paper mill sludge. These efforts have resulted in a wide variety of solid waste management techniques, of which some have proven to be viable environmentally safe alternatives.[5]

At the University of Stellenbosch, one such research program exists. The study involved the patent developed by Ysbrandy and Gerischer[6] in 1995 and the research by J. Crafford.[1] An inexpensive fibre cement composite, the so called "Sludge Panel" or "Deviro Panel", was developed by combining 55% by mass de-inking sludge with cement and fly ash in a simple manufacturing process. The Deviro panel was of medium density (approximately 1 g/cm^3), with a fair strength and acceptable fire rating.

To establish commercially viable products, which could be developed for appropriate market segments, the Deviro panel characteristics critical to potential end users needed to be optimised. Therefore the primary objective of this study was to research further the physical properties of the Deviro panel, such as flexural strength,

dimensional stability and panel durability by enhancing bonding and hydration of the cementitious materials. Focus was placed on improving the types of raw material such as using sodium silicate (Na_2SiO_3) as additive to improve cement hydration as well as improving curing methods by autoclave treatment to accelerate the curing time.

Process simplicity and a high level of de-inking sludge utilisation was maintained, keeping the final product viable with regards to manufacturing time and costs, while maintaining acceptable product properties. To establish the viability of an industrial process, the manufacturing method was transformed from a laboratory to a pilot plant type production process.

CHAPTER 1 – LITERATURE SURVEY

1.1 De-inking Sludge

1.1.1 Introduction

Although the focus is placed on de-inking sludge, the de-inking process is detailed as background information in appendix A to support the literature survey.

In the de-inking process, the surface layer of froth drawn off in flotation de-inking and the filtrate from the wash de-inking stage is usually collected at 2-5% solids. This slurry is partially dewatered using mechanical dewatering techniques, such as vacuum filters, followed by V-presses, or belt filters or screw presses. The solids content is raised to 30-50% and contains ink, coating and filler pigments and reject fibres. This wet mass is termed *de-inking sludge*, or *paper de-inking solids* (PDS).[1,14]

In 1996, approximately 100 dry tons de-inking sludge was produced daily by South African tissue mills alone.[15] This equates to 330 wet tons, or 190m^3 of sludge produced daily.[1]

While de-inking is generally considered an environmentally sound activity as it decreases our reliance on virgin fibre, it brings with it the problem of disposing of the de-inking sludge.

1.1.2 Characterisation of De-inking Sludge

The wet, grey sludge produced by de-inking plants, consists of 45-70% water, 5-20% inorganic materials and 10-25% fibres and fines.[12] Figure 1.1 illustrates the range of the bulk properties of sludge from various plants world-wide.[1,14,16,17,18,19]

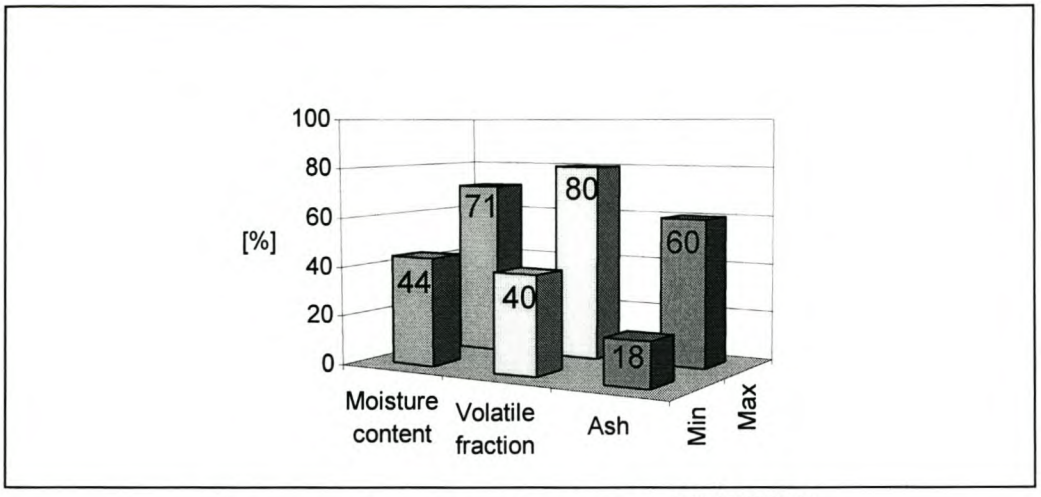

Figure 1.1. Bulk properties of sludge[1,14,16,17,18,19]

1.1.2.1 Ash Properties

The ash fraction of de-inking sludge consists mostly of SiO_2 (silica), Al_2O_3 (alumina), and CaO (lime), with traces of MgO, TiO_2, Fe_2O_3, P_2O_5, Na_2O and K_2O. The silica, alumina and lime are introduced primarily by kaolin ($Al_2O_3 \cdot SiO_2 \cdot 2H_2O$) and calcite ($CaCO_3$). MgO is derived from talc ($3MgO \cdot 4SiO_2 \cdot H_2O$) and TiO_2 from rutile or anatase.[14,20]

1.1.2.2 Fibre Properties

The fibres in de-inked sludge are of a degraded nature, being in a collapsed and fibrillated state. The fines fraction is high, resulting from mechanical actions and bacterial decay.

1.1.2.3 Metals

The trace metal content is very low.[17,21] These elements, include zinc, copper, chromium, nickel, cadmium, mercury, cobalt, arsenic, selenium, antimony and vanadium. They can be derived from sources such as de-inking chemicals, printing inks and impurities in filler materials.[21]

1.1.2.4 Polychlorinated biphenyls (PCBs)

Until the early 1970s, PCBs were used in the production of carbonless copy ink. Only de-inking sludge derived from waste plants using very old waste paper from file stock grades, could have a measurable PCB content.[17,21]

1.1.2.5 Heat Values

Heating values of de-inking sludge range from 6 to 16 MJ/kg (based on dry mass), depending on ash content. This is comparable to black liquor dry solids and municipal solid waste.[20,21] The high moisture and ash content, along with the large variation in ash and volatile content, makes de-inking sludge a difficult fuel to utilise.[20]

1.1.3 Management of De-inking Sludge

1.1.3.1 Land filling

Mills typically favour land filling their de-inking solids, whenever disposal sites are readily available and handling costs are low, because this is a relatively low capital investment. Landfill disposal is, however becoming more difficult.

The environmental impact of land filling is a concern. The runoff of liquid leached from the waste has the greatest impact.[4] This leachate contains conventional pollutants as well as traces of metals, volatile organic compounds (VOCs), phenolic compounds, volatile fatty acids and some base/neutral compounds. Should the leachate not be properly collected and treated, ground water and surface water bodies may become contaminated with these compounds. This has resulted in a tightening of international environmental regulations, which requires closer monitoring, environmental impact assessments (EIAs), closure plans and public consultation.[4]

Other problems are the difficulties associated with the availability of new landfill sites, which are rapidly decreasing. Additionally, the costs of building and maintaining landfills are increasing.[21] This has lead to the investigation and implementation of alternative sludge management programs.

1.1.3.2 Incineration

The most popular alternative to land filling, is the incineration of de-inking solids. Due to the high ash and moisture content of de-inking sludge, a refined combustion technology must be selected to insure complete energy recovery with minimum air emissions.[10] Difficulties are experienced using grate boilers, while fluidised bed incinerator systems have proved to be an effective system.[14,21,22,23] No serious sintering or emission problems occur when fluid-bed combustion is used. An advantage is that de-inking sludge can be burnt with other mill wastes such as chips and bark.

An example of a fluidised bed system, designed by the Fort James Company is described below, which can effectively incinerate sludge with a high ash and moisture content. A longer residence time and preheated combustion air is included in the design to assure complete combustion. An overbed natural gas burner is used to start the fluidised bed and afterburn the combustion products during the start-up transition. Process steam generated in the waste heat boiler is used in the paper making process and also to dry the sludge from 55 to 45% moisture prior to combustion. The system includes a fluidised bed combustion cell followed by a waste heat boiler, air preheater, economiser, and baghouse. A metering bin fuels the combustion vessel via a pneumatic injector. Feedback from an SO_2 analyser controls limestone addition with the fuel feed for acid gas abatement as` needed. Fluidisation air, preheated initially with a steam coil and secondarily with an air-to-air heat exchanger, assures sufficient heat is available to burn the sludge with low CO and VOC emissions. An aqueous ammonia injection system (SNCR) is used to reduce nitrous oxide gasses (NOx). A high efficiency baghouse completes flue gas cleanup prior to discharge.[23]

Even if combustion generates little or no energy, the amount of waste material is reduced and the sludge is deactivated.

1.1.3.3 Recovery of Raw Materials

A means to manage de-inking sludge is to reduce the amount of sludge produced. This is the objective of fibre and filler separation and recovery systems.

One such system is the fibre recovery system (FRS).[18] Rejects such as plastics polystyrene and metals are firstly removed. A secondary screening stage fractionates the waste furnish into a long fibre fraction and a short fibre, fines and ash fraction. A subsequent screening stage separates the short fibre fraction from the fines and ash. The fines and ash are then floated from the process water in a flotation cell, with the aid of a flocculating agent. The fibre fractions recovered in the different stages, can be re-introduced into the stock preparation system. The result is that the final sludge volume is significantly reduced.[18]

Fillers are recovered from the fractionation system by employing a thermal oxidation technique for destroying the organic fraction of the sludge to yield filler in the form of an ash. Exact control of the kiln temperature avoids the formation of fused agglomerates, which would otherwise cause the recovered filler to be excessively abrasive.[5]

Filler materials can also be recovered by wet air oxidation (WAO).[5,19] WAO oxidises the organic fraction of the sludge in a liquid environment, under high temperature and pressure. An ash composed of inert filler materials is produced, which can be re-used in the papermaking process. Problems with calcium sulphate and calcium oxalate scale deposition and low filler brightness has been experienced with this process.[19]

Direct reuse of sludge has been reported to be feasible at several board mills where furnish cleanliness is not critical.[24]

1.1.3.4 Pelletising

De-inking sludge can be pelletised with primary sludge and often waste paper for by-product applications.[5,25] The most common application is its use as a fuel supplement.[5,25] Another use is as a carrier material for agricultural, home and garden

pesticides. Pelletised sludge can also be used as an absorbent for oil spills[1], kitty and poultry litters and beddings for large animals.[5]

1.1.3.5 Land application

De-inking sludge and other paper mill sludge can effectively be composted.[5,26,27,28] The sludge must be stockpiled on-farm for some time before land spreading. Composting is achieved either by mechanical pile turning or by static pile forced aeration.[28]

Alternatively, de-inking sludge can directly serve as a soil amendment, should adequate nitrogen and phosphate supplements be provided.[26] Sludge added in soil could improve the germination and root development rate in many crops and increase the moisture holding capacity of the soil.[2]

1.1.3.6 Supercritical Water Oxidation (SCWO)

Organic and inorganic materials are decomposed in the aqueous phase above the critical point of water. In this state, organic materials become far more soluble in water and oxidise readily. Only laboratory scale research has been performed, with potential problems such as corrosion and salt and pyrolitic char depositions expected in large-scale systems.[5]

1.1.3.7 Building and Ceramic Materials

The ash generated from sludge incinerators can be used in the building industry for cement and concrete, or it can be used for road building.[21] Sludge can serve as a feed stock supplement to a cement kiln, because it contains significant quantities of the raw materials within the inorganic fraction required for the production of cement.[5]

Organic fibres are included in cementitious composites to increase durability and reduce shrinkage related cracking. The silica, alumina, lime and calcite contained within the inorganic fraction of de-inking sludge are expected to promote cement hydration, while the cellulose fibre would serve to reinforce a cement matrix.

Therefore the addition of de-inking sludge in cementitious products to produce building blocks, wall boards, panels, shingles, fire retardants, and filler materials in fire proof doors has been researched.[1,5,24] It is this research that serves as the basis for this study. To gain a better understanding of the interaction of sludge and cement, ordinary Portland cement (OPC) and cement chemistry will be reviewed.

1.2 Ordinary Portland Cement (OPC)

1.2.1 Introduction

Cements can be described as materials with adhesive and cohesive properties, capable of compactly bonding fragments or particles of solid matter. In cases of engineering purposes cements can be restricted to contain compounds of lime as their principle constituent, called calcareous cements or, sometimes, certain allied compounds of magnesium.

Two cement classifications exist.
Non-hydraulic cements: These are unable to set or harden in water (e.g. non-hydraulic lime) or which are unstable in water (e.g. plaster of Paris).
Hydraulic cements: These cements set and harden in water, producing a solid, which is stable in water and are therefore of interest in the making of concrete for building and civil engineering (e.g. Portland cement).
Ordinary Portland cement is defined as a cementing material which is obtained by intimately mixing together calcareous or other lime-bearing material with, if required, argillaceous and/or other silica-, alumina-, or iron oxide-bearing materials, burning them at a clinkering temperature and grinding the resulting clinker.[29,30]

1.2.2 Cement Chemical Composition

Portland cement consists mainly of the four oxides: CaO (lime), SiO_2 (silica), Al_2O_3 (alumina) and Fe_2O_3 (iron oxide). These comprise 90 % of the cement by weight. The remaining 10 % consists of MgO (magnesia), Na_2O and K_2O (alkali oxides), Ti_2O (titania), P_2O_5 (phosphorous pentoxide) and $CaSO_4$ (gypsum). The usual composition limits are given in table 1.1.[29] Lime and silica form compounds that will hydrate to

form cementing compounds. Alumina and ferric oxide act as flux agents in the process of clinker burning, by lowering the burning temperature of the cement, thus avoiding difficulties associated with high clinkering temperatures.

Table 1.1. Usual Oxide Composition Limits of Portland Cement [29]

Oxide	**Content [%]**	
	Minimum	Maximum
CaO	60	67
SiO_2	17	25
Al_2O_3	3	8
Fe_2O_3	0.5	6
MgO	0.5	4
Alkalis (asNa_2O)	0.3	1.2
SO_3	2	3.5

The mineralogical composition of cement, is listed in table 1.2.[1] It should be noted that the silicates are not pure compounds, but contain minor oxides in solid solution. These impurities have a significant effect on the atomic arrangements, crystal form and hydraulic properties of the silicate compounds.[29,30]

Table 1.2. Compound Composition of South African Portland Cement [1]

Compound	**Oxide Composition**	**Abbreviation***	**% by mass in cement**
Tricalcium silicate	$3CaO \cdot SiO_2$	C_3S	35-55
Dicalcium silicate	$2CaO \cdot SiO_2$	C_2S	20-40
Tricalcium aluminate	$3CaO \cdot Al_2O_3$	C_3A	5-12
Tetracalcium aluminoferrite	$4CaO \cdot Al_2O_3 \cdot Fe_2O_3$	C_4AF	5-10
Magnesia	MgO	M	0.3-4
Gypsum	$CaSO_4 \cdot 2H_2O$	-	4-7
Free Lime	CaO	-	0.5-2.5

*Shortened notation used by cement chemists:

C = CaO

S = SiO_2

A = Al_2O_3

F = Fe_2O_3

M = MgO

H = H_2O

C_3S is relatively stable at ambient temperatures, but slowly decomposes to C_2S and CaO between 700°C and 1250°C. Therefore, cooling after the manufacture of the

clinker must not occur too slowly, to ensure that C_3S remains unchanged. As previously stated, the silicate compounds are not pure. C_3S exists in an impure form called alite, which contains traces of Al_2O_3, Fe_2O_3, MgO, and Na_2O. Six forms of C_3S exist: three triclinic, two monoclinic and one triagonal form. The monoclinic form usually occurs in Portland cement.

Four forms of C_2S exist. The first, α-C_2S is stable above temperatures of 1420-1447°C and upon cooling, changes reversibly to the α'-form, which is stable in a temperature range of 800-1447°C.[30] Inversion to the β-C_2S occurs at about 650-670°C. Pure β-C_2S changes reversibly to the γ–form at approximately 520°C. At the rates of cooling of commercial cement and the delayed effect that impurities have on inversion, β-C_2S is preserved in the clinker. This impure β-C_2S (belite) forms rounded double grains.

C_3A is introduced in the manufacturing process because it acts as a flux agent in the kiln. C_3A forms rectangular crystals.

C_4AF exists as a solid solution ranging from C_2F to C_6A_2F, with the median being fairly close to C_4AF, which is therefore used for convenience.

Gypsum contributes almost 100% of the sulphur trioxide (SO_3) content in the cement. Optimum gypsum content exists, which imparts to the cement maximum strength and minimum shrinkage where excess would cause cracking and deterioration in the cement set. This optimum depends on the alkali oxide and C_3S content and on the cement fineness.

Free lime is present in cement, either because more lime is contained in the raw materials to combine with the acid oxides SiO_2, Al_2O_3 and Fe_2O_3 or because the reaction between the lime and acid oxides is not complete after the clinkering process. Free lime should be limited, because it may cause cement cracking and deterioration, a phenomenon known as "unsoundness due to lime".

$MgCO_3$, which is contained within the raw materials, dissociates to magnesium oxide (Magnesia) and CO_2 on burning. The magnesia does not combine with the major oxides. It is partly taken up in the clinker minerals, while the remainder crystallises as periclase (MgO). The hydration of periclase, similar to that of CaO, involves volume increase, which may cause unsoundness. The degree of unsoundness is dependant on the size of the periclase crystal. Smaller crystals tend to hydrate more rapidly or without creating excessive internal pressure. Crystal size decreases as the cooling rate of the clinker increases. Hence, cement made from rapidly cooled clinkers is more tolerant to a higher MgO content.

The alkali oxides (Na_2O and K_2O) are introduced into the cement through the raw materials. On burning, they usually combine with SO_3 producing a solid solution of sodium-potassium sulphate, the approximate formulation being $3K_2SO_4 \cdot Na_2SO_4$. The alkali content usually exceeds the SO_3 content, with the excess being taken up in solid solution. These alkali oxides have been found to form products with alkali reactive aggregates, which may cause cracking and disintegration of the concrete.

Traces of titanium oxide (TiO_2) are introduced into the cement through the clay or shale used in the manufacturing process.

Phosphorus pentoxide (P_2O_5) is usually introduced through the limestone used in the manufacture of cement. It retards cement hardening and may cause unsoundness, which may result from CaO produced in reactions between P_2O_5 and C_2S or C_3S.

1.2.3 Cement Hydration Chemistry

1.2.3.1 Introduction

Portland cement becomes a bonding agent in the presence of water by virtue of the reactions of silicates and aluminates, in which hydration products are formed, which in time set and harden. This takes place either by a true reaction of hydration, or by hydrolysis.[29,30]

Hydration occurs when water molecules adhere directly to the compound. This reaction, known as a direct topochemical (solid state) reaction, takes place directly at the surface of the solid without the cement constituent going into solution. During hydrolysis, the reactants hydrolyse to produce ions in solution. The ions combine and the resulting products form a precipitate. The term hydration will however be applied to describe both these reactions.

To gain an understanding of the hydration of Portland cement, the reactions of the individual compounds will firstly be discussed, after which the chemistry and physical behaviour of their interaction in cement will be considered.

1.2.3.2 Calcium Silicate (C_3S and C_2S)

In limited amounts of water, calcium silicate hydrolyses and produces a less basic calcium silicate hydrate (CSH), with the released lime separating out as calcium hydroxide ($Ca(OH)_2$). Calcium silicates do not hydrate in the solid state, but instead the anhydrous silicates first pass into solution, which hence react to form less soluble hydrated silicates and those precipitate out of the supersaturated solution.[29] The hydrate exists in a variety of forms, with the predominant form being that of a fibrous particle. It is poorly crystalised, producing a porous solid defined as a rigid gel.[30] The chemical composition of the CSH gel varies. It is generally assumed that the approximate composition of the hydrate ultimately formed is $C_3S_2H_3$. As a guide, the reactions of hydration can be written as follows:[29,30]

for tricalcium silicate:

$$C_3S + 6H \rightarrow C_3S_2H_3 + 3Ca(OH)_2 \qquad (1.1)$$

for dicalcium silicate:

$$C_2S + 4H \rightarrow C_3S_2H_3 + Ca(OH)_2 \qquad (1.2)$$

It should be noted that these are not exact stoichiometric equations.[29]

The calcium hydroxide is released rapidly. Thin hexagonal plates are formed, which later merge into a massive deposit.

1.2.3.3 Tricalcium Aluminate (C_3A)

The reaction of pure C_3A with water is very violent. This leads to excessive heating and immediate stiffening of the paste known as flash set.[29] C_3A hydrates to C_4AH_{19} and C_2AH_8 in an excess of water.[30] These hydrates are metastable and transform into the less soluble and more stable cubic crystal C_3AH_6. At ambient temperatures, C_3AH_6 also forms directly in pastes with low water/solid ratios. An approximation of the hydration reaction can be written as follows:

$$C_3A + 6H \rightarrow C_3AH_6 \qquad (1.3)$$

It should be noted that this is once again not an exact stoichiometric equation.[29]

1.2.3.4 Tetracalcium Aluminoferrite (C_4AF)

C_4AF rapidly hydrates into tricalcium aluminate hydrate and an amorphous phase, probably $CaO \cdot Fe_2O_3 \cdot aq$. It is also possible for some Fe_2O_3 to be present in solid solution in the tricalcium aluminate hydrate.[29]

1.2.3.5 Cement Hydration

The hydration of cement is an exothermic reaction, therefore the rate of evolution of heat is an indication of the hydration rate. Figure 1.2 shows that there are three exothermal hydration peaks within the first few days, from the time that the dry cement is mixed with water.

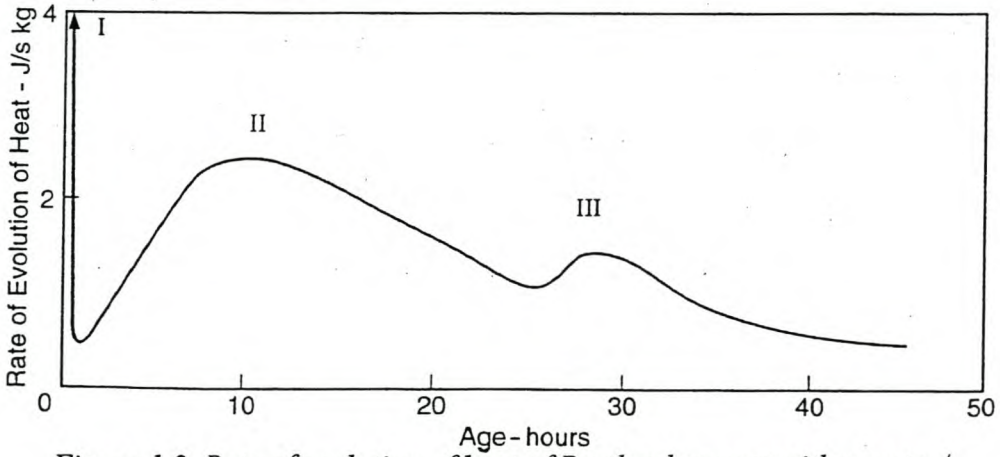

Figure 1.2. Rate of evolution of heat of Portland cement with a water/ Cement ratio of 0.4.[29]

The first peak is very high. This is the **pre-induction period** where contact is made between cement and water and only lasts a few seconds.[31] It corresponds to the initial hydration at the surface of the cement particles C_3S and C_3A.

The hydration of C_3S leads to a rapid release of $Ca(OH)_2$ into the solution, while a dense CSH gel coating forms on the surface of the cement grain.

To avoid flash set, gypsum ($CaSO_4 \cdot H_2O$) has been added to the cement clinker, which is supposed to delay the formation of calcium aluminate hydrate. However, the rate of C_3A hydration during this stage is so high, that calcium aluminate hydrate is formed directly. This means that the conditions for the retardation by gypsum cannot be established immediately.[29]

The ferrite phase reacts with gypsum and $Ca(OH)_2$ to produce needle-like crystals in solid solution consisting of high-sulphate sulphoaluminates and sulphoferrites. The hydration reaction may be written as follows, assuming the ferrite phase to be C_4AF:

$$4CaO{\cdot}Al_2O_3{\cdot}Fe_2O_3 + CaSO_4{\cdot}2H_2O + Ca(OH)_2 \rightarrow$$
$$CaO(Al_2O_3,Fe_2O_3){\cdot}3CaSO_4{\cdot}aq$$

During the next period, which is known as the **dormant or induction period**, the cement hydration rate is low. This period lasts for one to two hours, during which the cement paste remains plastic and workable.

The C_3S hydration reaction is inherently self-retarding, largely due to the inhibition of nucleation of crystalline $Ca(OH)_2$ by soluble silica.[32] Silica ions adsorb onto the liberated $Ca(OH)_2$ nuclei, which prohibits hydration product growth until some level of super-saturation of $Ca(OH)_2$ is reached. Super-saturation is achieved slowly, because $Ca(OH)_2$ must leach from C_3S into a solution of increasing chemical potential, while the CSH layer acts as a diffusion barrier. Only when super-saturation is achieved, does crystal growth continue.[32]

Gypsum and C_3A react to form needle-like crystals of a high-sulphate calcium sulphoaluminate known as ettringite ($3CaO \cdot Al_2O_3 \cdot 3CaSO_4 \cdot 31H_2O$). The ettringite forms an insoluble layer on the surface of the tricalcium aluminate grains, retarding further hydration. There is some evidence that the $Ca(OH)_2$ released by the hydrolysis of C_3S also retards the hydration of C_3A.[29,33] $Ca(OH)_2$ reacts with C_3A and water to form C_4AH_{19}, which forms a protective coating on the surface of the unhydrated C_3A grain. It is also claimed that $Ca(OH)_2$ possibly reduces the concentration of alumina ions in solution, thus slowing down the rate of hydration of C_3A.[29,33]

The break up of the CSH coating signifies the beginning of the **setting period**. An osmotic mechanism or calcium hydroxide crystal growth is suggested to be the cause of the disintegration of the gel coating. The cement grains are once again exposed, resulting in an increase in the rate of hydration. The rate of heat evolution reaches a second peak during this stage.

The volume of the hydration products is more than double that of the anhydrous cement. Therefore, as hydration proceeds, spaces are filled, points of contact are made and stiffening of the paste occurs.[29]

The **hardening period** follows the second hydration peak and lasts for a few days. The rate of hydration slows down over a long period, the controlling factor being the diffusion through the pores of the hydration products. The concentration of the hydration products and the resulting points of contact, restrict the mobility of the cement grains to such an extend that the paste becomes rigid and final set is achieved.[29,34]

Until now, ettringite has continued to form. When the gypsum (sulphate ions) has been exhausted, another increase in the rate of hydration occurs, forming a third hydration peak. This is the result of the further hydration of C_3A whereby ettringite converts into either low sulphate sulphoaluminates ($3CaO \cdot Al_2O_3 \cdot CaSO_4 \cdot 12H_2O$), referred to as monosulphates or into hexagonal plate solid solution of C_4ASH_{12} and C_4AH_{13}. The remaining C_3A hydrates to C_4AH_{19}, which depending on the temperature, may convert to cubic C_3AH_6 or to a hydrogarnet by taking up silica.[35]

Similarly, upon the depletion of sulphate ions, the solid solution of high-sulphate aluminoferrites convert into a low-sulphate aluminoferrite solid solution ($3CaO(Al_2O_3,Fe_2O_3)\cdot CaSO_4\cdot aq$) and/or into a solid solution phase in which sulphate ions are replaced by hydroxide ions, i.e. $3CaO(Al_2O_3,Fe_2O_3)\cdot Ca(SO_4, (OH)_2)\cdot aq$.[30]

Furthermore, CSH hydrates to short fibres, while $Ca(OH)_2$ grows steadily.

After the third peak of hydration, heat of hydration decreases, as the hydration reaction rate decreases. At the onset of this period, the cement is expected to have at least 90% of its final strength.

1.2.4 Structure of Hydrated Cement

The hardened cement paste is a heterogeneous solid consisting of an undifferentiated amorphous mass, unhydrated cement grains and void volumes of either air or water.

The amorphous mass is a CSH-gel containing hexagonal crystals of calcium hydroxide and occasionally small amounts of hexagonal and cubic aluminate and sulphoaluminate crystals. It is a rigid gel of colloid-sized particles and is characterised by a porous structure and large specific surface area.

1.2.5 Factors Affecting Cement Hydration and Setting Properties

1.2.5.1 Cement Composition

From figure 1.3 below, the rate of hydration of the various compounds are shown.[2] It can be concluded from this figure that selective hydration occurs at the early stages, while the degree of hydration proceeds at equal fraction rates thereafter. C_3A only contributes to strength during the early stages. C_3S (alite) contributes to strength during the first four weeks, while C_2S (belite), contributes after that.

When hardened cement is attacked by sulphates, the C_3A form more calcium-sulphoaluminates, which causes expansion and leads to cracking. The gypsum required, increases, with an increase in C_3A and the alkali content.

The cement composition must therefore be varied to manipulate the setting of cement according to the factors above, to achieve the desired properties, as shown in table 1.3.

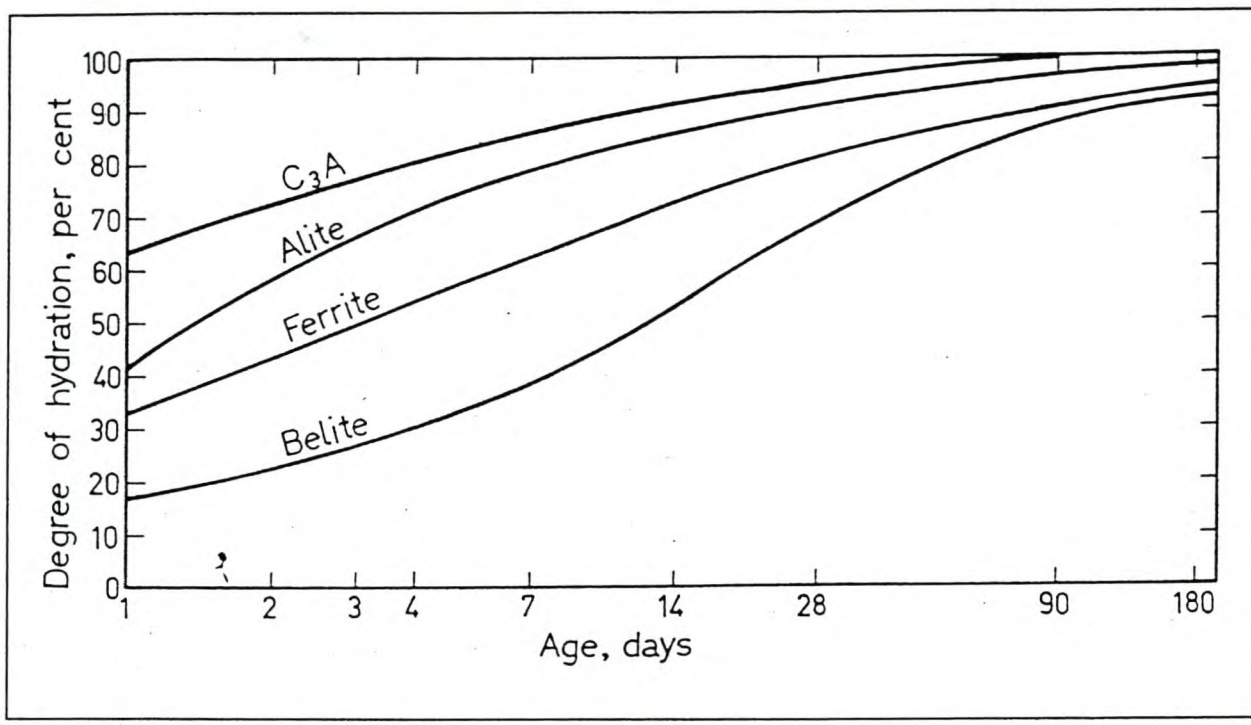

Figure 1.3. Rate of hydration of various compounds in Portland cement[30]

Table 1.3. Composition and fineness of type I-V ASTM classified USA cements[31]

ASTM Type	ASTM Designation	C_3S [%]	C_2S [%]	C_3A [%]	C_4AF [%]	Fineness [cm^2/g]
I	General purpose	50	24	11	8	1800
II	Moderate sulphate resistant – Moderate heat of hydration	42	33	5	13	1800
III	High early strength	60	13	9	8	2600
IV	Low Heat	26	50	5	12	1900
V	Sulphate resisting	40	40	4	9	1900

The alkalis (Na_2O and K_2O) in the cement paste accelerate the advent of the second hydration peak, which implies an increase in hydration rate.

The alkalis contribute to deleterious chemical reactions, particularly with active silica constituents. The reaction is initiated by the alkaline hydroxide in the pore water derived from the alkalis in the cement paste. An alkali-silicate gel is formed in planes of weakness, pores in the aggregate or on the surface of the aggregate particles. In the latter case, the bonds between the aggregate and surrounding hydrated cement paste may be destroyed. The gel increases in volume when in contact with additional water. Because the surrounding confines the gel hydrated cement paste, internal pressure results and may eventually lead to expansion, cracking and disruption of the hydrated cement paste.

1.2.5.2 Fineness of Cement

The rate of hydration increases as the fineness of the cement increases, because of an increase in surface area exposed to water. Rapid-hardening cement makes use of this concept (see table 1.3).

1.2.5.3 Water/Cement (W/C) Ratio

W/C ratio does not affect the initial rate of hydration, but a lower W/C ratio will accelerate the advent of the decreased hydration at the latter stages.[31]

The W/C ratio required for complete hydration of all the cement constituents is approximately 0.23. However, a higher level of water addition will increase the initial paste volume to equal that of the final paste volume. This will provide for the increase in cement volume during hydration without inhibiting strength development. A W/C ratio of approximately 0.4 has been reported for optimum paste strength.[1,31]

1.2.5.4 Curing Temperature

1.2.5.4.1 High Temperature Curing (< 100^{0}C)

An increase in temperature during and after the initial contact between cement and water accelerates the hydration rate. The dormant period is reduced so that the overall

structure of the hydrated cement paste is established very early. The effect on the ultimate degree of hydration is however very small.[29,83,84]

When placing and setting cement under atmospheric conditions and increasing the curing temperature between 60°C and 100°C, very early strength is increased, but strength, particularly flexural strength, from about 7 days and onwards may be adversely affected.[29,30,31] The rapid initial rate of hydration under such elevated temperatures retards subsequent hydration and produces heterogeneously distributed products of hydration within the paste.[29,30] The reason for this effect is that during high temperatures of hydration, there is insufficient time to facilitate the diffusion of the products of hydration away from the cement particle or for uniform precipitation in the interstitial spaces. The result is the formation of a highly concentrated and dense gel around the hydrating cement grains, and the formation of a less concentrated and therefore weaker gel, in the spaces between the grains. The loss of durability is affected due to a deleterious effect known as delayed ettringite formation.[83] Also, the difference in the thermal expansion coefficients of the various constituents of the paste may produce internal stresses. This in turn increases the porosity of the paste and increases micro-cracking.[29, 83]

1.2.5.4.2 Steam Curing at Atmospheric Pressure

Steam curing at atmospheric pressure is a special case of moist curing, where the temperature remains below 100°C, while the vapour saturated atmosphere ensures a supply of water. Sufficiently high early strength is obtained, which facilitates product handling soon after casting. As with high temperature curing, long-term retrogression of strength occurs. A partial explanation is that the thermal expansion of air is far greater than the surrounding solid material. The expansion of the air bubbles are restrained and tensile stresses are induced, which may lead to the formation of very fine cracks.[29,30]

A delay of 2-6 hours in the application of steam curing or a lower rate of temperature rise during the curing process reduces the disruptive effects of the expansion of air bubbles. It has been established that such delayed steam curing can completely offset the negative effect of the rapid heating.[29]

1.2.5.4.3 High Pressure Steam Curing (Autoclaving)

This process involves the curing of the cement paste in a pressure vessel with a supply of wet air. This allows curing at temperatures greater than 100°C (typically between 160 and 193°C), without causing the cement paste to dry out.

Autoclaving causes structural and chemical changes resulting in a detrimental effect on strength. This effect is even greater than for curing conditions under 100°C. At temperatures above 100°C, the gel pores are absent and the specific area of the hydration products is lower. A gel with a coarser structure, increased porosity and a reduced strength results.[29]

Autoclaving reduces the degree of hydration which in part also contributes to the reduction in strength. The composition of the hydration products is also affected. The phase diagram presented in figure 1.4 illustrates that for a CaO/SiO_2 (C/S) ratio of 2 to 3, which is typical for Portland cement, the hydration product $C_2SH(A)$ forms at temperatures above 100°C (see area 2 in figure 1.4). This is in contrast to the CSH gel formed at temperatures 70-100°C. The formation of $C_2SH(A)$ also contributes to the reduction in strength associated with autoclaving. This detrimental effect may be eliminated by reducing the C/S ratio to approximately one, by increasing the silica content through the addition of condensed silica fume. This results in the formation of tobermorite as hydration product and a strength increase greater than the strength reducing effects associated with autoclaving.[29,83,84]

Additionally, the lime in the paste is reduced, because of secondary lime-silica reactions. Efflorescence is resultantly reduced, because no lime remains to be leached out. The products of hydration are stable and no retrogression of strength occurs. Resistance to sulphate attack is also improved.[29]

1.2.5.5 Porosity

The strength of cement is fundamentally a function of the void volume within.[29] An increase in porosity equates to a decrease in cement strength. [1,30]

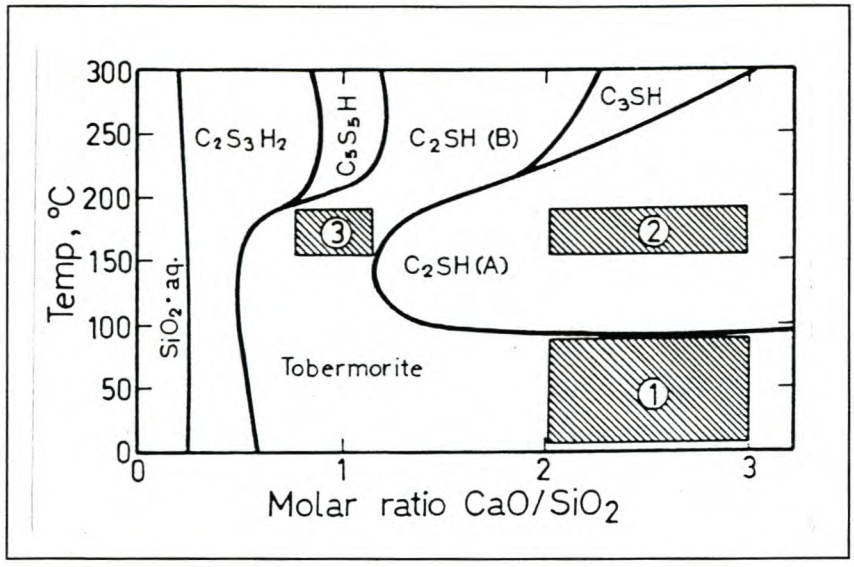

Figure 1.4. Phase diagram of the CaO-SiO_2-H_2O system[30]

1.3 Cement Composites

1.3.1 Introduction

It can be noted from the above discussions that cement-setting properties differ greatly with changing parameters. Cement can be further modified to achieve specific objectives. This can be done by the addition of other components and admixtures.

Cement can be combined with cement extenders and admixtures that participate in the cement hydration reactions to enhance cement hydration. Alternately, cement can be combined with *aggregates* that serve as filler materials. The aggregates are chemically inert materials that do not participate in cement or pozzolanic reactions.

1.3.2 Wood- and wood fibre-composites

1.3.2.1 Wood and cement interaction

1.3.2.1.1 Physical interaction

When a composite is subjected to a flexural force, the composite can be seen to experience a large number of parallel shear forces perpendicular to the force. The

function of the wood-fibre reinforcement is to spread, absorb and dissipate the resultant stresses and strains, to withstand a much higher tensile force than a pure mineral matrix. These stress and strain forces are endured until fibre debonding, pullout or rupture occurs.[68] Hence, the length and percentage fibres in the composite is of importance to reinforcement, where a higher fibre slenderness ratio (length/diameter) will produce higher strength properties. An optimum strength is achieved at approximately 8-10 % fibre addition by mass.[68,70]

The density of the composite is a function of the pressure during pressing. At higher pressures, the density will be greater, where improved intimacy between the cement matrix and fibre bonding is achieved, while fibres are collapsed.[66] This principle was applied during the manufacture of the Deviro panel and its enhancements, where at a given press pressure, the desired density could be achieved.

The fibre content will also affect the density of the composite. The theoretical density can be calculated by equation 1.4, where the gross density of the fibrous material is used for the minimum density, and the dry cell wall density is used at the maximum density, because it is expected that the cell is collapsed under high compression.[69]

$$\rho = \frac{1 + \omega_0 + X_f}{1/\rho_b + \omega + X_f/\rho_f} \qquad (1.4)$$

with ρ = theoretical density

ω = water/ binder ratio

ω_0 = hydration water/ binder density

X_f = fibre/ binder ratio

ρ_b = binder density = 2,86 g.cm^{-3} for cement

ρ_f = density of fibre (for minimum density) or density of dry cell wall for maximum density

In turn density has a significant effect on the composites strength properties. Equation 1.5 has been established to express modulus of rupture and compressive strength for wood cement composites as a function of density. As with findings for cement bonded excelsior board and MDF board, a linear relationship is established.[87,92,48,97]

$$MOR = (a \bullet \rho) + b \quad , \quad r^2 \in [72\%;98\%] \qquad (1.5)$$

with MOR = panel modulus of rupture, MPa

ρ = panel oven dry density

a,b = empirically determined constants

1.3.2.1.2 Chemical interaction

Cement contains reactive metal hydroxyl groups such as –Ca-OH, -Si-OH, -Al-OH and -Fe-OH at its surface, while wood fibre contains mainly hydroxyl groups, -C-OH and carboxyl groups, -C-OOH. Hence, it is believed that bonding between the cement and wood fibre occurs through chemical interaction between these hydroxyl groups through hydrogen bonding.[1,68] Because maximum fracture energy is achieved when frictional energy is dissipated by fibre pull-out, the strength of these bonds will significantly impact on the tensile and flexural strength of the fibre reinforced composite.[68]

During cement hydration, the water-soluble sugars in wood are split from the ends of cellulose chains and the higher carbohydrates (hemicelluloses, starch and pectin) are degraded by alkaline peeling reactions while water insoluble carbohydrates solubilize under the alkaline conditions.[65,66] These compounds contain acidic groups, which retard cement hydration by primarily forming complexes with C_3A, creating an impermeable sheath that prohibits hydration.[66,67] This leads to the investigation of curing accelerators and other cement composite enhancers known as pozzalans and additives.

1.3.2.2 Cellulose-fibre reinforced cement composites

Wood-fibres that are held together by a cement matrix, form a composite used in a variety of industrial applications. Such composites exhibit improved tensile and flexural strength and fracture toughness, water resistance and fire retardancy properties, because of the combined characteristics of the components.[64,91]

Two processes are used to manufacture wood fibre reinforced cement composites, namely the *Hatschek* process for composites at higher densities of approximately 1,5

g/cm^3, and the *Magnani* process for lower density panels.[68] Softwood kraft fibre is ideally suited, but recycled fibre has served as replacement with slight reduction in flexural strength and a marginal increase in density.[70]

In the *Hatschek* process, wood fibres are pulped, deflaked and refined to the required degree of freeness. The fibre is homogenised with cement and other admixtures as a slurry at a low consistency of 5-10%. This slurry is dewatered into thin layers on vat formers and delivered to the forming roll. The wet boards are cut and delivered to a corrugating, flat sheet or embossed board line for pressing. Stacking and hydration is done between caul plates.[66,68,85,86] This process holds the advantage that fibres are distributed evenly, but board thickness is restricted due to the high water drainage requirements.[68]

In the less popular *Magnani* process, a low density board, thicker than 12 mm is produced. The slurry is prepared to approximately 50% solids, formed over a belt conveyor and dewatered by vacuum boxes after which, the boards are air dried. This composite is of a lower strength and is used for fire retarding purposes.[66,68]

1.3.2.3 Cement bonded particle board

Passing round wood or waste wood such as construction waste through hammer mills, chippers and/ or refiners produces wood chips.[90] The chips are mixed with Portland cement and water at a typical cement:wood:water ratio of 60:20:20 while a cement accelerator is often added. This mixture is spread as a continuous mat onto caul plates, cut, stacked and pressed to a predetermined pressure. The cement is hardened at elevated temperatures of 70-80°C for 6-8 hours in the compressed state. Thereafter the cauls are removed and the boards are conditioned for 12 to 18 days.[89]

Injecting carbon dioxide into the board during pressing reduces the cement setting period to 5 minutes because of the formation of lime that causes bonding and high initial strength. No heat treatment is required and the process is not limited to a few wood species, but instead is suited to most species.

1.3.2.4 Wood wool cement board

Wood Wool Cement Boards (WWCBs) are increasingly being used as construction material as roof decking, ceilings and walls. They have good water, fire and decay resistance and insulating properties, in addition to being lightweight. These properties and the low manufacturing costs make them ideal and cost-effective in the construction of inexpensive shelters in developing countries.[21]

Wood wool (excelsior) is typically manufactured from softwood wood logs that are shred into long strands and dipped into a salt solution such as calcium chloride to accelerate cement curing. Portland cement, wood wool and water are mixed to the ratio 1:2:1 respectively and spread into a mat which is cold pressed and stacked. The boards are cured within moulds, under pressure for the first 24 hours to allow initial set and then conditioned for two to three weeks for final hydration to occur.[60,61,66,88]

Boards manufactured using CO_2 injection are pressed in a sealed gas injection press. Pressing time is 400 seconds, during which a gas pressure of 400kPa is maintained for the first 220 seconds of the pressing time.[62]

1.3.2.5 Comparison between commercially available wood composites

To understand the applications for wood mineral composites, panel characteristics were compared with other wood composites in figure 1.5. The densities of cement bonded wood and fibre boards are up to twice that of the resin bonded composites, but without a concomitant increase in flexural strength. Dimensional stability, fire resistance and long term durability are however substantially improved.[59,50]

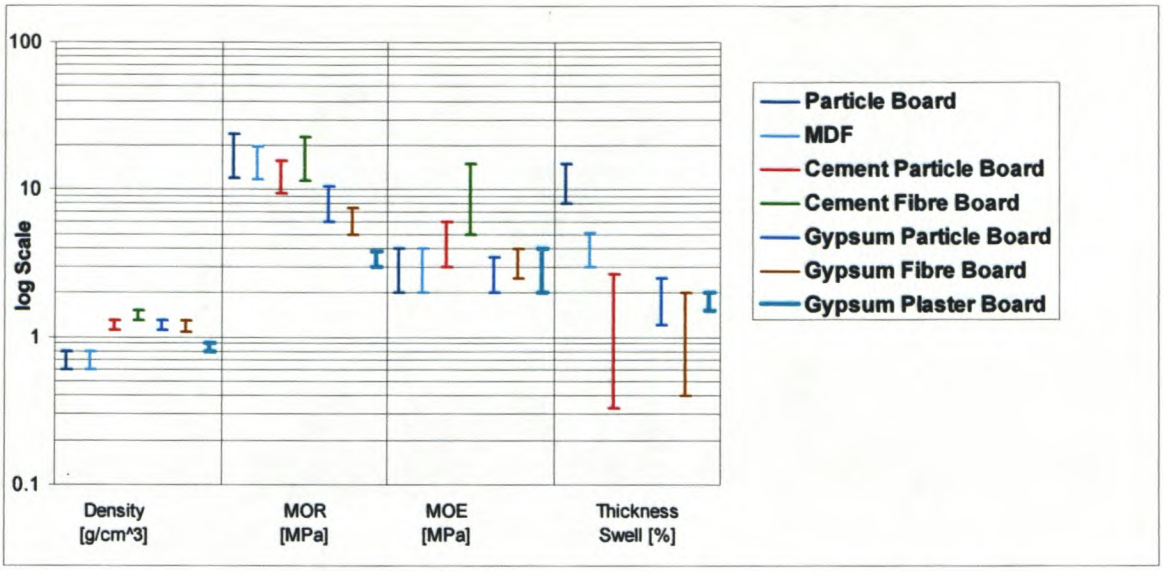

Figure 1.5. Comparison of wood- and wood-fibre composites[48,49,50,66,89,93,94,95]

The broad range in the properties may be attributed to the various wood species, fibre types, wood and fibre contents within the composites, density, binder and production process differences.

1.3.3 Pozzalans

Material, which have cementing tendencies and are used with cement to gain technical and/or economic benefit, are termed cement extenders or pozzalans.[41] These pozzalans can be defined as siliceous or siliceous and aluminous materials with little or no cementing value. When reacted with cement, $Ca(OH)_2$ reacts with the silicates to form cementing compounds consisting of calcium silicate hydrate.[37,73] Equation 5.2 simplifies this reaction:[37]

$$2S + 3CH \rightarrow C_3S_2H_3 \qquad (1.7)$$

1.3.3.1 Fly Ash

1.3.3.1.1 Characterisation

Coal fired boilers at power plants generate energy from carbon and combustible matter that is incinerated, while mineral impurities become fused. A portion of this

mineral matter can fuse into agglomerates and form at the bed of the boiler, while the 72-80% ash is removed with the flue.[71] This so-called fly ash is removed from the gas by electrostatic precipitators.[1,72] Fly ash consists of small, hollow spherical particles and varies widely in physical, chemical and mineralogical properties.[71,72] The course particles are relatively unreactive, thus only the fine fraction (approximately 10% on the 45mm sieve) is used as cement extender.[37]

When fly ash is derived from the combustion of anthracite and bituminous coal, the CaO content is determined to be less than 5% and is classified as class F fly ash. When lignite and sub-bituminous coal are combusted, a fly ash rich in CaO (15-35%) is produced, classified as class C fly ash. Because CaO is beneficial for strength development, the class C fly ash provides the highest pozzalanic reactivity.[1,74] The chemical composition of South African fly ash is shown in table 1.4.

Table 1.4. Chemical composition of South African fly ash[37]

Oxide	**% by Mass**
SiO_2	45-50
Al_2O_3	25-30
CaO	4-8
FeO	9-11
MgO	2-4
$N_2O + 0.658\ K_2O$	1-3

1.3.3.1.2 Reaction with cement

When mixed with cement, fly ash acts as an inert fine aggregate in the early stages of cement curing. As cement hydration continues, pozzalanic activity is initiated as the tetrahedral layer, forming the glass phase of the fly ash, is exposed and dissolved under the alkaline conditions.[1,75] Silica and alumina from the fly ash reacts with $Ca(OH)_2$ to produce calcium silicate and calcium aluminate.[74] The result is a retarding of the cement setting and hardening reactions, but enhanced strength development of the resulting concrete. Further effects are:[71,73,74,76]

- improved plasticity and workability
- reduced expansion normally caused by alkali-aggregate reaction
- higher sulphate resistance
- reduced contraction and cracking

- reduced density
- reduced permeability.

The addition of fly ash requires an increase in water/cement (W/C) ratio. Table 1.5[73] indicates the suggested W/C and W/C_E[a] ratios required at various fly ash addition levels. The table also provides for the addition of aggregates, which would be de-inking sludge for purposes of this study.

Table 1.5. Water/ cement (W/C) and water/ equivalent cement (W/C_E) ratios required for different blend and mix proportions[73]

Binder (% cement/ % fly ash)	Binder/ Aggregate							
	10/90		20/80		30/70		40/60	
	W/C	W/C_E	W/C	W/C_E	W/C	W/C_E	W/C	W/C_E
100/0	0.73	-	0.42	-	0.31	-	0.28	-
80/20	0.90	0.82	0.52	0.47	0.43	0.39	0.40	0.37
60/40	1.17	0.93	0.72	0.57	0.60	0.47	0.53	0.42
50/50	1.42	1.01	0.87	0.62	0.74	0.53	0.67	0.48

Partial replacement of cement with fly ash has been shown to be possible to levels of 15-30%.[71,74]

1.3.3.2 Condensed silica fume (CSF)

1.3.3.2.1 Characterisation

Quartz is reduced to ferosilicon and silicon alloys at high temperatures in electric arc furnaces.[77,78] Silica fume is released as a by-product, which cools down and condenses on contact with air, to form condensed silica fume (CSF). CSF is highly pozzalanic, due to its extremely fine (specific surface of approximately 20,000 m^2/kg), non-crystalline structure.[37,78] From table 1.6[37] is can be seen that CSF consists mostly of SiO_2.

[a] Equivalent cement (C_E) is considered as cement + 0.4 fly ash

Table 1.6. Chemical composition of CSF[37]

Oxide	% by Mass
SiO_2	92
Al_2O_3	1.5
Fe_2O_3	1.2
CaO	0.6
MgO	0.6
K_2O	0.6
H_2O	0.8

1.3.3.2.2 Reaction with cement

Cement replacement levels with CSF are from 5 to 10%.[1,77,78] The hydration reaction is quicker than for fly ash, commencing after one day and glass dissolution starts at pH 12, instead of pH 13.[79] Due to the fineness of CSF, a denser cement matrix is formed. The high specific surface implies that water is more readily absorbed and hence a W/C ratio greater than 0.55 is required.[77,78]

CSF serves as a very effective replacement for cement, improving concrete compression strength greatly.

1.3.3.3 Perlite

Perlite is a volcanic glass rock, which is processed by first crushing the ore to the desired grain size. These crushed grains are passed through a furnace and heated to the softening point, which ranges from 760 - 1090°C.[80] The water within the structure expands, expanding the grains to about 20 times its original volume. Much of the trapped water escapes by diffusion, with the remaining water being absorbed into the glass structure. Hence, the chemistry of the glass is altered, increasing its melting point.[81]

Perlite is used in the building industry for its:[80,81]

- excellent thermal properties
- ultra low density (bulk density of 110 -130 kg/m^3)
- exceptional fire resistance, no smoke evolves during combustion, and is resistant to spalling (does not loose its integrity due to fire and water quenching)

- compatibility with OPC and other inorganic binders
- strength
- low water permeability

1.3.4 Admixtures

An admixture is a chemical added to a concrete mix, in quantities no greater than 5%, to achieve a specific modification to the normal properties of concrete.

1.3.4.1 Accelerating Admixtures

The primary function of accelerators is to increase the rate at which early strength development occurs, which may also accelerate setting.

Calcium chloride ($CaCl_2$) is the most commonly used accelerator. It is effective in accelerating the hydration of the calcium silicates, mainly C_3S, either by a slight change in alkalinity of the pore water or as a catalyst in the hydration reaction.[1] The addition of $CaCl_2$ also results in the formation of a double sulphoaluminate salt. At $CaCl_2$ concentrations above 1%, the solubility of alumina is increased. This accelerates the hydration of C_3A, which accelerates cement setting.[2] $CaCl_2$ reduces the danger of frost attack during the first few days after placing, but freeze-thaw resistance at later ages is adversely affected. Abrasion and erosion resistance is also improved.

Other accelerating additives are sodium chloride, calcium nitrite, calcium nitrate, calcium formate and sodium formate. Calcium nitrate also appears to be a corrosion inhibitor. Calcium formate is only effective when used with cement with a low sulphate content and a C_3S/SO_3 ratio greater than four.

1.3.4.2 Retarding Admixtures

Retarding admixtures (retarders) delay the setting of the cement paste. The hardening of the cement paste is also generally slowed down. Retarders do not alter the

composition of the hydration products. Sugars, carbohydrate derivatives, soluble zinc salts and soluble borates, and possibly methanol exhibit retarding action .[1]

Setting may be delayed by reducing the solubility of the alumina. This will reduce the formation of the lime-poor gel, thereby delaying the setting of the cement paste, provided the cement has a low alkali oxide content.[1] Alternatively, they modify the crystal growth or morphology, becoming adsorbed on the rapidly formed membrane of hydrated cement and retarding the growth of calcium hydroxide nuclei. This results in forming a more efficient barrier against further hydration.

Retarders tend to increase the plastic shrinkage because the duration of the plastic stage is increased, but the drying shrinkage is not affected.

1.3.4.3 Water-reducing Admixtures

These admixtures have the effect of reducing the water content of the cement paste by 5 to 15%, thus reducing the water/cement ratio, while retaining the desired workability or to improve the workability at a specific water/cement ratio. Water reducing admixtures such as lignosulphonic acids and their salts or hydroxylated carboxylic acids adsorb onto the products of hydration, thereby retarding hydration.

The surface area of the cement, which can undergo initial hydration, is effectively increased by the active components (surfactants) of the admixture. The amount of water available for hydration is as a result also increased. Also, the strength increases because of a higher rate of hydration in the early stages. Some Type D admixtures adsorb onto the products of hydration, thereby retarding hydration.

1.3.4.4 Superplasticizers

Superplasticizers have a water-reducing effect, significantly more so than normal water-reducing admixtures. They are water-soluble polymers, namely: sulphonated melamine formaldehyde condensates; sulphonated naphtalene- formaldehyde condensates; modified lignosulphonates; sulphonic acid esters and carbohydrate esters.

The main effect is deflocculating and dispersion of cement particles, thereby improving workability. The structure of the hydrated cement paste is not fundamentally altered, the main effect being a better distribution of cement particles and consequently their better hydration. The result is a general increase in strength, with no retrogression of strength at later ages. Furthermore, superplasticizers retard the hydration of C_3A. The ettringite crystals so formed are small and cubic, rather than needle-like. This also improves the mobility of the cement paste.

1.3.5 Silicates

1.3.5.1 Introduction

Soluble silicates are water soluble glasses generally manufactured at different proportions of an alkali metal and SiO_2. Sodium silicate is an alkaline salt prepared by calcining sand, diatomaceous earth or quartz with sodium carbonate or sodium hydroxide.[45] The salt consists of a varying proportion of sodium oxide (Na_2O) and silica (Si_2O). The degree of alkalinity increases with an increase in Na_2O:Si_2O ratio.[46]

Sodium silicates are available either in a hydrated or anhydrous powder or as a liquid. In powder form, it is commonly manufactured as sodium metasilicate (Na_2SiO_3).[47] The powders are transparent, glassy or crystalline solids, water soluble and have high melting points. The solubility increases with an increase in Na_2O:Si_2O ratio.[46] Colloidal silicates are available as concentrated liquids, known as "water glass".

Sodium silicates are widely used as high temperature adhesives and binders due to the following properties:

- Low Cost
- Inorganic
- Easy to Handle
- Rapid Controlled Set
- High Strength
- Chemical Stability

The following section will focus on the application of sodium silicate in wood cement and cellulose-fibre cement composites.

1.3.5.2 Sodium silicate in wood and wood-fibre mineral composites

Problems arise during the manufacture of cement bonded composites (CBCs) if wood is incompatible with cement. Wood contains low molecular weight carbohydrates and extractives that interfere with the normal hydration and setting of cement (refer to section 1.3.2.1.2). The dissolution of these products when wood is in contact with cement paste, inhibits normal cement hydration resulting in poor wood/cement bonds. To improve wood/cement compatibility, sodium silicate, could be employed.[41]

Sodium silicate also serves as a fireproofing agent and fortifier in wood and wood fibre composites.

1.3.5.2.1 Cement-bonded Particleboard

Wood cement boards usually require pressing at 50°C for 8 – 12 hours, to allow for the initial setting of cement. This results in high capital and installation costs and low productivity. Attempts are therefore made to accelerate the curing process and increase production rate. The addition of sodium silicate serves as a curing accelerator for cement bonded composites and as a fortifier with the further addition of CSF.[41,88]

Na_2SiO_3 is firstly dissolved in water if in powder form. It is then mixed with saw dust, wood shavings or wood chips after which the cement is blended into the bulk. Mats are formed and then pressed. The pressing cycle can be hot or cold, with an optimum press temperature of approximately 95°C for hot pressing being reported.[41] Pressure should be released slowly at the end of the hot pressing cycle so as to avoid blow-out of the boards. Pressing time can be shortened to 12 minutes. Boards can further be dipped in a 2% aqueous solution of $MgCl_2$ to increase the acceleration process. Condensed silica fume (CSF) can be added to accelerate cement hydration and to fill the gaps in the cement structure.[42] Boards produced with CSF can be autoclaved at a curing temperature greater than 135°C.[43]

During the initial hardening of cement, amorphous calcium silicate hydrate (CSH) and cementation of SiO_2 gel occurs when Na_2SiO_3 is used as a fortifier. Cement hydration is brought about by the production of CSH TypeIV with the addition of $MgCl_2$ after pressing.[60]

For Na_2SiO_3 addition in a range of 5 to 15% (based on cement mass), an increase in silicate content relates to an increase in MOR and MOE. This can be attributed to the increase in cement hydration with an increase in silicate content, which results in less springback of the boards. The post treatment of dipping the board in a 2% aqueous solution of $MgCl_2$ improves bending strength.[41] When CSF is added, optimal strength properties are achieved at 15% addition levels. If the board is further autoclaved, the silica content must be increased, requiring CSF additions to range between 20-25% for optimum results.[43]

An increase in water glass addition relates to increased water absorption and thickness swell. This implies that the dimensional stability of the boards decrease with an increase in Na_2SiO_3. The addition of $MgCl_2$ improves the dimensional stability of the boards.[41] The addition of CSF has a slight improvement on the hygroscopic properties of the CBCs. Optimum addition rates are the same as those for optimal strength properties.[43]

Wood chips may be mixed with OPC in a slightly basic solution of sodium silicate. The mixture is moulded and then set by passing a direct current through it, with sodium silicate serving as the electrolyte. The material is chip and crack proof and weathers well. It also has exceptional acoustic properties.[60]

1.3.5.2.2 Low Density Wood-Cement Composites

Early strength improvements are realised with the addition of sodium silicates, most likely due to the increase in slurry pH. No significant improvement in long term strength or hygroscopic properties have been observed with the addition of sodium silicate to the wood wool.[61,62] This is in contrast to claims that physical and mechanical properties improve as a result of an interphase layer formation at the boundary of the mineral binder / wood-filler phase.[63]

CHAPTER 2 - EXPERIMENTAL

2.1 Standard Deviro Panel

2.1.1 Introduction

The Deviro panel can be classified generically as a wood fibre-cement composite, but is dissimilar to commercial wood fibre reinforced cement composites, in that the wood fibre fraction of such composites is significantly less. Commercial products contain a small percentage of fibre (8-12% by mass), versus the Deviro panel that contained 55% de-inking sludge or approximately 25% fibre by mass.

Testing critical properties versus commercially available wood and wood-fibre composites in order to evaluate its commercial viability benchmarked the Deviro panel. Such comparisons identified the extent that physical properties needed further development to meet demand requirements.

2.1.2 Raw materials

De-inking sludge, collected from *Nampak Tissue Bellville*, a local tissue mill, was transported in 50 kg polyethylene bags. The sludge was subsequently placed in cold storage at 4 ±2°C, for a maximum of 12 weeks prior to use, to reduce the risk of bacteriological decay. Moisture and ash content were determined prior to storage.

A general purpose, type I ordinary Portland cement (OPC), with a specific surface area of 2800-3300 cm^2/g manufactured by PPC was used in all the panels.[37]

A grade 4, Malta fly ash, supplied by Ash Resources, was used as a cement extender for the standard Deviro panel. This was the least reactive, but also least expensive commercially available grade of fly ash.

The cement and fly ash were screened through a 20 mesh sieve prior to mixing to remove any lumps in the bulk bags. Table 2.1 summarises the components of the cement and fly ash used for the study.[1]

Table 2.1. Chemical composition of cement and fly ash[1]

Chemical component	OPC [%]	Fly ash [%]
SiO_2	20	54
Al_2O_3	4	33
CaO	59	4
TiO_2	0.2	2
MgO	0	1
Fe_2O_3	3.4	3
Na_2O	0.1	0
K_2O	0.3	0.5
P_2O_5	0.1	0.3
L.O.I. (Loss on ignition)	2.5	1

2.1.3 Manufacturing process

De-inking sludge, cement and fly ash were mixed in a ratio 55:30:15 by mass for 10 minutes using a 10-litre food processing kneader. To afford homogenous mixing, while striving to optimise the water/cement (W/C) ratio (refer to 1.3.3.1.2), additional water was added to produce a slurry of approximately 35% consistency.

The slurry was subsequently poured into a mould and spread evenly, using a plastering tool. A perforated PVC square, 313 x 313 mm, 10mm thick with holes 13mm ϕ, covered with a 60 mesh wire placed over a 20 mesh wire served as the base. A 5mm thick, 65mm high, stainless steel frame fitted on the base. The paste was covered with a 60 mesh wire and 2 stainless steel plates, 300 x 300 x 0.75 mm in size. This design allowed for a high rate of dewatering during the pressing stage.

The mould was then placed in a Bürkle LA150 press fitted with a press form. The pressure was applied intermittently to allow the slurry to relax after each increase in load. The reological properties of the slurry, during the initial phase of pressing, contributed to a more even paste distribution, homogenizing panel density and thickness. After further pressing, panel de-watering started.

Crafford controlled panel density and thickness by steel spacers placed within the press.[1] This would not be possible if panel enhancements were made where the panel could not be pressed to the thickness of these spacers due the expected bulking effect of additives such as sodium silicate and perlite. Hence a pre-set maximum pressure

was established to achieve a predetermined oven dry density[48,92]. A pressure of 4MPa was set to achieve an oven dry density of 1 g.cm^{-3}. This would afford a more accurate comparison with further panel enhancements that could also be pressed at the same pre-set pressure.

Thereafter the panel was de-moulded and placed between two rigid wire racks, by a stepwise removal of all the sub-assemblies. The wet panel had no handling strength at this stage, and was constantly supported. The drying racks were constructed of a stainless steel sieve (3 mesh size), supported by a square steel frame. A 20 mesh wire covered the rough sieve, which prevented impressions from forming on the soft wet panels, during the initial setting period. These racks were stacked horizontally in a steel holding frame. The design afforded effective curing (hydration), while maintaining the panel's shape and structure. Hydration was achieved in a controlled environment of 20°C and 65% relative humidity (RH).

The panel was rigid after 48 hours and could be easily handled at this stage. After 28 days, the panel was considered fully cured and was removed from the curing racks.

2.1.4 Testing of physical properties

2.1.4.1 Static bending tests

Modulus of rupture (MOR) and modulus of elasticity (MOE) were determined in accordance to SABS Method 1015[51,52], with the exception that the recommended size for a test specimen was not the same. Therefore due to the experimental panel dimensions, 180 mm x 65 mm instead of the recommended 300mm x 600mm test pieces were cut, as tested by Crafford (1997)[1].

Static bending tests were performed on test specimen cut from the dry panel after 7, 14, 21 and 28 days. Conventional wood working machinery was adequate to cut the dry panels. The outer 5mm of the panel was cut away, because the panel edge dehydrated quicker than the remainder of the panel, and was not considered representative. The dry panel was cut in a configuration, which produced five test

pieces. Each test piece was finished with a belt sander to achieve even, parallel surfaces.

The static bending properties were evaluated on a computerised Instron strength testing machine. The data was downloaded to an Excel spread sheet. A module was developed in Visual Basic 5.0 to chart the load-deflection graph, and determine the modulus of rupture and modulus of elasticity according to SABS method 1015. This yielded a static bending test, after the data had been processed (see appendix B).

The modulus of rupture was calculated from the bending moment at the maximum load and the cross-section of the test specimen, according to equation 2.1.[52] The modulus of elasticity was determined from the load-deflection curve. The gradient at the most linear section of the curve was determined by linear regression. This gradient ($m = \Delta F/\Delta l$) was used in equation 2.2[52] to determine the MOE.

$$MOR = \frac{3 \cdot F \cdot l}{2 \cdot b \cdot t^2} \qquad (2.1) \qquad MOE = \frac{l^3 \cdot m}{4 \cdot b \cdot t^3} \qquad (2.2)$$

MOR in MPa

F = maximum load, N

MOE in MPa

m = $\Delta F/\Delta l$ at the linear portion of the load-deflection curve, $N.mm^{-1}$

l = distance between the centres of the supports, mm

b = width of test piece, mm

t = thickness of test piece, mm

The integral beneath the curve was calculated to determine the energy to failure, expressed in Joule. The load-deflection charts were investigated to further understand of the nature of fatigue.

2.1.4.2 Moisture content

Moisture content (mc) for de-inking sludge samples was determined according to equation 2.3. Equation 2.4 was used to determine the moisture content of dry panels and test pieces.

$$mc = \frac{m_g - m_0}{m_g} \times 100\% \qquad (2.3)$$

$$mc = \frac{m_g - m_0}{m_0} \times 100\% \qquad (2.4)$$

mc = moisture content, %

m_g = wet mass, g

m_0 = oven dry mass, g

The composite samples and the test specimen were oven dried at 103 ± 2°C. The oven dry mass (m_0) was determined to be the constant mass, when two successive weighing operations, did not differ by more than 0.1% of the final mass of the test piece.

2.1.4.3 Oven dry density

The dimensions of the oven dried test pieces were measured to determine the oven dry volume, with density expressed as $g.cm^{-3}$, according to equation 2.5

$$\rho_0 = \frac{m_0}{V_0} \qquad (2.5)$$

ρ = density, $g.cm^{-3}$

m_0 = oven dry mass, g

V_0 = oven dry volume, cm^3

2.1.4.4 Ash content

Ash content was determined by incinerating the oven dried sample or test specimen at 550°C, in a muffle furnace for a period of 6 hours. The sample was placed in a desiccator for 10 minutes before weighing.

2.1.4.5 Water absorption and thickness swelling

The Deviro panel was compared with the following commercially available wood- and wood-fibre composites:

- Urea formaldehyde (UF) bonded particle board
- Standard fibre board ("pressed-wood")
- Tempered fibre board

- Medium density fibre board (MDF)
- Cement particle board
- Cement fibre board
- Paper overlaid gypsum board

25,0mm x 25,0mm test specimen were cut from the panels. In the case of the Deviro panel, samples were cut after 28 days of curing. The test specimen were sanded until all surfaces were square and parallel and then conditioned at 20°C and 65% RH for 48 hours. Sample mass and dimensions were measured. Water absorption tests were conducted as per SABS Method 1012[53], whereby the samples were immersed in distilled water for 2 hours, removed and blotted to remove excess water and accurately weighed and measured. The samples were again immersed for an additional 22 hours (total immersion period = 24 hours). Sample mass and dimensional measurements were repeated. These measurements were used in equations 2.6 and 2.7 to calculate water absorption and thickness swelling.

$$WA_x = \frac{m_x - m_g}{m_g} \times 100\% \qquad (2.6) \qquad TS_x = \frac{t_x - t_g}{t_g} \times 100\% \qquad (2.7)$$

WA_x = water absorption after x hours, %

m_x = mass after being immersed for x hours, g

m_g = conditioned mass, g

TS_x = thickness swelling after x hours, %

t_x = thickness after being immersed for x hours, mm

t_g = conditioned thickness, mm

2.1.4.6 Dimensional stability

A dimensional environmental control chamber (DECC) was used to determine sorption characteristics.[54] The purpose of the experiment was to identify the linear expansion of the test specimens from a lower relative vapour pressure to a higher vapour pressure. This was achieved by conditioning the test specimens at 30% relative humidity (RH) and 45°C, and then suddenly changing the environment to 90% RH and 30°C. The difference in dry bulb temperature from 45°C to 30°C ensured

that the enthalpy of dry air did not increase when switching conditions. (Refer to the psychometric chart in appendix C.)

The DECC consisted of two chambers which could be set to the desired temperature and humidity. This was achieved by spraying a fine mist of water over an electric heating element in each chamber. A fan moved this warm, moist air through the chamber over a cooling element that served to cool the air to the required temperature and condenses the excess moisture. The samples were placed in measuring holders in one central chamber. These were equipped to register dimensional change as a change in electrical current. The air from each chamber could either be directed to move through these sample holders, or by-pass the chamber in which the test specimens were kept. A simple gate selected which condition prevailed in the sample chamber. This afforded for a quick change in environmental conditions. The air was reticulated once it moved through or past the sample chamber. This apparatus is shown in figure 2.1.

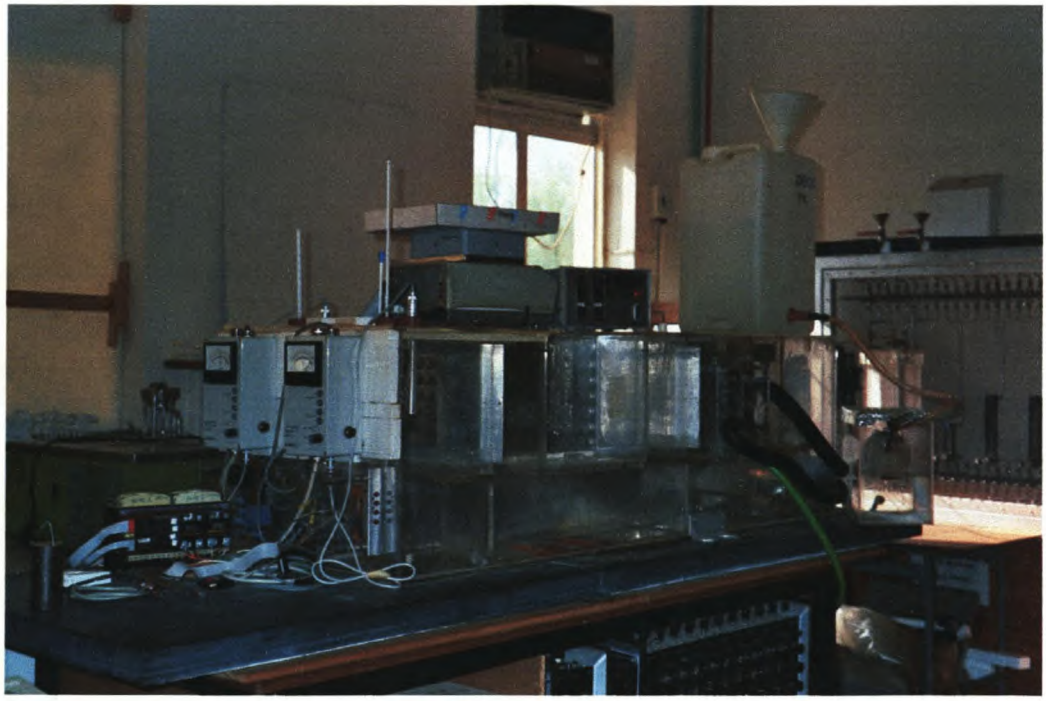

Figure 2.1. Dimensional environmental conditioning chamber

2.1.4.7 Accelerated aging

The ability of cellulose fibre re-inforced cement composites to withstand severe exposure conditions is of critical importance. Deppe had concluded that at least 5 years of outdoor aging is required to reliably characterise wood based panel aging.[56] This is however not practical, hence accelerated aging procedures have been developed to simulate conditions of natural outdoor weathering. Accelerated aging tests induce cyclic swelling and shrinkage to generate internal stresses.[57]

The test method applied in this study was the ASTM D1037: Accelerated aging.[55] This procedure had been shown to be more severe on resin bonded particle boards than the British standard (BS) 5669 cyclic test, the cyclic soak-dry test and the cyclic boil-dry test.[57] Hence, differences in durability between the different panels would be more easily identified.

This procedure provided high rank correlations with the 1, 5 and 10 year outdoor aging of wood and phenolic bonded wood composites.[58] This correlation was assumed to be extrapolated with all test specimens.

According to ASTM D1037 procedure, each specimen was subjected to six complete cycles of accelerated aging, with each cycle consisting of the following treatments:

1. The test pieces were immersed in a water bath at 49°C ±2°C for an hour;
2. The test specimens were transferred to a steam chamber, where they were treated with saturated steam at 93°C ±3°C for 3 hours. A steam generator was used to purge live steam at atmospheric pressure into the steam chamber. The temperature in the chamber was controlled by regulating the steam flow;
3. The test pieces were then stored in a closed, but not sealed box in a cold storage room at -18°C ±2°C for 20 hours;
4. Thereafter, the specimens were heated in an oven at 99°C ±2°C for 3 hours;
5. The pieces were again sprayed with saturated steam at 93°C ±2°C for 3 hours;
6. The cycle was completed with a further heating period of 18 hours, at 99°C ±2°C.

One cycle took 48 hours, while the full aging period equalled 12 days. Inspections were made after each stage, to identify any signs of weathering. The test specimen were conditioned for 48 hours at 20°C and 65%RH, prior to testing the static bending strength, according to section 2.1.4.2.

2.2 Panel Enhancements

All panel enhancement tests were evaluated according to methods set out in section 2.1.4.

2.2.1 Condensed silica fume (CSF) reacted sludge panel

Crafford (1997) questioned whether the flexural strength of the sludge panel increased on replacing fly ash with more reactive CSF.[1] The densifying effect of CSF also increased the panel density. A linear increase in flexural strength was established, with an increase in density for the standard Deviro panel (refer to section 3.3.3.2). Apart from an increase in strength due to an increase in density, it should be established if this was further enhanced by the pozzalanic reactivity of the CSF.

The manufacturing process remained unchanged. The fly ash was directly replaced with CSF, hence the CSF addition was at 15% by mass. The pressure for the press was set at 4 MPa to achieve a $1 g/cm^3$ oven dry density.

2.2.2 Autoclaving

Given the corrected CaO/SiO_2 ratio, autoclaving the standard panel increased panel strength and reduces the curing period.[1] In order to achieve the required CaO/SiO_2 molar ratio of approximately 1, the 15% fly ash added in the standard panel was fully replaced with CSF. OPC contained 59% CaO and 20% SiO_2 (refer to table 2.1, in section 2.1.2) and CSF contained 92% SiO_2 and 0.6% CaO (refer to section 1.3.3.2.1). Hence, for 300g of cement and 150g CSF:

$m(CaO)_{cement} = 0.59*300 = 177$ g in cement

and $m(CaO)_{CSF} = 0.006*150 = 0.9$ g in CSF

molar mass of CaO $= 56.08$ g.mol^{-1}

$\Rightarrow$ $n(CaO) = (177+0.9)/56.08 = 3.172$ mol

Also $m(SiO_2)_{cement} = 0.2*300 = 60$ g in cement

and $m(SiO_2)_{CSF} = 0.92*150 = 138$ g in CSF

molar mass of $SiO_2 = 60.08$ g.mol^{-1}

$\Rightarrow$ $n(SiO_2) = (60+138)/60.08 = 3.296$ mol

$\Rightarrow$ CaO/SiO_2 molar ratio $= n(CaO)/n(SiO_2) = 0.96$

This meant that the very practical and simple change of pozzalan from fly ash to CSF afforded the required change in CaO/SiO_2 molar ratio. This had the advantage of making meaningful comparisons with the panel enhancements with CSF and the standard Deviro panel, because the fibre and inorganic fractions were unchanged.

The panel was manufactured as the CSF enhanced panel (section 2.2.1 above). Autoclaving at too high a moisture content would result in structural failure of the panel, resembling *blow-out*,[1] where as fully air dried panels would have passed the setting period and the full benefits from autoclaving would be lost. Therefore, once the panel was placed in the drying rack, it was immediately transferred to a pre-drying kiln prior to autoclaving. A laboratory oven with an air circulation fan was used for this purpose. Dewatering rates were investigated at the temperature set points of 40, 50, 60, 70, 80 and 103°C. After 6 to 15 hours, the panels were removed from the oven. The moisture contents were measured and the panels were placed in an autoclave within 2-3 hours.

Initially a laboratory autoclave, depicted in figure 2.2, was used. After an untimely failure of this autoclave, the panels were treated in the industrial autoclaves at Everite Building Products, Brackenfell. The conditions in the laboratory autoclave and industrial autoclaves were both set at a peak temperature of 175°C, for a 10 hour cycle. Subsequently the autoclaved panels from the autoclave were allowed to cure further in the curing racks, under the control conditions of 20°C, 65% RH. for 28 days.

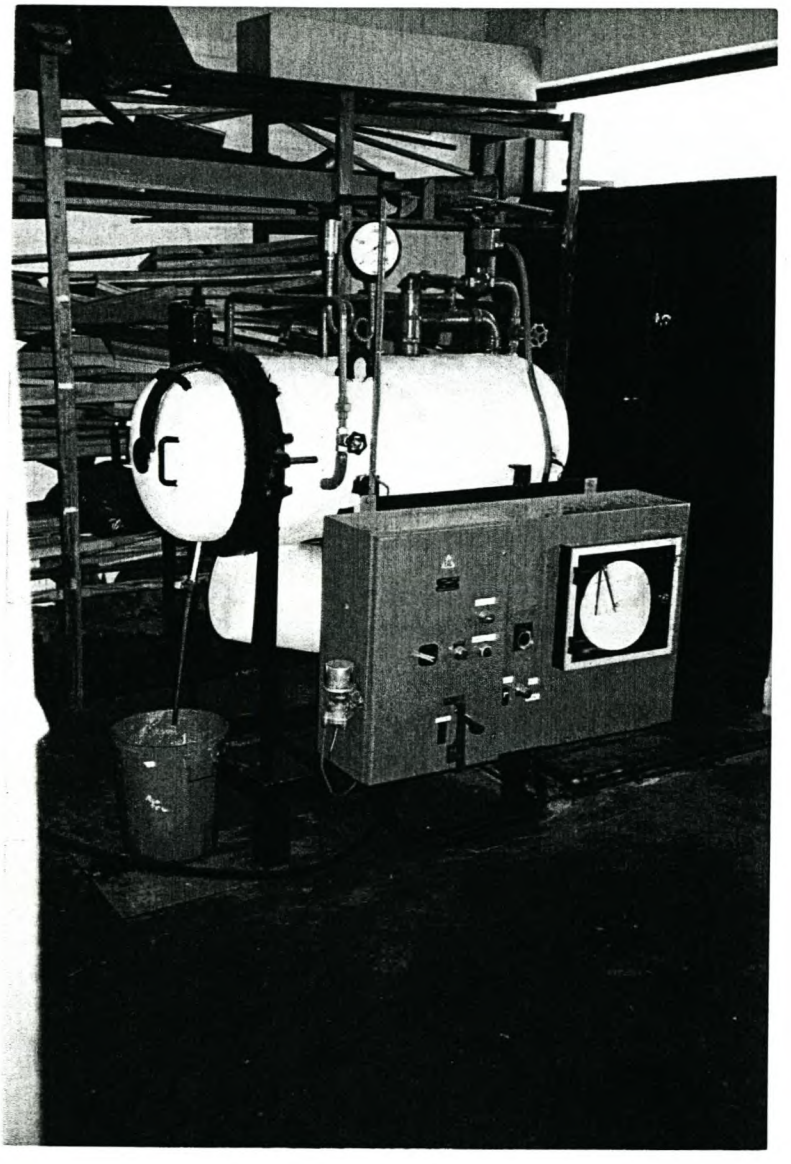

Figure 2.2. Laboratory autoclave

2.2.3 Addition of sodium silicates

The objective with the sodium silicate (water glass) addition was to increase early strength development due to improved bonding, curing acceleration, and improved

cement-fibre compatibility.[41] Hygroscopicity was also expected to be reduced, due to fortification, especially with the inclusion of CSF.[41,43]

Introducing sodium silicate during the mixing stage allows the silicate to coat the fibres, rendering them less hydrophilic.[38] The water based sodium silicate should act as a curing compound and adhesive upon the introduction of cement and pozzalan (fly ash), hardening and densifying cement products.[39,40] Sodium silicate also accelerates the curing process, which offsets the negative interference of carbohydrates.[41]

Soluble sodium silicate at 40% solids, supplied by Silchem Industries, was diluted with the water used to mix the sludge slurry. This silicate solution was mixed with the sludge for 5 minutes prior to cement and fly ash addition, allowing the silicate to coat the fibres. 1% to 10% water glass was added, based on the oven dry mass of the panel. The same manufacturing process was followed as that used for the standard Deviro panel. The filtrates were collected and pH was determined, to measure the effect water glass had on the slurry pH. An increase in slurry pH should promote hydration, thereby accelerating the curing of the panel.

2.2.4 Addition of Perlite

Perlite is added to reduce panel density, without incurring flexural strength loss, while improving the fire rating of the panel. The Perlite is supplied by Pratley, and marketed as pretreated Pratliperl®. The density of this pozzalan in the loose state is approximately 100 kg/m^3, and when mixed with cement, the practical concrete densities are expected to range from 300 kg/m^3 to 1000 kg/m^3, depending the addition rate.[44]

Due to the lower density of Perlite, the masses of the other components in the panel were reduced. All gravimetric measurements were based on a target density, assuming a final panel volume of 1000 cm^3, while pressing the panels to a pressure of 4 MPa.

2.2.5 Surface coating

The purpose of applying a surface coating, was to extend the durability of the panel. Two types of surface coats, Cemwash® and Stipplecrete®, supplied by Cemcrete were evaluated. Cemwash®, a coloured cement finish, having a base of white Portland cement served as a water proofing cement finish, which was ultraviolet resistant and highly durable.[82] Stipplecrete® was also a coloured cement based finish, to increase panel durability. Stipplecrete® contained polypropylene fibre in the dry powder mix, and could be supported with a polypropylene mesh to increases surface hardness.[82]

The surfaces of the fully cured and cut standard Deviro panels were cleaned with a dry cloth. The coating was applied by brushing the slurry over the panel surfaces. The test panels were wetted three times within the next 24 hours by immersing in distilled water for a period of 5 minutes. Thereafter, they were conditioned at 20°C, at 65% RH for 28 days to ensure a fully cured coating. Then these panels were tested for durability according to the ASTM D1037 accelerated aging and performing flexural strength tests.

2.3 Pilot Scale-up

In all previous work, 300 by 300 mm panels were manufactured and evaluated for curing, strength, aging and dimensional stability. It is important to understand whether these characteristics remain unchanged on a larger scale. Hence, a panel, approximately ½ the size of a standard door, with an area of $1m^2$ was manufactured. Such a panel was tested for homogeneity and curing characteristics.

2.3.1 Press design

2.3.1.1 Requirements

The most important criteria was that the process had to be simple and manufactured at a cost advantage. The press had to consists of detachable subassemblies such as a

pressing device, moulding frame, press platen and press frame to ensure ease of transport and handling.

The thickness of the standard Deviro was 12mm, when pressed to 4MPa. The large panel was manufactured to a thickness of 30 mm. Based on this final thickness, the wet slurry was expected to be 120 mm deep, therefore a moulding frame was designed with 160 mm depth. This afforded an opportunity to produce a thicker panel of approximately 60 mm if required. To ensure the frame fits easily into the greater press structure, a gap of 20 mm between the press platen and the moulding frame was accommodated. This implied that when producing a 30 mm thick panel, the full travel of the pressing mechanism was 150 mm.

The moulding tray had to handle easily, as to facilitate smooth and gentle demoulding, without disturbing the panel, which required the design to be of minimal weight. To accommodate the large amount of dewatering during slurry compression, the base of such a mould was perforated. Since the wet panel had no intrinsic strength, the base had to be sufficiently rigid to support the wet panel, upon removal from the press.

To facilitate the ease of sliding the mould with the wet slurry, the tray design was slightly tapered to the back, to ensure ease of removal after pressing. Therefore, the back edge was 5 mm shorter than the front, while fitting the base with handles to pull the tray.

Although a 4 MPa pressure was required to press a 1 $g.cm^{-3}$ panel, it was not practical to press to such a high density or achieve the loading force of $4x10^{6}N$. The panel would be too heavy to handle and the press design would require cost prohibitive engineering, which would impact negatively on the commercial viability of such a solution. A loading force of $4.10^{5}N$ was engineered by employing two 20-ton hydraulic jacks. Hydraulic loading was selected because of the high force and the great distance the tray had to travel within the press assembly. It was essential that the tracking of the tray and press platen was true, hence a mechanical guiding system was included.

Finally, although the press was designed to accommodate a maximum pressing force, the panel was pressed to a predetermined thickness by employing mechanical stops.

2.3.1.2 Initial design

Central Mechanical Services, University of Stellenbosch, designed an initial frame as in figure 2.3 to 2.6. This frame fit an existing 100 ton hydraulic, single ram, vertically down stroking press. Because this was a single ram press, with a ram diameter of 130 mm, the force line would be generated at the centre of the panel. Any variation in the wet slurry mass in the moulding frame would induce initial uneven loading, which would damage the ram. Hence an alternative press design with more than one action line was required.

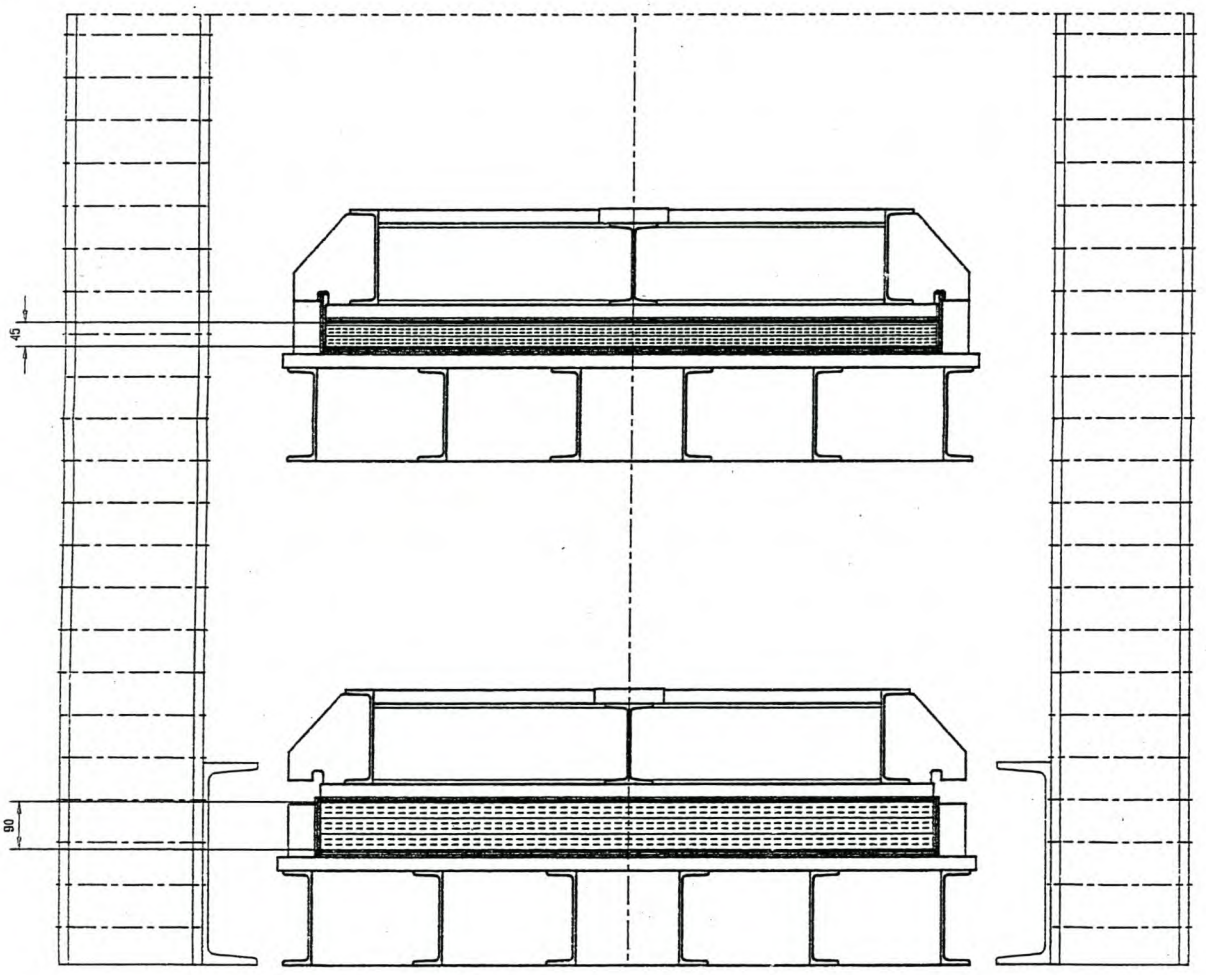

Figure 2.3. Full press – Front view (unloaded and loaded to full travel)

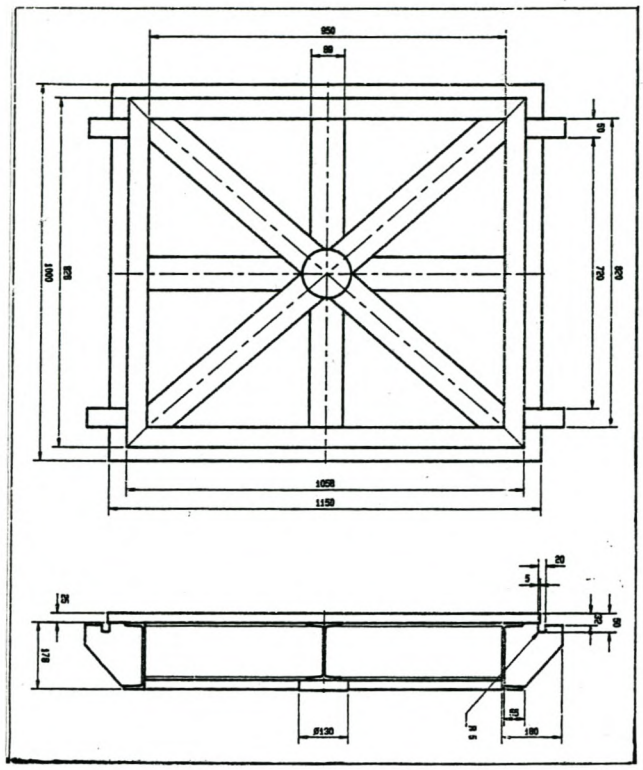

Figure2.4. Press platen – Top and front view

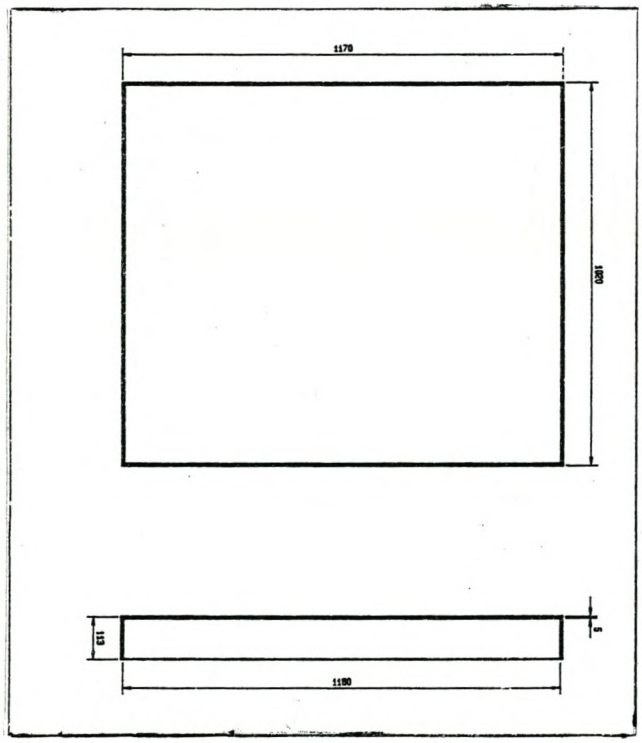

Figure 2.5. Molding frame – Top and front view

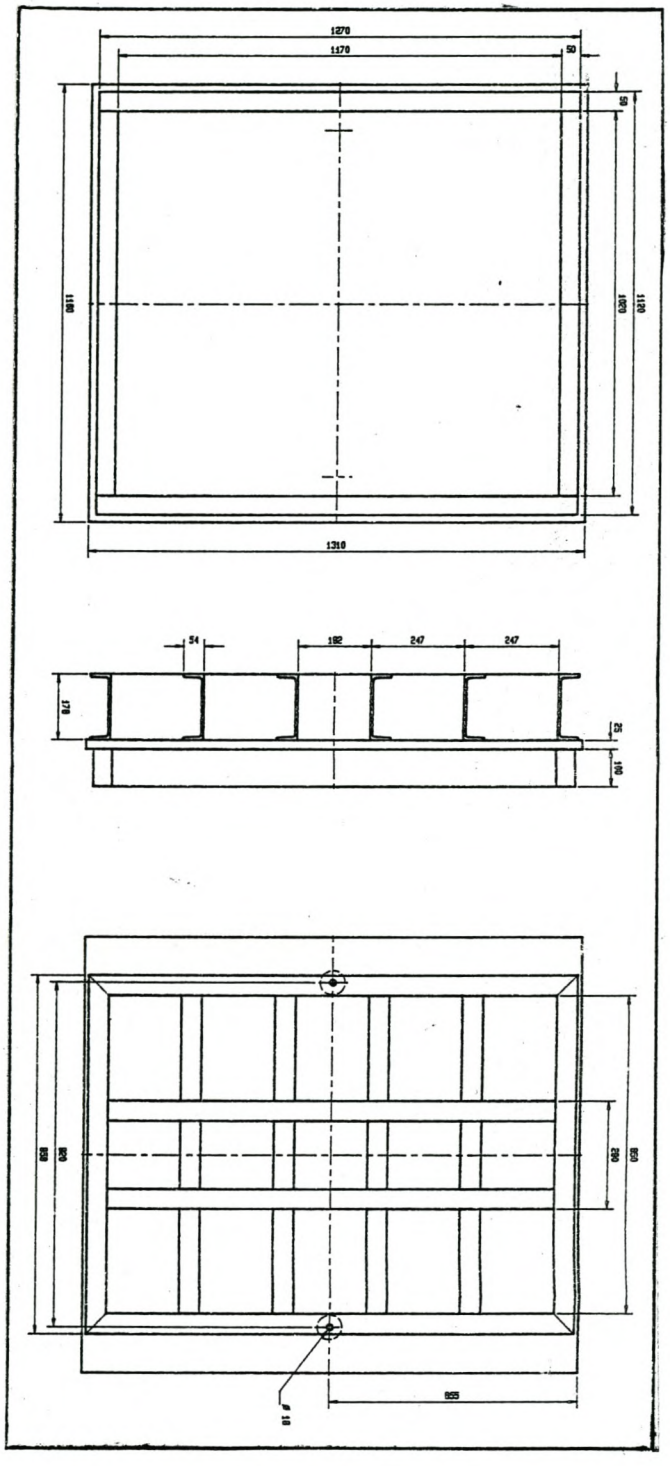

Figure 2.6. Press base – Top, front and bottom view

2.3.1.3 Press design and manufacture

Based on the initial design and experiences from the laboratory Bürkle press, a press was developed for the larger panel (figure 2.7). The press was transported and handled as the following subassemblies (refer to figure 2.8 and 2.9):

- Press frame
- Hydraulic pistons
- Moulding assembly
- Moulding tray
- Press platen and horizontal support beams

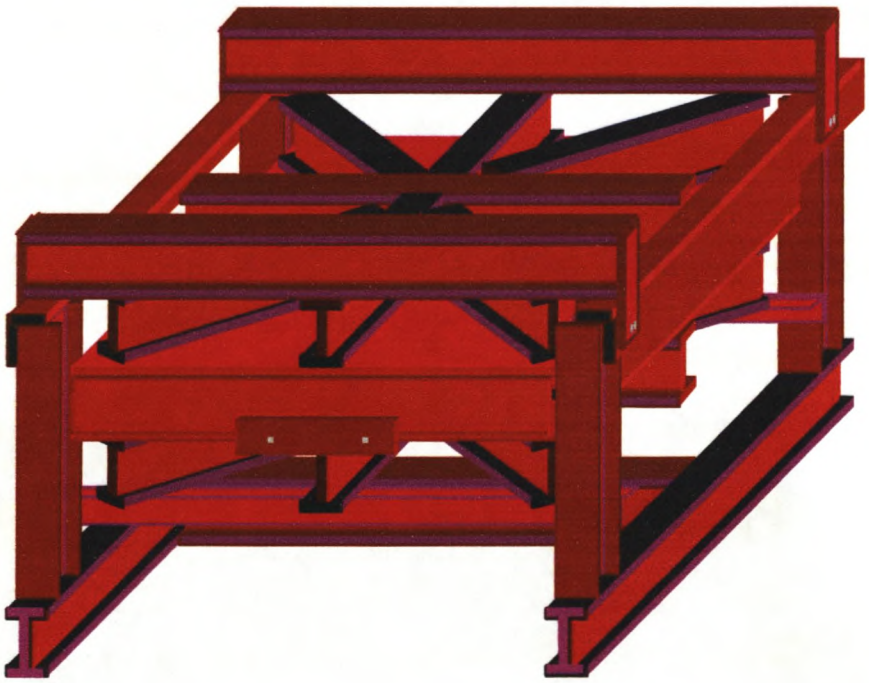

Figure 2.7. Final press design

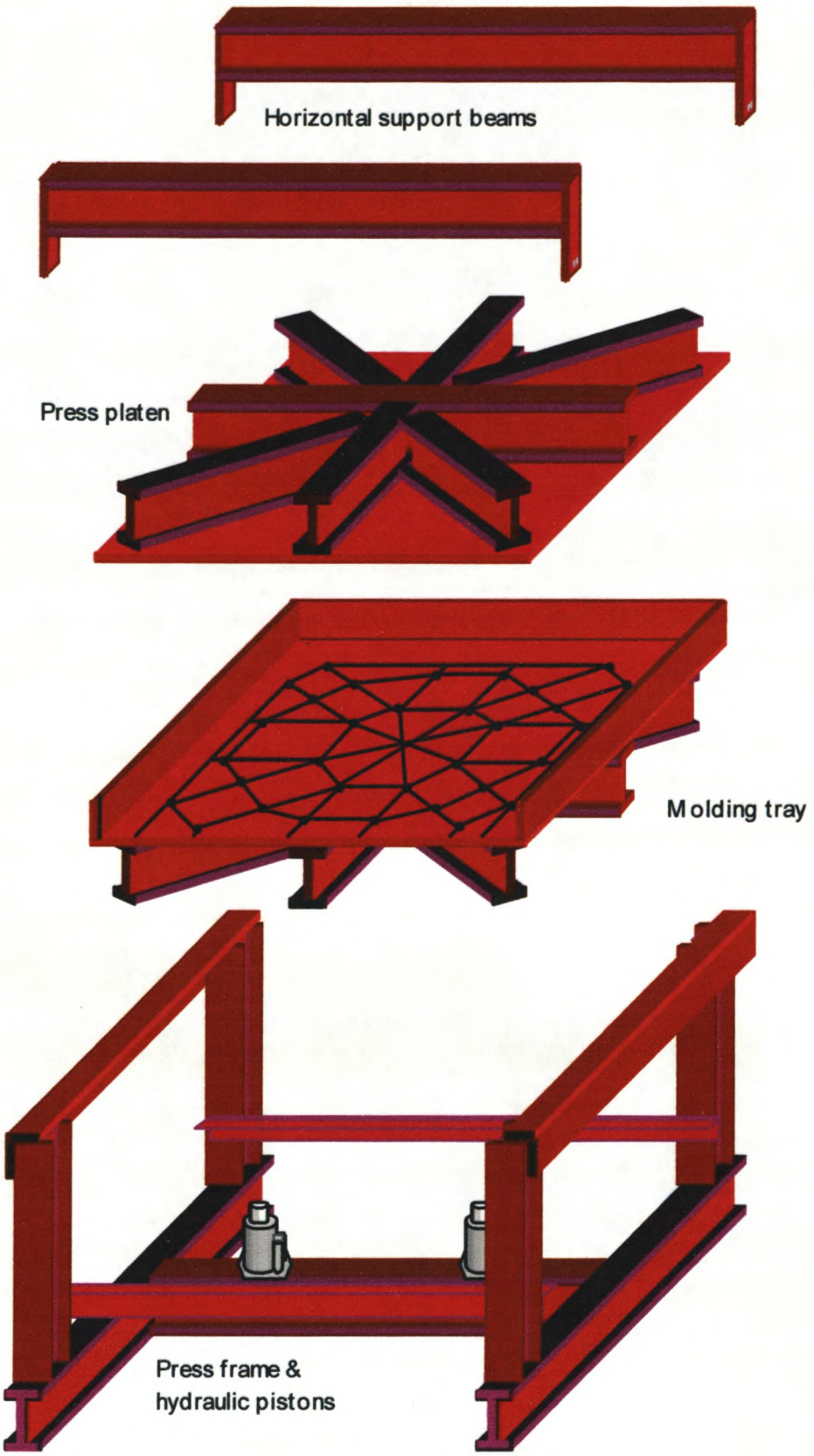

Figure 2.8. Press sub-assemblies

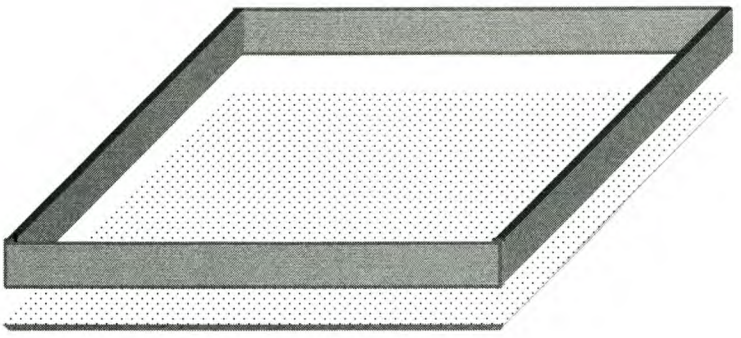

Figure 2.9. Moulding tray

The **press frame** was designed for even load and stress distribution throughout the structure. The greatest stresses were generated in the base due to strong moment forces acting on this structure. Hence, 180 mm I-beams were used to manufacture the base. The vertical beams supported the frame and guided the moulding tray through its full travel. All beams were fully welded to together.

To achieve a load of 4.10^5N, two **hydraulic piston jacks** with a maximum capacity of 20 tons (196kN) each were used. The supporting I-beam beneath the hydraulic pistons was supported by vertically positioned 6 mm channel iron to prevent crimp failure of this I-beam.

The **moulding assembly** consisted of a 10 mm thick, perforated, high density polyethylene (HDPE) base. 1mm deep longitudinal and latitudinal channels ran square between the 6 mm ϕ holes, which were 20 mm apart in the HDPE. The base was first covered with a polyester netting and then a 60 mesh stainless steel wire. A 5 mm thick, stainless steel moulding frame fitted on top of the base completed the moulding assembly.

The moulding assembly slid into the **moulding tray**. A large amount of dewatering occurred when pressing the panel. For this reason, 20 mm ϕ holes were drilled in the base of the tray to allow the high volumes of water to escape. 3 mm deep channels connected these holes to carry the water from the 6mm ϕ holes in the moulding assembly to these 20 mm ϕ holes. The base was supported below by I-beams similar to the initial design to prevent the base from buckling under maximum load. The 20 mm thick sides of the tray supported the lightweight moulding tray, preventing it from

buckling or breaking. Because the moulding assembly was inserted from the front, the front support plate was detachable by it sliding into position in channels on either end and supporting it in the centre by an additional support plate that was bolted into position.

The paste in the moulding assembly was pressed against a 20 mm thick **press platen,** which was supported like the base of the moulding tray. Two 180 mm I-beams welded onto the press platen and bolted over the frame, served as **horizontal support beams**.

2.3.2 Manufacturing procedure

2.3.2.1 Mixing and forming

A 50 litre industrial cement mixer was used to mix the slurry (figure 2.10). The volume of the large panel was 24 times the volume of the standard panel increasing the mass of the raw materials to the following:
Sludge (55% by mass) = 13,2 kg (O.D) = 36 - 44 kg @ 37 - 30 % consistency;
Cement (30% by mass) = 7.2 kg;
Fly ash (15% by mass) = 3.6 kg;
Water = 20 - 30 kg (depending on the consistency of the sludge)
Total mass = 75 kg

The capacity of the cement mixer was less than this mass, therefore half the required mass was weighted off and mixed with the water in the mixer for 20 minutes. After forming the first portion of mat in the moulding assembly, the second portion was mixed for 20 minutes. This tray assembly was placed on plastic crates that were double stacked to match the height of the press tray. Each layer formed a separate set of 9 crates that were firmly tied together into one rigid assembly.

The second portion was then transferred to the mould and spread to a homogenous, even paste, seen in figure 2.11. A measuring block was used to ensure even paste thickness. Thereafter the paste was covered with another 60 mesh wire and then by a

polyester shade net. This lay-up allowed for dewatering at the top of the panel during pressing.

2.3.2.2 Pressing

The moulding tray was pushed into the frame and its front secured by a reinforcing cover. A level gauge was placed on the supporting plate to ensure the mould remained level. Spacers placed at each corner of the tray ensured that the tray assembly travelled to a predetermined height.

Pressing was achieved by raising the mould against the press platen with 2 hydraulic jacks. The filtrate collecting on the top of the press platen was sponged away frequently to prevent it from being absorbed again, while the filtrate passing through the base ran to drain. Figure 2.12 shows the press loaded, at half its maximum travel.

After pressing to the desired thickness, the hydraulic lifts were simultaneously released, and the releasing the mould assembly to its original position.

2.3.2.3 Demoulding and curing

The front cover was removed and the tray pulled on the double layered crate assembly (figure 2.13) to remove the top mesh and the moulding frame (figure 2.14). A third layer of assembled crates was placed on top of the panel with a polyester shade netting between the panel and crates for protecting the soft panel surface. The panel and HDPE base were firmly secured between the second and third layers of crates. While removing the bottom layer of crates, the assembly was turned upside down and partially loosened to replace the HDPE base with a polyester net. The panel was again secured between the two rigid crate assemblies and tilted vertically to prevent the panel from *sagging*.

The panel assembly was air cured for 28 days and rotated through 90^0 each day to prevent the material from sagging down to one end of the panel (Figure 2.15). The netting was removed after 2 days and the assembly was removed after the panel was fully cured (figure 2.16). Premature removal of the assembly, resulted in panel warp and deformation.

Figure 2.10. Mixing the raw materials

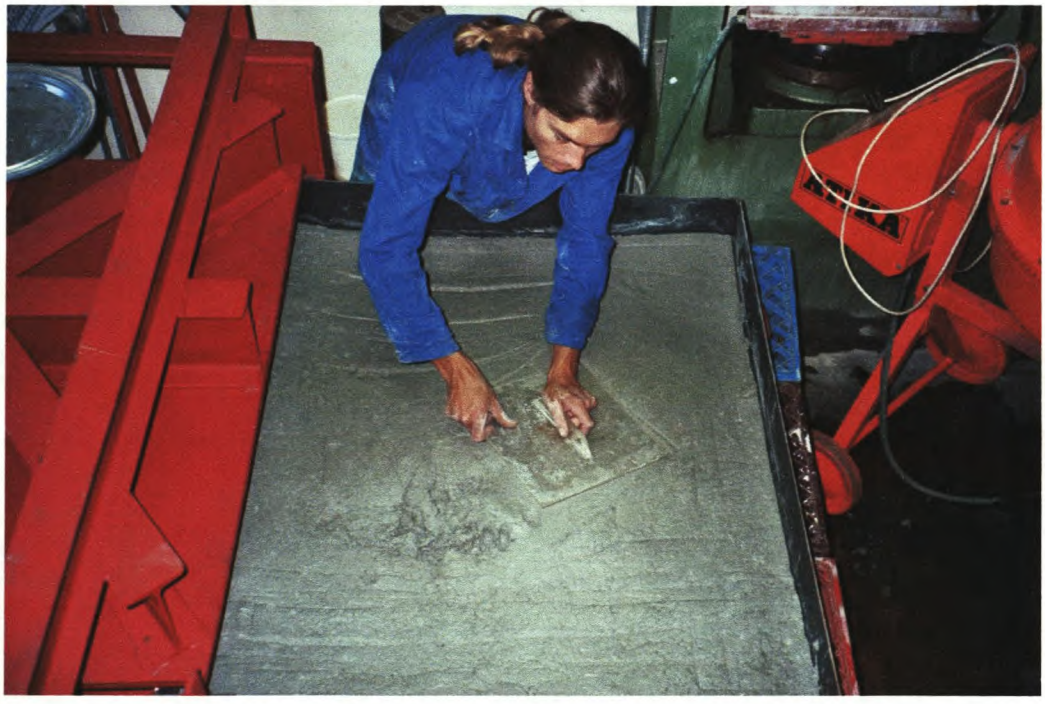

Figure 2.11. Forming the mat

Figure 2.12. Loaded press at half the maximum travel

Figure 2.13. Wet panel after pressing

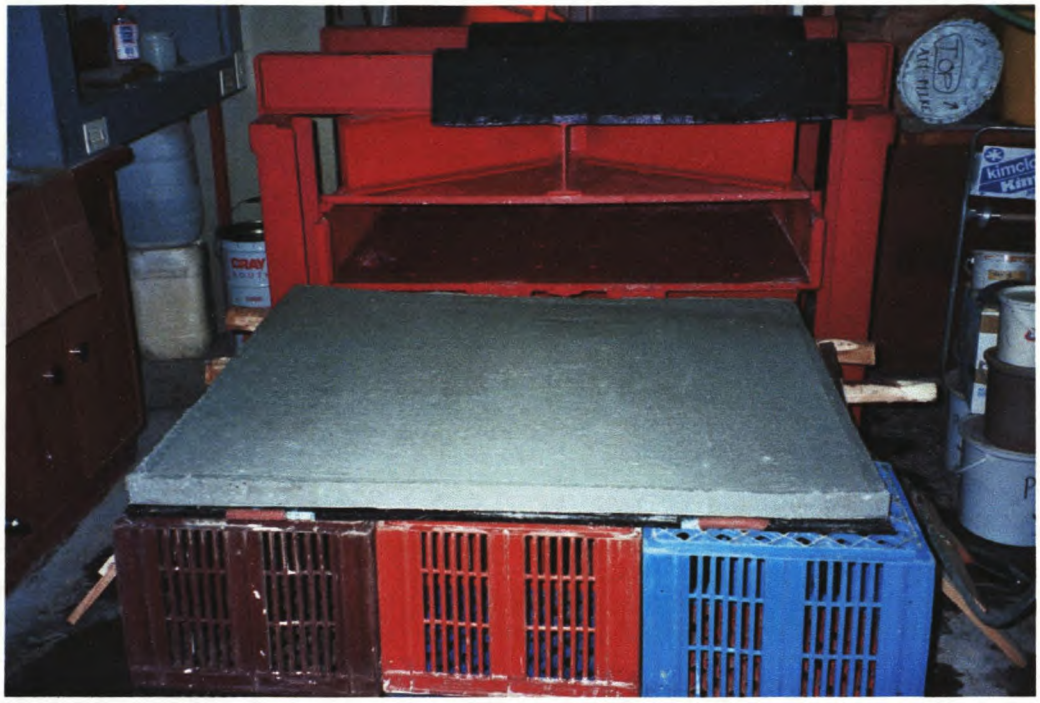

Figure 2.14. Demoulded panel after pressing

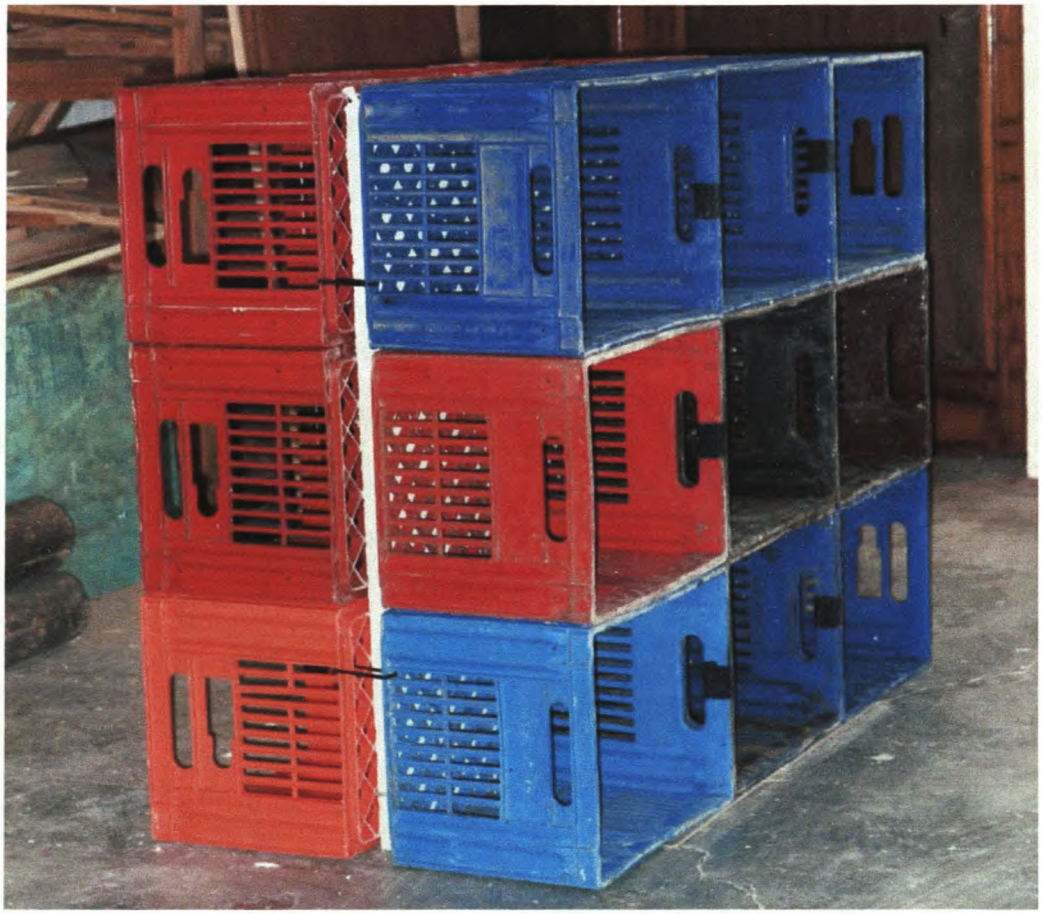

Figure 2.15. Curing of large panel

CHAPTER 3 - RESULTS AND DISCUSSIONS

3.1 Standard Deviro panel

3.1.1 Raw materials

Table 3.1 compares the moisture and ash content of the de-inking sludge collected during this study period, with the properties of the de-inking sludge from Crafford's study (1997).[1] The de-inking sludge was all collected from the same tissue mill. At the end of 1997, the mill invested in improvements that increased the consistency of the sludge. From the table, a decrease in moisture content was evident.

Table 3.1. Tissue mill de-inking sludge characterization

Study period	Moisture content		Ash Content	
	Average [%]	Std deviation	Average [%]	Std deviation
Previous study -J.Crafford ('95-'97)	70.33	0.58	49.67	10.97
1997 (present study)	71.33	2.28	48.74	4.01
1998 / 1999 (present study)	63.7	1.85	49.52	4.89

3.1.2 Manufacturing procedure

To achieve the target density for a fully cured panel, the slurry was pressed to a specified wet mass, as can be seen from figure 3.1. For an oven dry density range of 0,7-1,1 $g.cm^{-3}$, a wet mass of 1500 g to 2400 g after pressing needed to be achieved. This equated to a moisture content of 55-120% and a W/C ratio of 1,8 to 4. To achieve a panel density of 1,0 $g.cm^{-3}$, the ideal wet mass of 1700 g was achieved at a pressure of 4MPa.

The theoretical W/C ratio to achieve optimum panel strength is 0,4 (refer to section 1.2.5.3). In accordance to these findings, it was expected that the denser the panel, the stronger the panel would be, due to the lower W/C ratio.

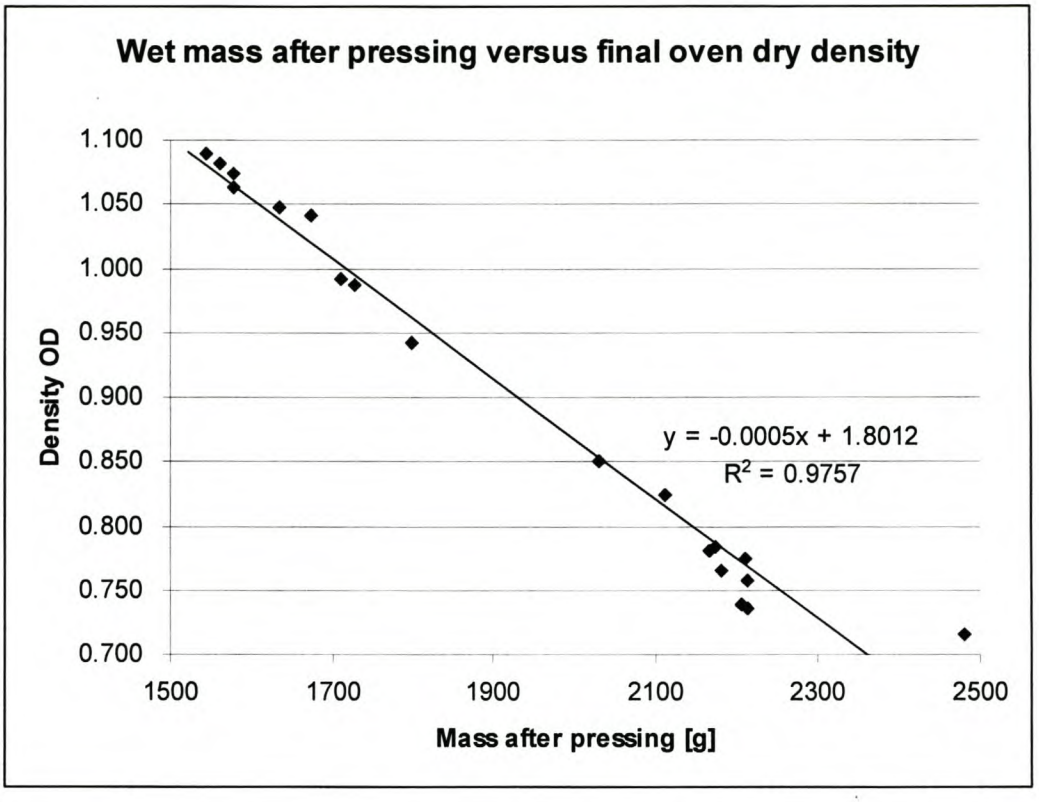

Figure 3.1. Relationship between the wet mass of the panel after pressing and the panel density after curing

3.1.3 Physical properties

3.1.3.1 Density and moisture characteristics

The density and moisture content of the standard panels produced in this study are summarised in Table 3.2.

Table 3.2. Density and moisture content of the standard panel

	Moisture content [%]	Density OD [g.cm^{-3}]
Average	4.22	0.873
Std Deviation	0.58	0.133
n (number of sections)	31	31

As the panel density (ρ_0) increased, the moisture content (mc) decreased. This strong linear correlation ($R^2 = 0.8$) is illustrated in figure 3.2. This may be explained in that a less dense panel will be more porous in structure. This should lead to more water being absorbed into the substructure, resulting in an increase ian moisture content.

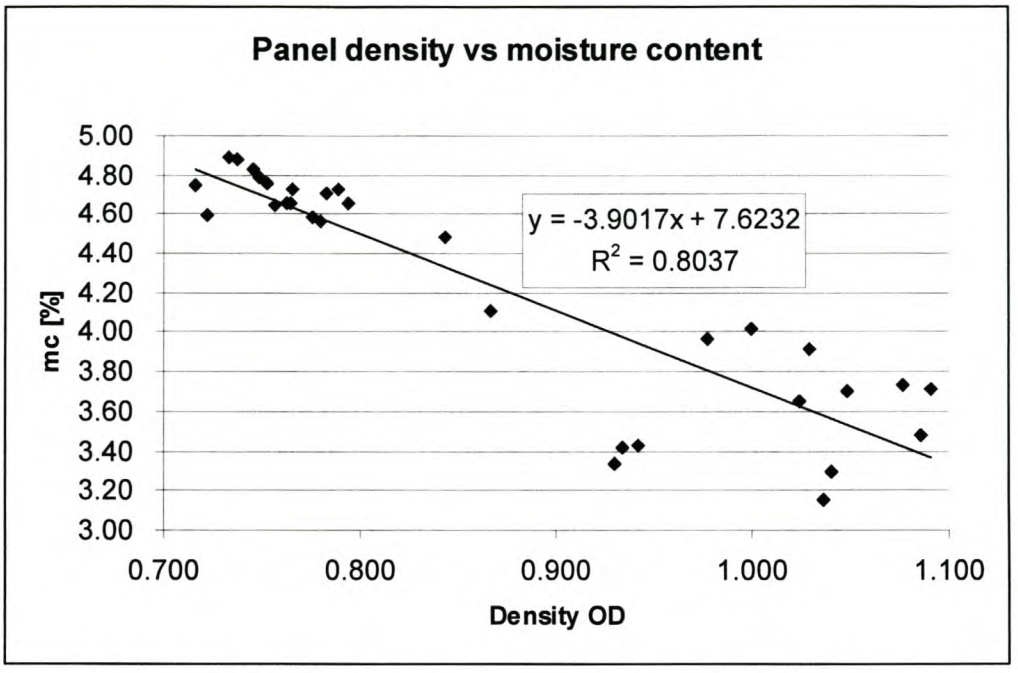

Figure 3.2. Correlation between panel density and moisture content

3.1.3.2 Static bending strength

The static bending strength of the standard panel is tabulated in table 3.3.

Table 3.3. Static bending strength of the standard panel

	MOR [MPa]	MOE [MPa]
Average	4.18	1550
Std Deviation	1.30	765
n (number of sections)	31	31

Crafford (1997) had identified that the static bending strength of the panel increased as the density of the panel increased. A comparison of bending strength, based on a strength to weight ratio had been proposed.[1] Hence the investigation into the effect of panel density was further analysed against the static bending strength. Static bending strength was measured against the oven dry density of each standard panel. A linear correlation was determined through regression analysis for the relation between MOR and MOE versus panel density, as shown in figure 3.3.

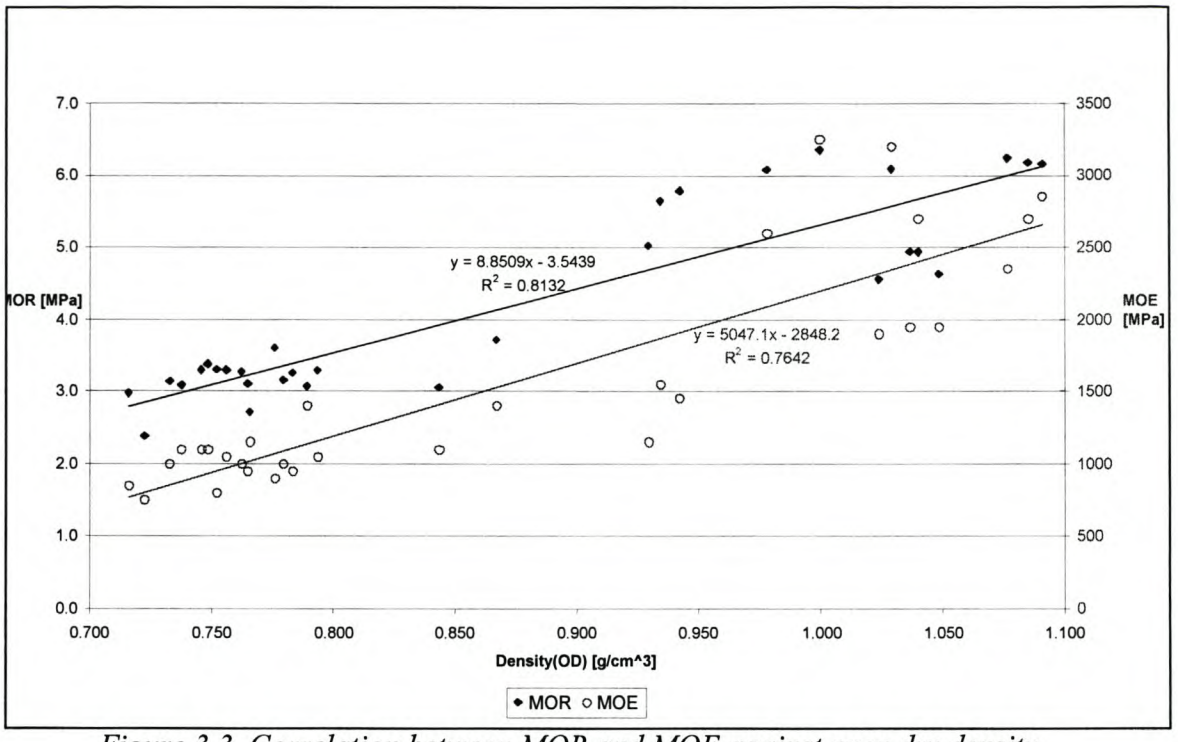

Figure 3.3. Correlation between MOR and MOE against oven dry density

The regression formulae are:

$$MOR = 8.85*\rho - 3.54, \qquad (R^2 = 0.81) \qquad (3.1)$$

$$\text{and } MOE = 5047*\rho - 2848, \qquad (R^2 = 0.76) \qquad (3.2)$$

MOR = Modulus of rupture, MPa

MOE = Modulus of elasticity, MPa

ρ = Oven dry density, $g.cm^{-3}$

Hence, for the standard panel at a density of 1 $g.cm^{-3}$, **MOR = 5.31** MPa and **MOE = 2200** MPa.

The Pearson's correlation coefficients of 81% and 76% were slightly lower than for commercial wood cement composites where the raw material is more homogenous, but very comparable to wood cement composites manufactured from construction waste wood.[49,87,90]

To compare enhanced sludge panels of various densities, these regression formulae were applied according to equations 3.3 and 3.4 to standardise all panels to a density of 1 $g.cm^{-3}$ (refer to appendix D for derivation of the formulae).

$$MOR' = 8.85(1- \rho) + MOR \qquad (3.3)$$

$$MOE' = 5047(1- \rho) + MOE \qquad (3.4)$$

MOR' = Modulus of rupture corrected to a density of 1g.cm^{-3}, MPa

MOE' = Modulus of elasticity corrected to a density of 1g.cm^{-3}, MPa

MOR = Modulus of rupture, MPa

MOE = Modulus of elasticity, MPa

ρ = Oven dry density, g.cm^{-3}

When comparing the flexural strength of the standard panel against other wood composites (refer to section 1.3.2.5), it was identified that the MOR of 3-6 MPa fell within the lower range of 5 to 20 MPa for wood- and wood-fibre composites, while the lower MOE of the Deviro panel indicates that it was less rigid. The regression formulae made it possible to compare the panel static bending properties against further panel enhancements.

To compare the various de-inking sludge batches, static bending results of standard panels were compared for 4 different sludge batches. The slight variability in strength properties can be seen in table 3.4, with a variance calculated for these properties to be less than10%.

Table 3.4. 28 day static bending strength determined for standard panels from various de-inking sludge batches

	Minimum [MPa]	Maximum [MPa]	COV [%]
MOR'	5.4	6.1	9.4
MOE'	1700	2500	9.8

3.1.3.3 Sorption characteristics

The water absorbed and thickness swelling, expressed as a percentage increase is charted against oven dry density in figure 3.4. It is evident that density strongly affects the water absorption characteristics of the sludge panel. An increase in panel density resulted in an increase in thickness swelling, and a decrease in water absorption.

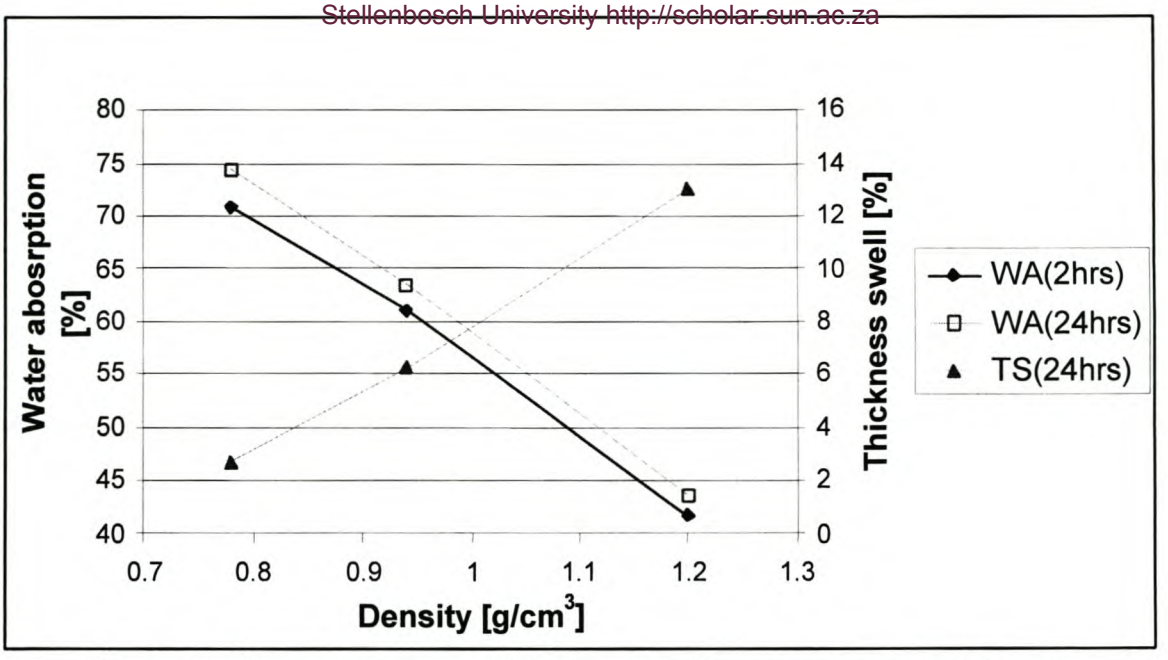

Figure 3.4. Water absorption and thickness swelling at various panel densities

Because of this great variation, the standard panels at three different densities (i.e. 0.78; 0.94 and 1.2 g.cm^3) were compared with commercially available wood- and wood-fibre products. The composites used for this comparison are tabulated below:

Table 3.5. Commercially available composites tested in sorption tests

Composite	**Density [g.cm^{-3}]**
Urea formaldehyde (UF) bonded particle board	0.56
Standard fibre board ("pressed-wood")	0.85
Tempered fibre board	0.95
Medium density fibre board (MDF)	0.64
Cement particle board	1.27
Cement fibre board	1.32
Paper overlaid gypsum board	0.76

In figure 3.5 it is evident, that although the water absorbed by the low density panel was 2nd greatest after UF-bonded particle board, the thickness swelling was only 2.7%. This was greater than the cement bonded products, which exhibited very little thickness swelling, but was lower than any of the organically bonded composites. When comparing the higher density panels, the thickness swelling was between that of MDF, presswood and UF-bonded particle board.

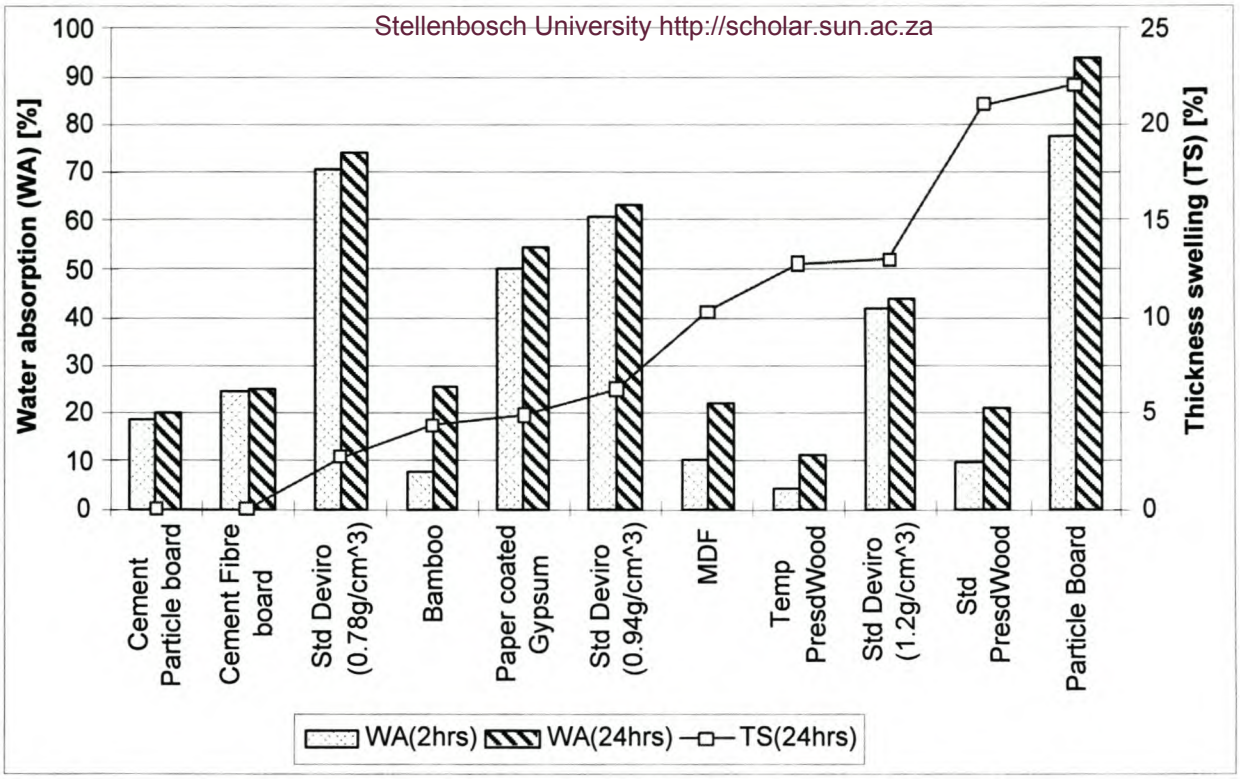

Figure 3.5. Sorption characteristics of commercially available wood and wood-fibre composites compared to the Deviro panel

Dimensional stability of the panel was identified by determining the water adsorption curves in the DECC as explained in section 2.2.3.7. The mA signals representing the linear expansion proved to be erratic at times, reducing the repeatability of the results. Hence tests were performed in triplicate, with a set being discarded should it differ from the other test results by more than 10%.

Figure 3.6 compares these sorption curves. Each curve represents results from two or three tests, depending on whether a data set had been discarded as erroneous. Most of the linear expansion of the samples occurred within the first 12 hours, while no or little further expansion was observed after 24 hours. The ranking of the dimensional stability determined in the DECC compared well with the ranking for the thickness swelling tests, whereby the standard Deviro panel compared favourably against the organically bound composites, but was less stable than the other inorganic composites.

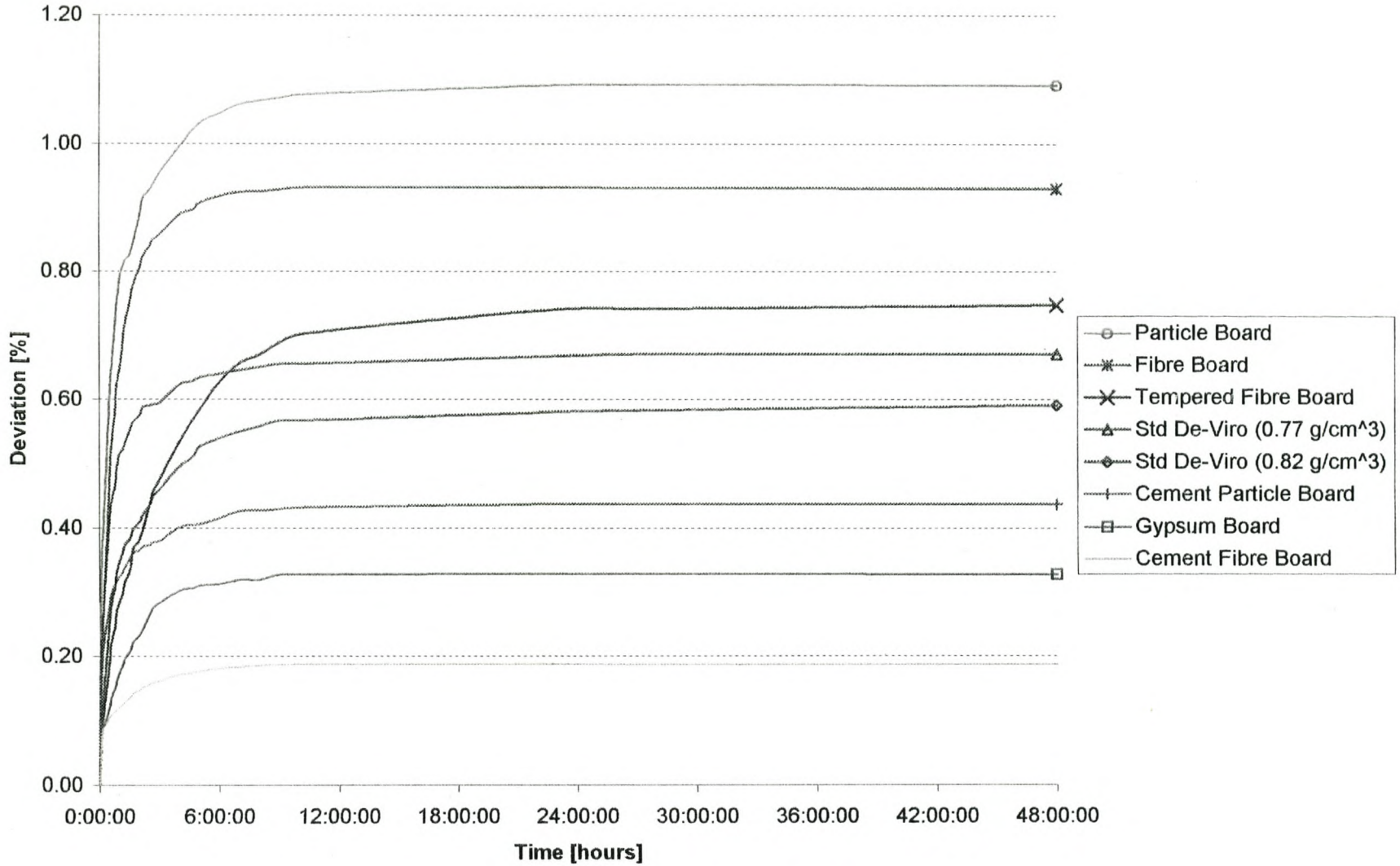

Figure 3.6 Linear expansion of wood & wood- fibre composites

3.1.3.4 Accelerated aging

Figures 3.7 and 3.8 show the test panels before and after the accelerated aging procedure. The following visual observations were concluded from the tests:

- The standard Deviro panel retained its initial form, with no visual degradation.
- The UF-bonded medium density fibre board (MDF) had lost internal bond strength after the first steam cycle resulting in springback.
- UF bonded particle board delaminated on the rough particle core and fine surface layer after the first steam stage in the first test cycle. It is believed that the resin hydrolysed, resulting in internal bond failure.[57]
- The coated layers of the paper overlaid gypsum board partially delaminated during the first cycle, and the panel fractured at the start of the second cycle.
- Gypsum board without paper overlay exhibited surface checks during the first cycle and disintegrated at the start of the second cycle.
- The tempered fibre board started to buckle slightly after 2 cycles of weathering. Edge checks appeared during the 1st steaming treatment of the 3rd weathering cycle, but did not propagate to initiate delamination or springback. The panel showed significant darkening.
- The cement fibre board retained its initial shape, with no visual degradation.

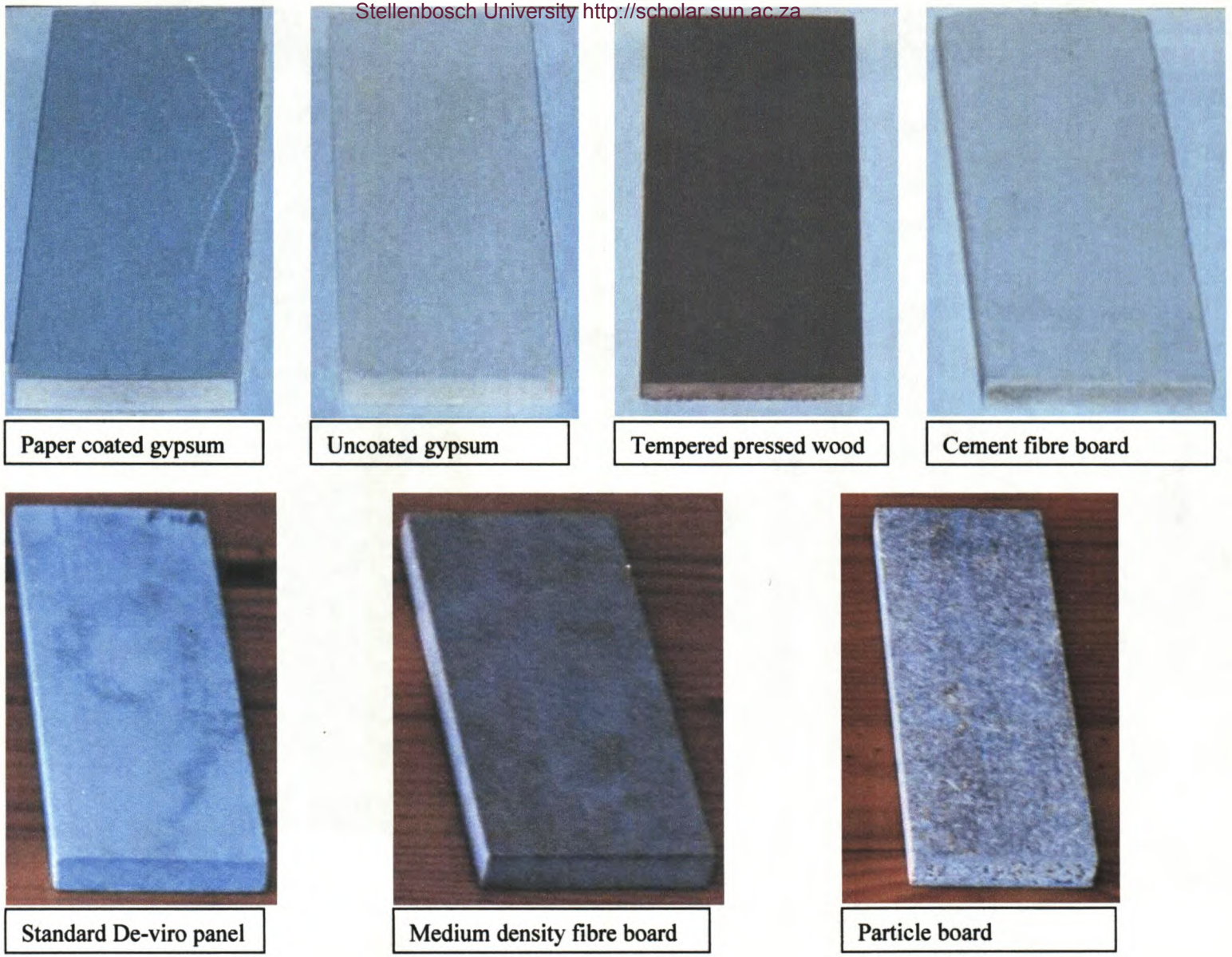

Figure 3.7. Test specimens before accelerated aging

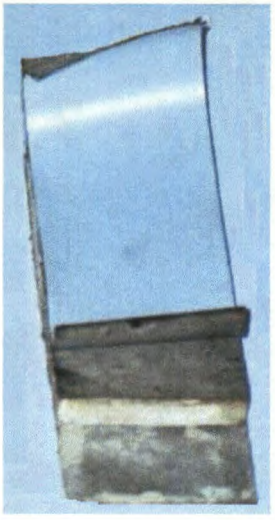

Paper coated gypsum

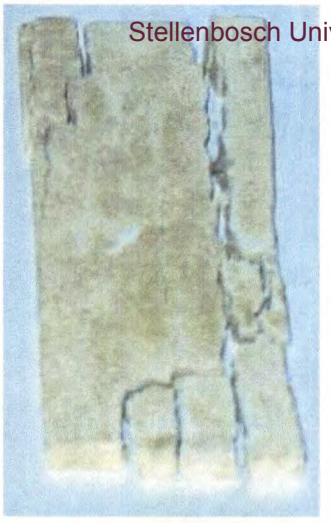

Uncoated gypsum

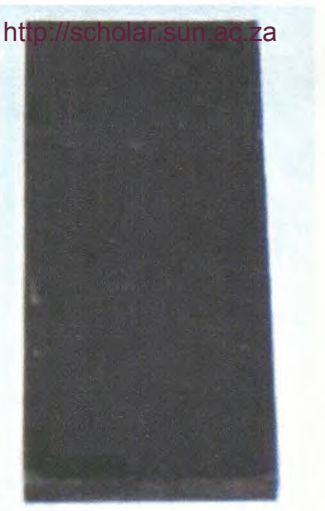

Tempered pressed wood

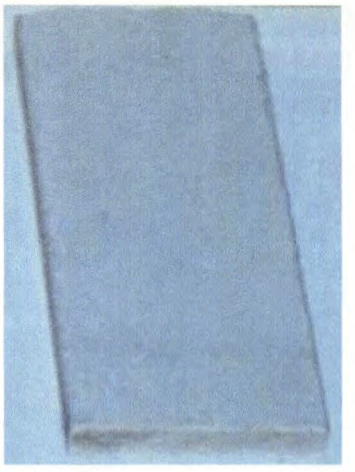

Cement fibre board

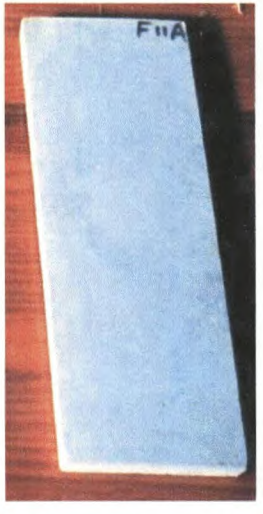

Standard De-viro panel

Medium density fibre board

Particle board

Figure 3.8 Test specimens after accelerated aging

Static bending tests were performed on the test samples that did not disintegrate or delaminate. Although the 1,0 g.cm^{-3} Deviro panel did not lose its shape during the accelerated ageing test, it lost more of its flexural strength than cement fibre board. This decrease in strength of cellulose fibre cement composites can be attributed largely to the polymer breakdown of cellulose components by the alkaline pore water.[59] Marikunte also established that an increase in cellulose fibre content, increased the drop in flexural strength, which agrees with these results.[60] The results are summarised in table 3.6, where n is the number of samples tested and COV the coefficient of variation. The oven dry density did not change after the accelerated aging of these test samples, given a 95% confidence coefficient.

Table 3.6. Retained static bending strength after accelerated aging treatment

	n	Density [g.cm^{-3}]	Retained MOR [%]		Retained MOE [%]	
			Average	COV	Average	COV
Standard Deviro panel	8	1.01	85.1	9%	80.9	11%
Cement fibre board	1	1.32	91.9	-	88.2	-
Tempered fibre board	1	0.95	48.7	-	47.2	-

3.2 Sludge Panel Enhancements

3.2.1 CSF-reacted sludge panel

The objective of the CSF is to enhance early hydration, hence improve panel strength at an early age. The oven dry density of the fully cured CSF panel and its wet mass after pressing are compared with the standard panel pressed at similar conditions in Table 3.7. A difference of 3.8% between the average oven dry densities was measured which considering the variability in the manufacturing process, was not significant.

Table 3.7. Wet mass after pressing and final density of CSF and standard sludge panel pressed at 4MPa

	Standard panel		CSF-reacted panel	
	Average	Std Dev.	Average	Std Dev.
Wet mass after pressing [g]	1595	50	1656	6.7
O.D. Density after cured [g/cm^3]	1.066	0.019	1.025	0.010

When CSF is added to cement, a denser cement matrix is formed,[78] but in the sludge panel, the cement served as a binder, hence a looser cement matrix was hypothesised.[1] From these results it was evident that because the cement served only as a binder, the formation of a significantly more dense matrix was inhibited. This disagreed with the densification experienced by Crafford (1997).[1] In Crafford's study, the panel was pressed to spacers to achieve a controlled thickness, and not to a pressure set point to afforded density comparisons. It may be that the dewatering mass was greater at the same wet panel thickness, which would result in a denser dry panel.

Figure 3.9 and 3.10 compare the modular strength properties of the CSF panel against the standard panel static bending strength values which have been normalised to a density of 1g/cm^3 (refer to section 3.1.3.2). Each curve represents the average flexural properties of 6 test panels. After 7 days of curing, the CSF-reacted panels showed a 12,0 % greater modulus of rupture and 11,6% greater modulus of elasticity. After 28 days of curing, there was no significant difference in MOR between the composites (given a 95% confidence coefficient). The 11.6% MOE gained from the addition of CSF after the first 7 days was held throughout the curing period.

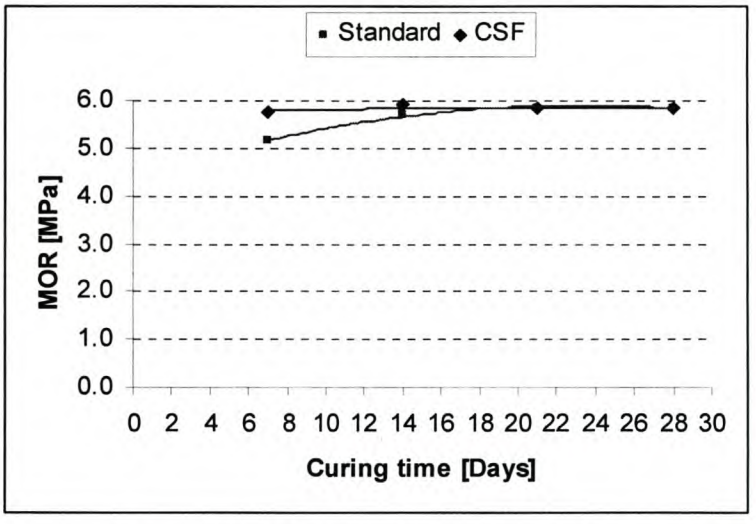

Figure 3.9. MOR for standard and CSF-reacted sludge panels after different curing times

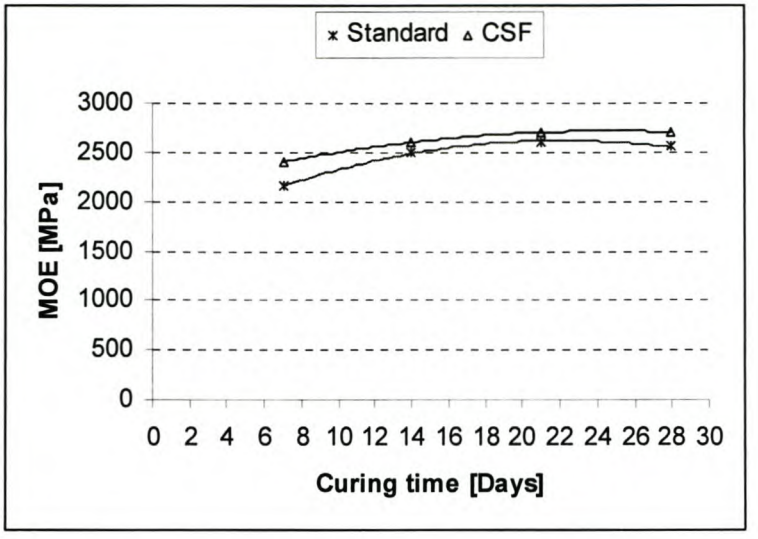

Figure 3.10. MOE for standard and CSF-reacted sludge panels after different curing times

Producing a lower density panel established the effect density had on the flexural strength. Properties of CSF-reacted panels produced of O.D. density 0.85 g/m^3 were measured against those of 1.025 g/cm^3 panels. The comparison made in table 3.8 shows a decrease in density resulted in a reduction in flexural strength. This was expected as the amount of hydration water available after pressing was higher for the lower density panel than for the higher density panel.

Table 3.8. Comparison between *low* and *high* density CSF-reacted panels

	n	Density [g/cm^3]	MOR [MPa]	MOE [MPa]
Low density	3	0.85	2.94	1200
High density	8	1.025	5.75	2650

3.2.2 Autoclaving

Boards autoclaved in both, the laboratory autoclave and the industrial autoclaves, exhibited a "burnt" appearance on the panel surface, as shown in figure 3.11.

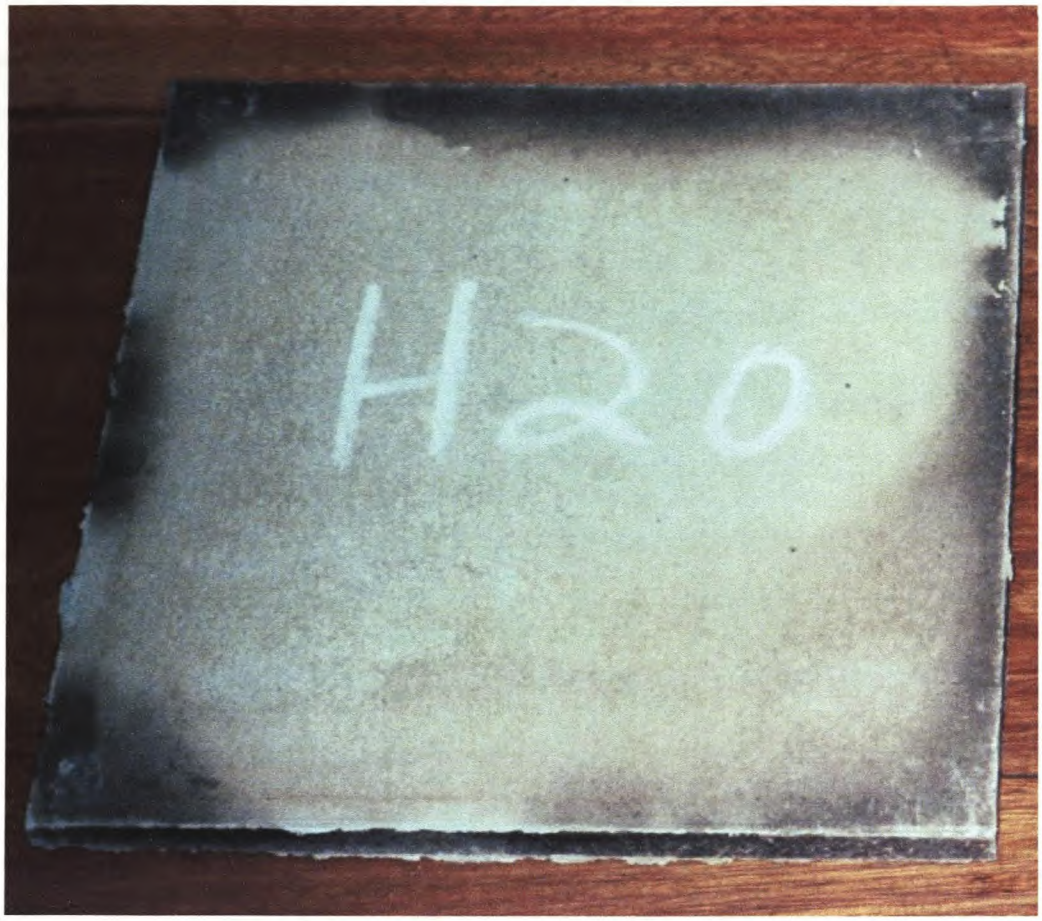

Figure 3.11. A typical autoclaved sludge panel

The panel moisture content ex-oven to autoclave proved to be the most critical parameter in the manufacturing process. For instance, a too high moisture content resulted in *blow-out* occurring and internal panel failure. It was established that when drying the panel below 100°C, this critical moisture content was 32%, and when drying above 100°C, it reduced to 28%. From the panels shown in figure 3.12, it can be seen that blow-out occurred at varying levels, but did not occur at the panel edges. This can be attributed to uneven drying in the laboratory oven, where the panel edges were dried more quickly, resulting in a wetter panel centre. It is expected that the pore water encapsulated by the fibre that reached boiling temperature, but was unable to evenly evaporate from the matrix caused the blow-out. Internal stresses were subsequently generated as this water rapidly expanded, resulting in internal bond failure. Table 3.9 summarises the physical properties of the autoclaved panels and figures 3.13 and 3.14 graphically display these results.

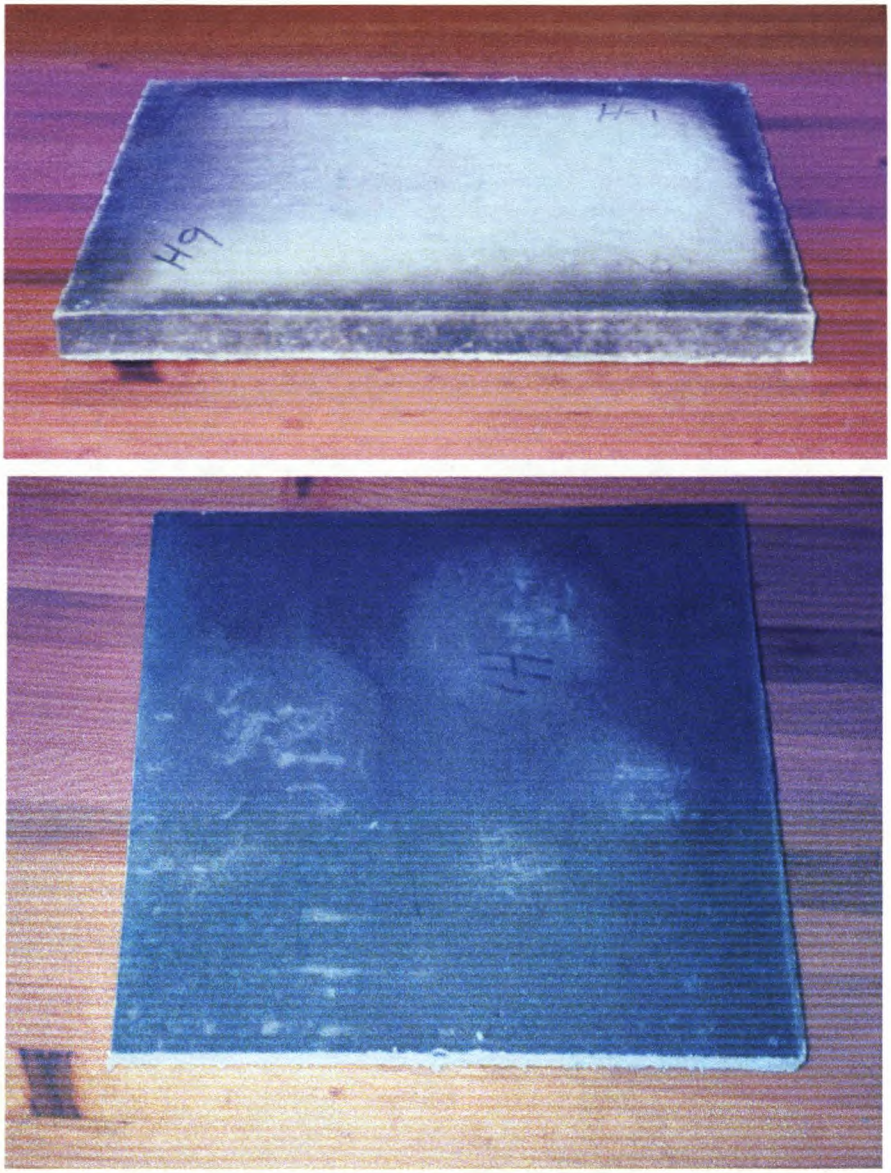

Figure 3.12. Autoclaved panels exhibiting blow-out

Table 3.9. Average physical properties of CSF-reacted autoclaved panels

Moisture content to autoclave [%]	Oven temperature [°C]							
	40		50		60-80		103	
	ρ	mc	ρ	mc	ρ	mc	ρ	mc
<15%	1.115	3.42	1.015	3.72	0.967	2.74	1.022	3.09
15-20%	1.161	4.47	0.906	4.44	1.063	4.48	0.980	2.83
20-25%	1.018	4.09	0.958	4.65	0.996	4.83	0.940	2.87
25-30%	0.963	3.94	0.986	4.53	1.016	4.02	0.937	2.84
>30%	0.934	4.74 / b_{32}	0.911	4.79 / b_{32}	0.895	4.15 / b_{32}	0.884	3.11 / b_{28}

with ρ = density of the fully cured panel, g/cm^3
mc = moisture content of fully cured panel, %
b_i = blow-out when the moisture content to autoclave is greater than i

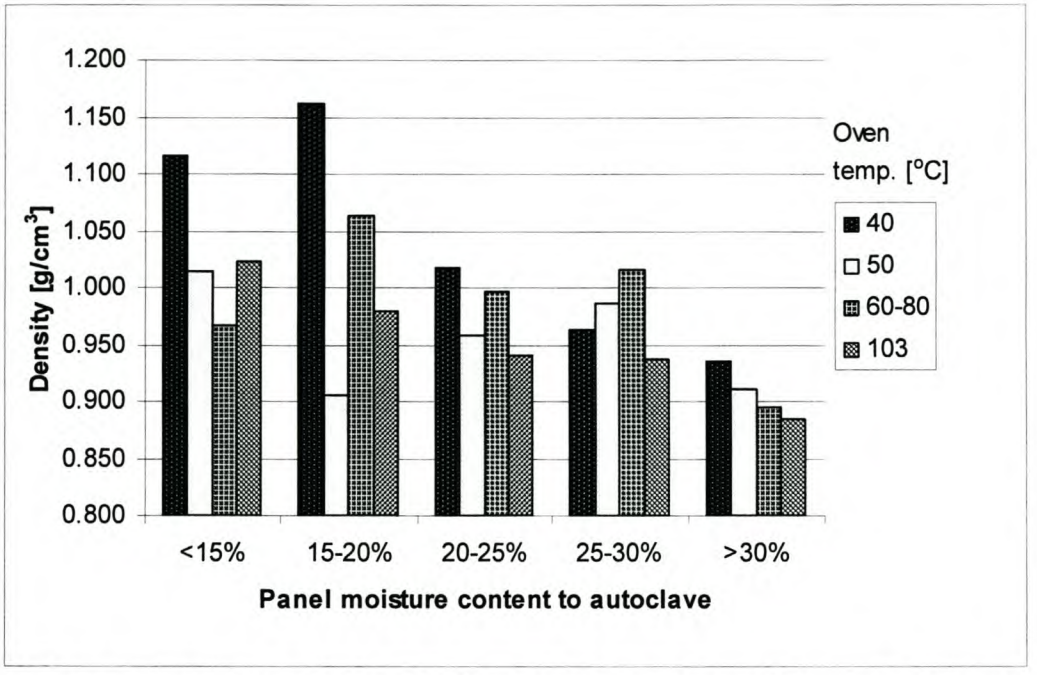

Figure 3.13. Oven dry density of the cured panel versus the oven temperature and the panel moisture content from the oven to the autoclave

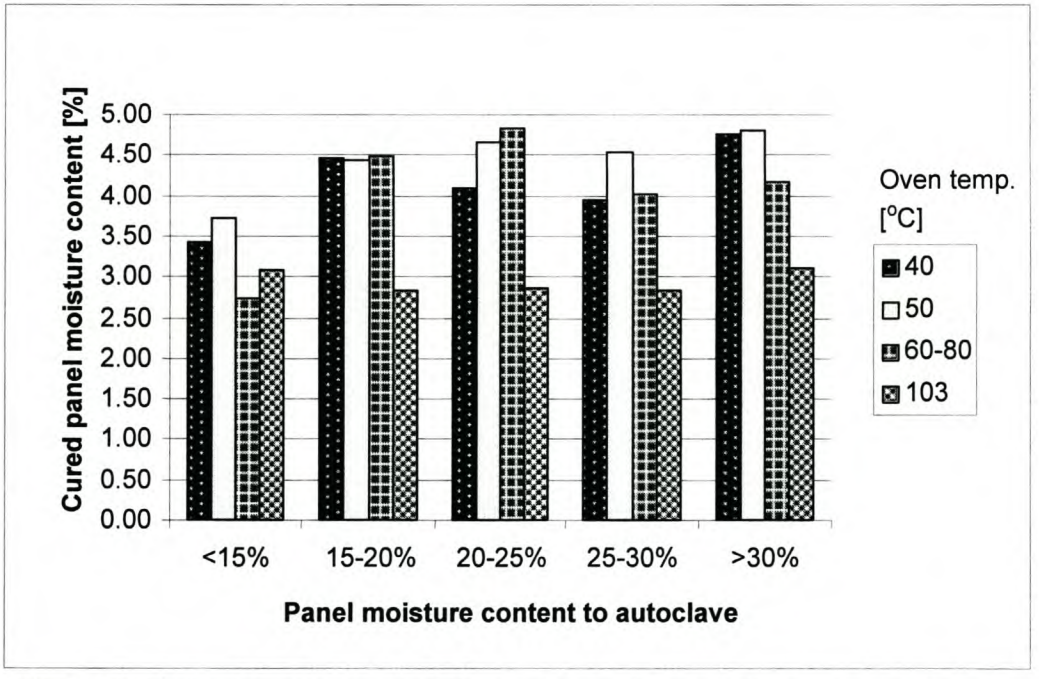

Figure 3.14. Moisture content of the cured panel versus the oven temperature and the panel moisture content from the oven to the autoclave

The panel density increased as the panel was dehydrated more slowly in the oven. A significant decrease in density was realised when the oven temperature exceeded

100°C. This would imply a more porous structure, when the panel was dehydrated above the boiling point of water. A decrease in the moisture content of the panel exiting the oven, also typically increased the panel density. This may be attributed to the difference in hydration reactions during the dehydration in the oven at temperatures well below that experienced in the autoclave (refer to phase diagram, section 1.2.5.4.3).

As with the panel oven dry density, the cured panel moisture content increased with a decrease in oven temperature. However, the panel moisture content decreased as the panel moisture content ex-oven to autoclave decreased. This may be explained in that the water that did not evaporate in the oven, would also not do so in the autoclave, where under the elevated temperature, more moisture was added through steam. Hence, more water may be contained within the pores, when the panel was wetter into the autoclave.

Static bending tests were performed on the CSF-reacted autoclaved panels that were dried at various oven temperatures and to various moisture contents. The results are tabulated, in table 3.10 and graphically represented in figure 3.15 and figure 3.16.

Table 3.10. Static bending strengths of CSF-reacted autoclaved panels

	Oven temperature [°C]							
Moisture content to autoclave [%]	40		50		60-80		103	
	MOR	MOE	MOR	MOE	MOR	MOE	MOR	MOE
<15%	6.07	2700	7.17	3250	4.15	1850	3.98	1000
15-20%	11.23	5850	6.38	3050	9.65	4050	3.20	800
20-25%	8.60	4250	7.01	3400	8.18	3900	3.02	600
25-30%	7.70	3950	6.57	3000	9.46	4050	3.29	750
>30%*	6.87	3300	7.09	2950	5.42	1250	3.07	750

* Includes panels with blow-out

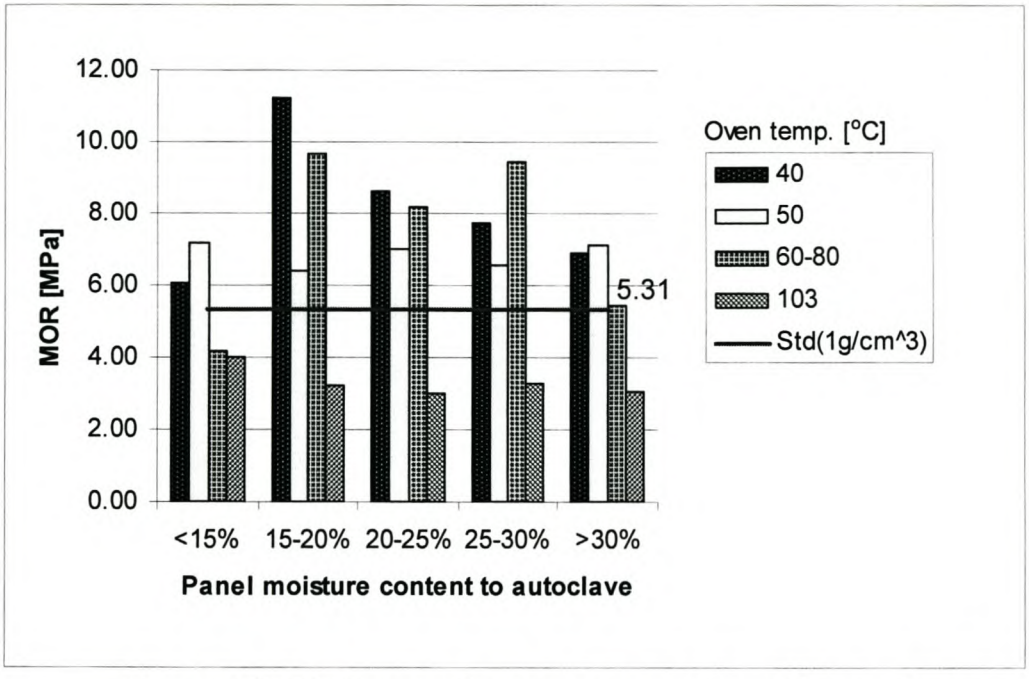

Figure 3.15. MOR versus the oven temperature and the panel moisture content from the oven to the autoclave

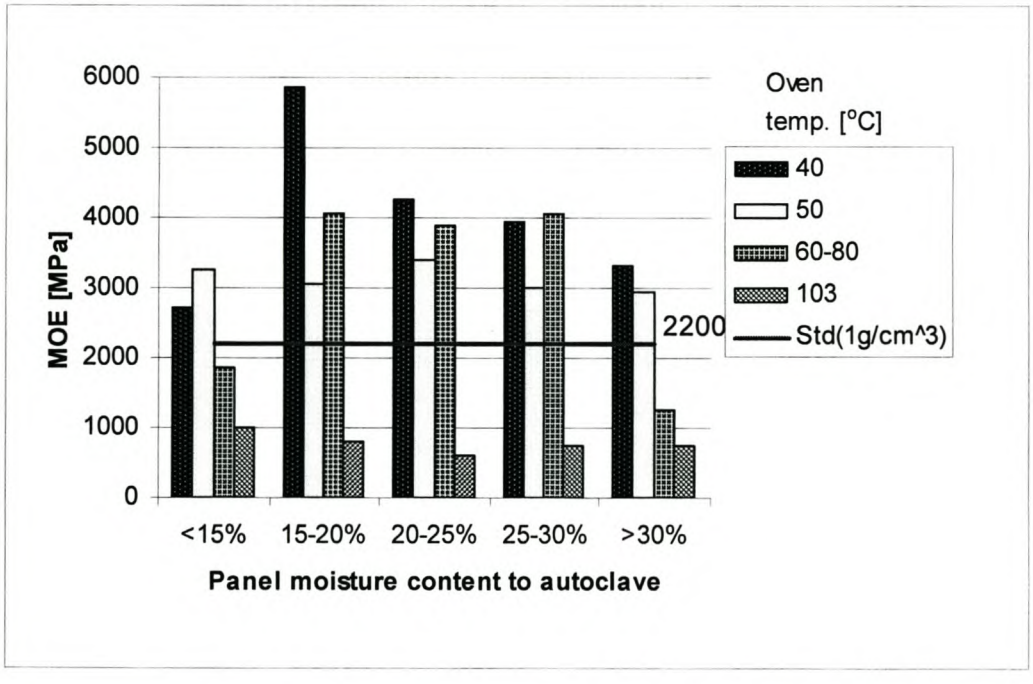

Figure 3.16. MOE versus the oven temperature and the panel moisture content from the oven to the autoclave

From these results, it can be seen that the strength properties of the panels dried at temperatures greater than 100°C was poor and inferior to the standard panel strength. The panels became brittle when dewatering occurred too rapidly, especially above the boiling point of water. Undesirable hydration reactions also resulted in this temperature range (refer to the phase diagram in section 1.2.5.4.3).

When the moisture content of the panel was too high (approximately 30%) ex-oven to autoclave, the panel exhibited blow-out (refer to table 3.9) and flexural strength was lost. But the flexural strength also decreased when the panel was dried below a moisture content of 15%. **Optimum strength development occurred when the moisture content ex-oven to autoclave was between 15 and 20%.**

Density played a more significant role in strength development with autoclaving the panels than with the standard panel. When comparing the strength results between the panels cured to the optimum moisture content (15-20%), the panels cured at 50°C exhibited poor flexural strength properties. This was due to the low density (density of 0.9 g/cm^3 vs. 1-1.1 g/cm^3) of these panels. This low density was achieved by pressing to a higher moisture content. The result was a longer curing time in the oven to achieve the desired moisture content into the autoclave. This increase in curing time reduced the strength properties (refer to section 1.2.5.4) and exaggerated the strength reduction at lower densities.

The greatest strength development was achieved at the lowest oven temperature of 40°C. The strength development was significant in comparison with the standard panel, where the MOR was almost double and the MOE 2½ times that of the standard panel.

3.2.3 Sodium silicate

The silicate treated panels were softer and had a smoother surface than the standard panel. An increase in sodium silicate addition was associated with panel *bulking*, with a concomitant reduction in density. Figure 3.17 shows the panel moisture content ex--press and final panel densities when pressed to 4 MPa, for various silicate addition levels. The composites dewatered less easily, as the silicate addition level increased.

This resulted in an increase in moisture content after pressing, and like the standard Deviro panel, resulted in a linear reduction in oven dry moisture content.

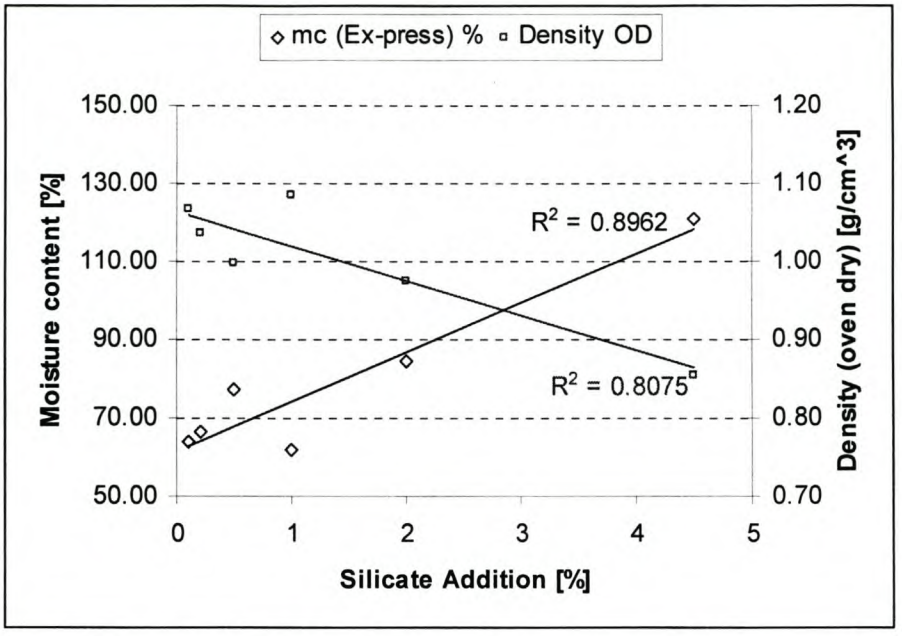

Figure 3.17. Sludge panels moisture content after pressing and density for various sodium silicate addition levels (press pressure set to 4 MPa)

The effect of sodium silicate addition on filtrate pH did not prove to be pronounced. Little or no increase in filtrate pH was identified at sodium silicate addition levels below 1%. The increase in pH at higher addition levels of 5% was approximately ½ a pH point, increasing the pH from an average of 11.8 to 12.3.

The bulking effect with the increase in silicate content complicated the comparison of the flexural properties, because at higher silicate addition levels, the density was reduced. Adjusting the MOR and MOE of the standard panel to the required density therefore made comparisons with the standard panel possible. This is achieved by using equations 3.3 and 3.4, as defined in section 3.1.3.2 for the standard panel. The physical properties are tabulated in table 3.11.

Table 3.11. Physical properties of silicate panels, at various silicate addition levels

Silicate addition [%]	Moisture content [%]	Density [g/cm^3]	MOR [MPa]	MOE [MPa]
0.1	3.66	1.066	6.788	2950
0.2	3.82	1.029	5.093	2750
0.5	4.04	0.997	5.790	2700
1	3.98	1.100	6.872	3200
2	4.32	0.985	6.544	2700
4.5	4.85	0.884	4.312	1500

The comparisons against the standard sludge panel (flexural strengths adjusted to the density of the silicate panel) are illustrated in figure 3.18 and figure 3.19. At a silicate addition level of 2%, an optimum increase of 26% in rupture strength and a 28% increase in elastic strength was realised. The strength improvements were not maintained at the higher silicate addition level of 4,5%. The cementitious products are believed to serve more as a binder than a matrix.[1] It is expected that the bulking effect of the high silicate addition sterically interferes with these bonds hence negatively impacting on the strength gain. Also it is expected that the fibres swell, which then after drying shrink leaving voids between the fibre and cement binder, more so than at no or low levels of sodium silicate addition.

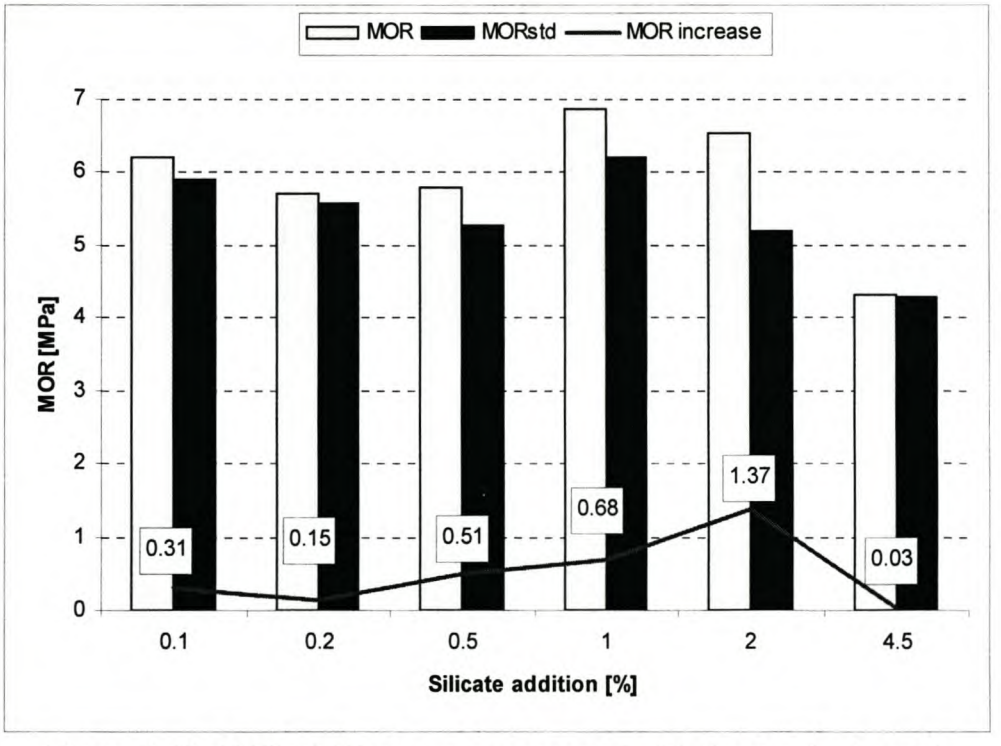

Figure 3.18. MOR of silicate panel compared with the standard panel

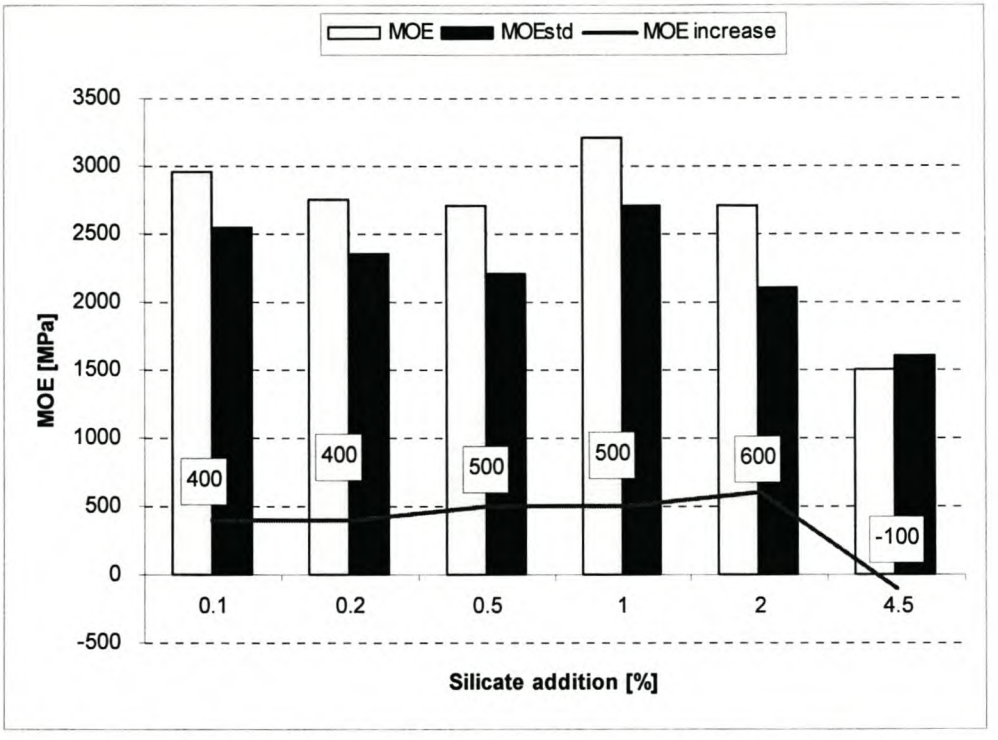

Figure 3.19. MOE of silicate panel compared with the standard panel

Due to the strength improvements achieved from autoclaving and the improvements when small quantities of sodium silicate were added, some silicate enhanced panels were autoclaved. The fly ash fraction was replaced with CSF and the silicate addition rate between 0.5 and 2%. The panel was dried at 50°C for 12 - 15 hours (which was the most practical drying cycle to follow), and autoclaved in the industrial autoclaves at 175°C for 10 hours.

The moisture content of these panels after drying was higher than the CSF-panel, when drying at the same temperature for the same length of time. The moisture content ranged from 20 to 40%. The panels with a moisture content above 30%, did not induce blow-out when autoclaved.

The silicate enhanced autoclaved panel, as seen in figure 3.20, did not exhibit the same burnt appearance as the autoclaved CSF-reacted panels. It is assumed that the fortification of the composite structure must be the contributing reason. The properties for these panels are tabulated in table 3.12 and compared with the standard panel in

figure 3.21. The static bending strength values for the standard panel is normalised to the density at each silicate addition level.

The panel density decreased as the silicate content increased. This may be attributed to the higher panel moisture content from the oven to the autoclave when the sodium silicate addition was increased. Panel *bulking* was also observed with an increase in silicate levels. An increase in flexural strength was achieved, when compared to the standard panel. When comparing these strength properties against the standard autoclaved panels, no additional strength developments were achieved.

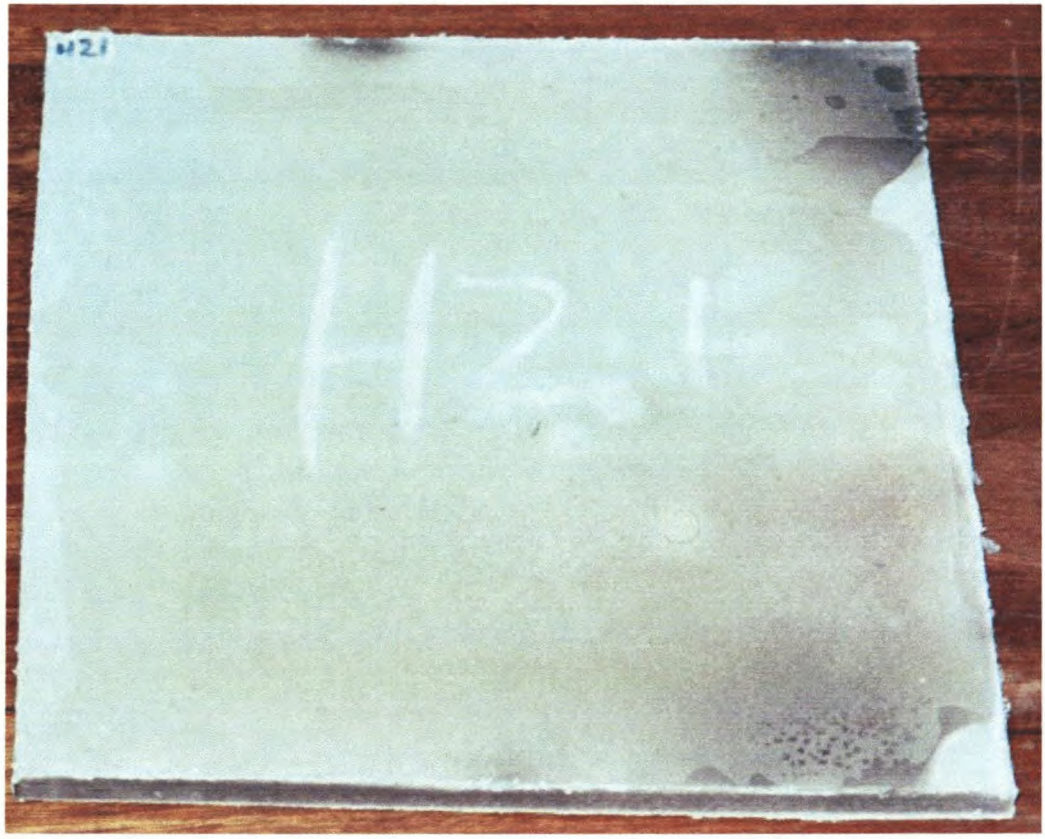

Figure 3.20. Silicate enhanced autoclaved panel

Table 3.12. Silicate enhanced autoclaved panels

Silicate [%]	Moisture content [%]	Density OD [g/cm^3]	MOR [MPa]	MOE [MPa]
0.5	3.88	0.997	8.27	4250
1.0	4.63	0.929	6.37	3000
1.8	4.09	0.865	5.33	2600

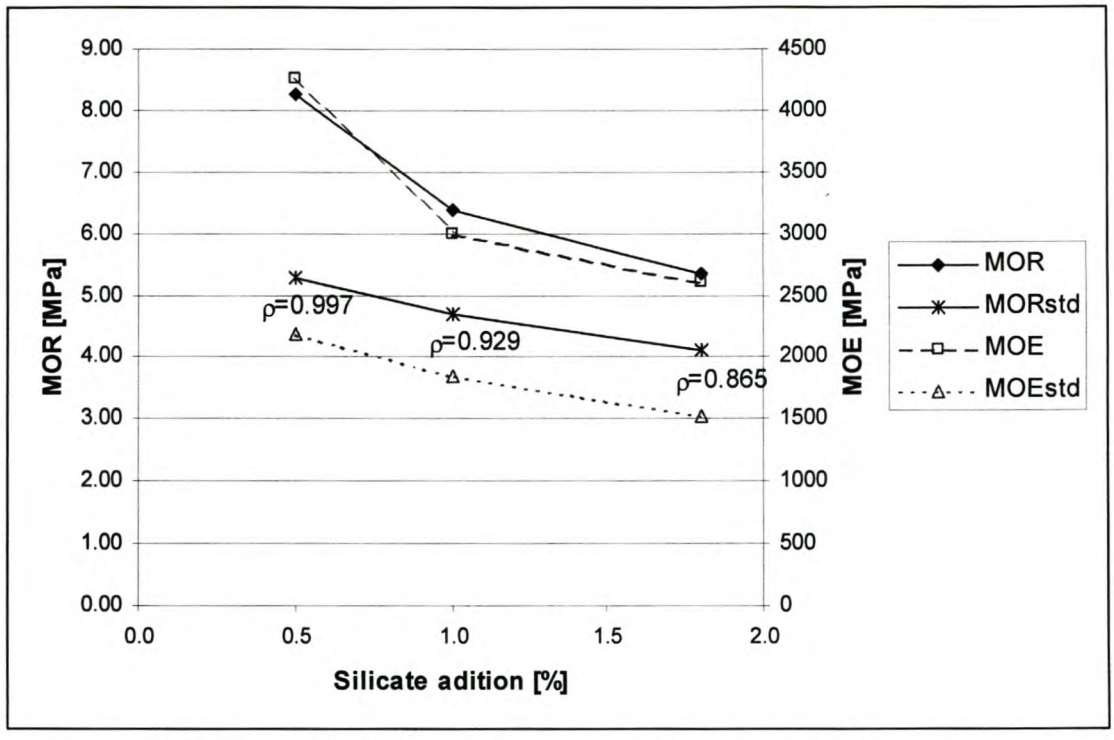

Figure 3.21. Flexural strength comparison between the silicate enhanced autoclaved panel and the standard panel

3.2.4 Perlite

Perlite addition, made the panel less workable. To keep the W/C ratio after pressing similar to that maintained for the standard Deviro panel, a limit to the Perlite addition level was established at a maximum of 5% by volume. Panel flow in the press was also a concern, and this maximum limit ensured homogeneous pressing of the panel.

The regression graph in figure 3.22, correlates the oven dry density and moisture content of the cured panel against Perlite addition (% by mass), when pressing to a pressure of 4 MPa. This graph illustrates, that the final panel density can empirically be predicted for a given pressure set point. For the pressure set at 4 MPa, the final oven dry density can be determined by equation 3.5:

$$\rho_4 = 0.048 \times P_{\%} + 1.1 \qquad (3.5)$$

with ρ_4 = density (oven dry) when pressing to 4 MPa, g/cm^3

$P_{\%}$ = Perlite fraction by mass, %

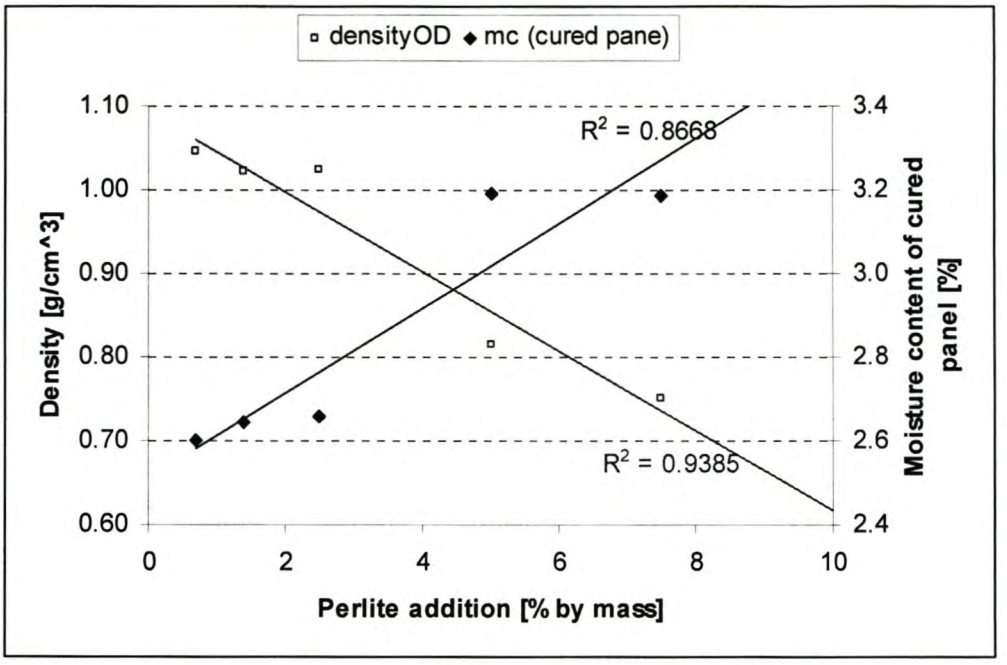

Figure 3.22. Sludge panels moisture content and density for various Perlite addition levels (press pressure set to 4 MPa)

The objective of adding Perlite was not to increase the maximum flexural strength, but instead to produce a panel of low density, which retained its strength properties. When evaluating figures 3.23 and 3.24, it can be seen that this objective is partially achieved. The graphs compare the static bending strength of the Perlite treated panels with the strength properties of the standard panel. The flexural strength values reported for the standard panel are adjusted to agree with the density of the Perlite panel. The loss in strength, when reducing the density, is not eliminated with the addition of Perlite, but is minimized.

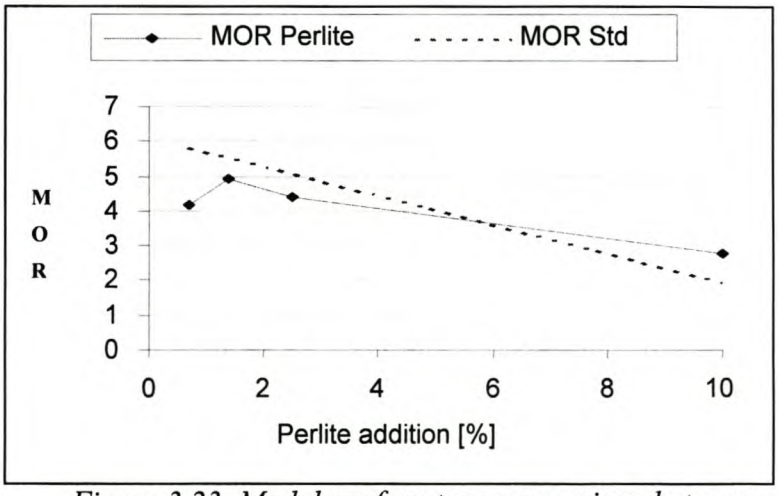

Figure 3.23. Modulus of rupture comparison between Perlite treated panels and the standard panel

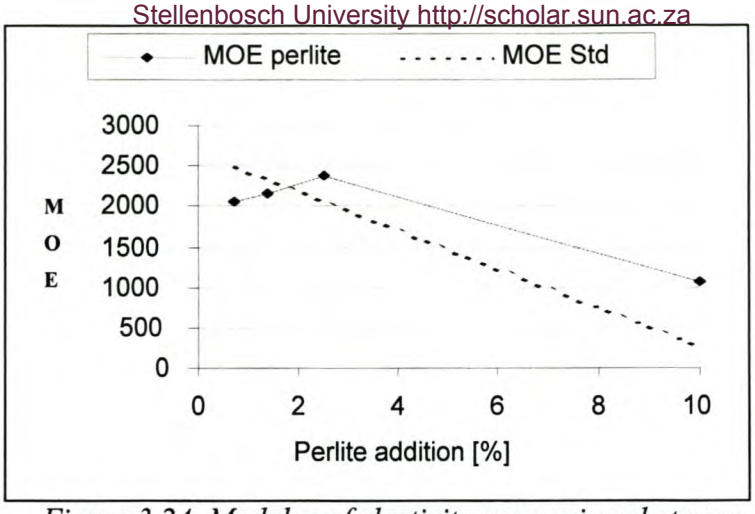

Figure 3.24. Modulus of elasticity comparison between Perlite treated panels and the standard panel

3.2.5 Surface coating

The white Portland cement based coating and the polypropylene containing coating applies easily to the standard panel surfaces. The textured surface finish exhibited signs of deflaking or chipping when subjected to a surface shear force, e.g. when sanding the panel. The surface was very abrasion resistant, and could not be sanded down on the regular sanders used to finish the surface of the standard panel.

Static bending tests were performed on the test panels coated with Stipplecrete® and Cemwash® so that a base line could be established for the accelerated aging tests. The results are tabulated below in table 3.13.

Table 3.13. Base-line static bending tests for surface coated panels

Treatment	Panel Density [g/cm^3]	MOR [MPa]	MOE [MPa]
Cemwash®	1.027	5.909	1700
Stipplecrete®	1.065	4.468	1250

These results are only in duplicate, hence no conclusions have been drawn to determine whether the two coatings react differently with the substrate, and hence affect the flexural strength of the panel.

3.2.6 Accelerated aging

Accelerated aging tests were performed for the following panel enhancements,:

- CSF-reacted panel
- Autoclaved panel – CSF as replacement of fly ash fraction in panel; drying is set at 40°C, and the panel is dried to a moisture content of 20-25%
- Silicate treated panel – at 2% and 4.5% sodium silicate addition
- Surface coated panel – Cemwash® and Stipplecrete® coatings

It is clear from figures 3.25 and 3.26 that, as with the standard panel, no visual panel degradation can be observed. The density of the CSF reacted panel increased by 25% due to the aging treatment. This may be due to the densifying of CSF products from second hydration during the water submersion and steam treatments. Static bending tests were performed after accelerated aging and compared to the panels that were not aged. These results are shown it table 3.14.

Table 3.14. Static bending strength of improved panels after accelerated aging

	Retained MOR [%]	Retained MOE [%]
Standard panel	85.10	80.90
CSF-reacted[1]	94.46	78.26
Autoclaved[2]	71.46	89.41
Standard + 2% sodium silicate	76.81	89.36
Standard + 4,5% sodium silicate	69.16	87.18
Surface coat (Cemwash®)	97.27	93.55

Notes:

1. The static bending strength values were not normalised for density, because aged and not-aged panels of equal densities were tested. Due to the 25% density increase of the CSF-reacted panel after the aging treatment, the retained flexural strength was artificially high. When normalising the flexural strength values, using equations 3.3 and 3.4 (section 3.1.3.2), the retained strength drops to 51.7% for MOR and 28.2% for MOE.
2. Oven temperature = 50°C, moisture content from oven to autoclave = 25%

The aged CSF reacted panel improved rupture retention but did not retain panel elasticity longer than the aged standard panel. The aged autoclave and silicate enhanced panels retained MOR to a lesser degree than the standard panel, but remained more rigid. Only the surface coating treatment significantly improved the aging characteristics of the Deviro panel.

Autoclaved (oven=40°C; mc to autoclave=20%)

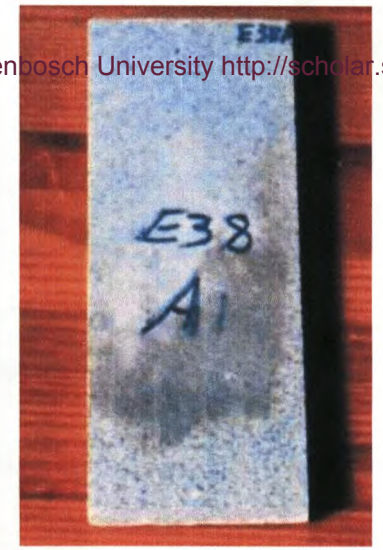

Autoclaved (oven=50°C; mc to autoclave=25%)

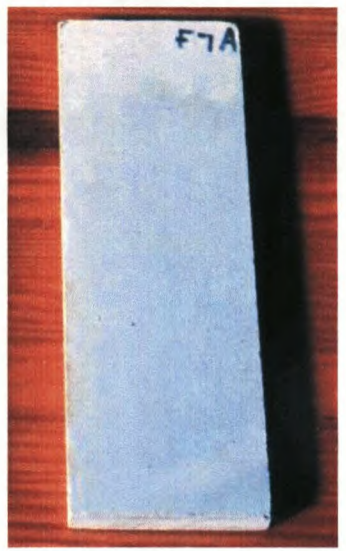

4,5% sodium silicate added

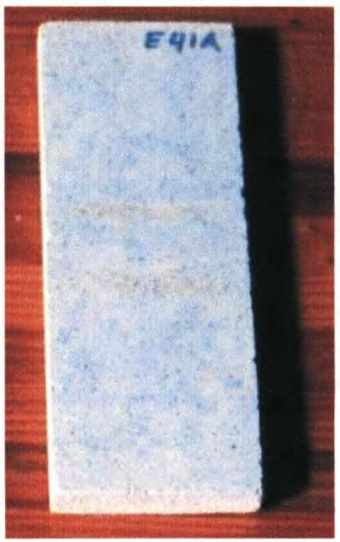

CSF-enhanced

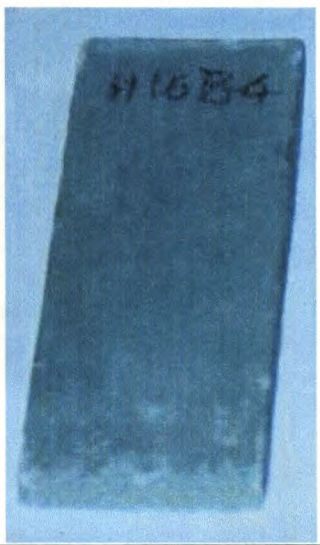

Std panel coated with Cemwash®

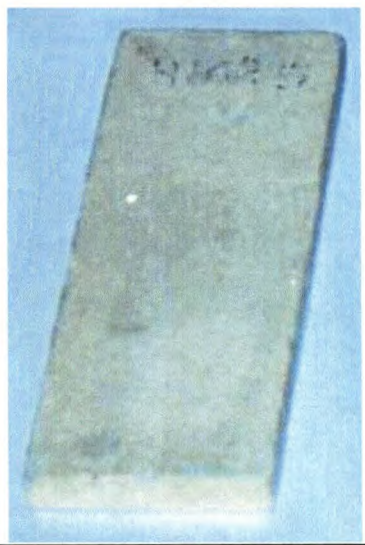

Std panel coated with Stipplecrete®

Figure 3.25. Enhanced sludge panels – before accelerated aging

Autoclaved (oven=40°C; mc to autoclave=20%)

Autoclaved (oven=50°C; mc to autoclave=25%)

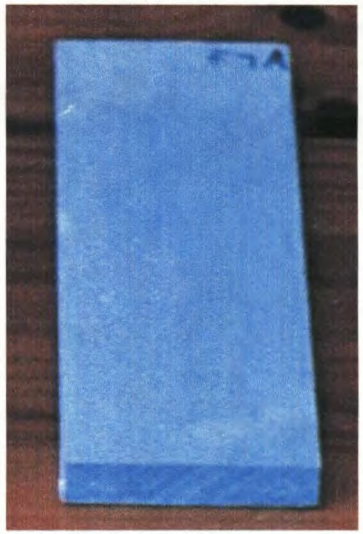

4,5% sodium silicate added

CSF-enhanced

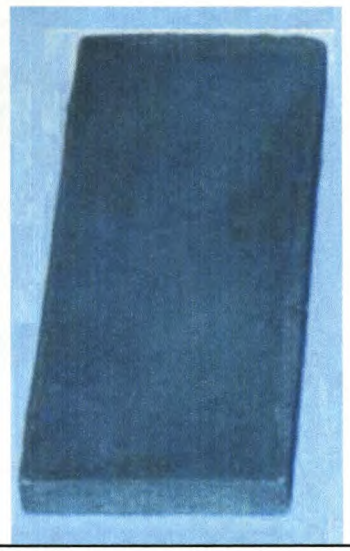

Std panel coated with Cemwash®

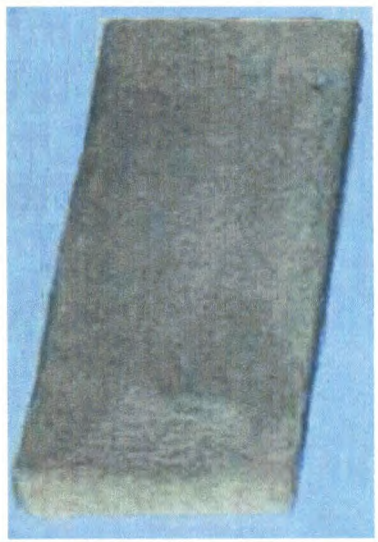

Std panel coated with Stipplecrete®

Figure 3.26. Enhanced sludge panels – after accelerated aging

3.2.7 Dimensional stability

The objective of the panel enhancements was not only to improve the flexural strength properties, but also to improve the sorption characteristics of the standard Deviro panel. It was identified that the standard panel was less dimensionally stable than other wood / wood-fibre inorganic composites. Figure 3.27 compares the water absorption and thickness swelling rates of the enhanced panels with the standard panel. The autoclave and surface coating treatments reduced the thickness swelling and water absorption properties, while silicate addition and CSF reacted panels contributed towards lower dimensional stability.

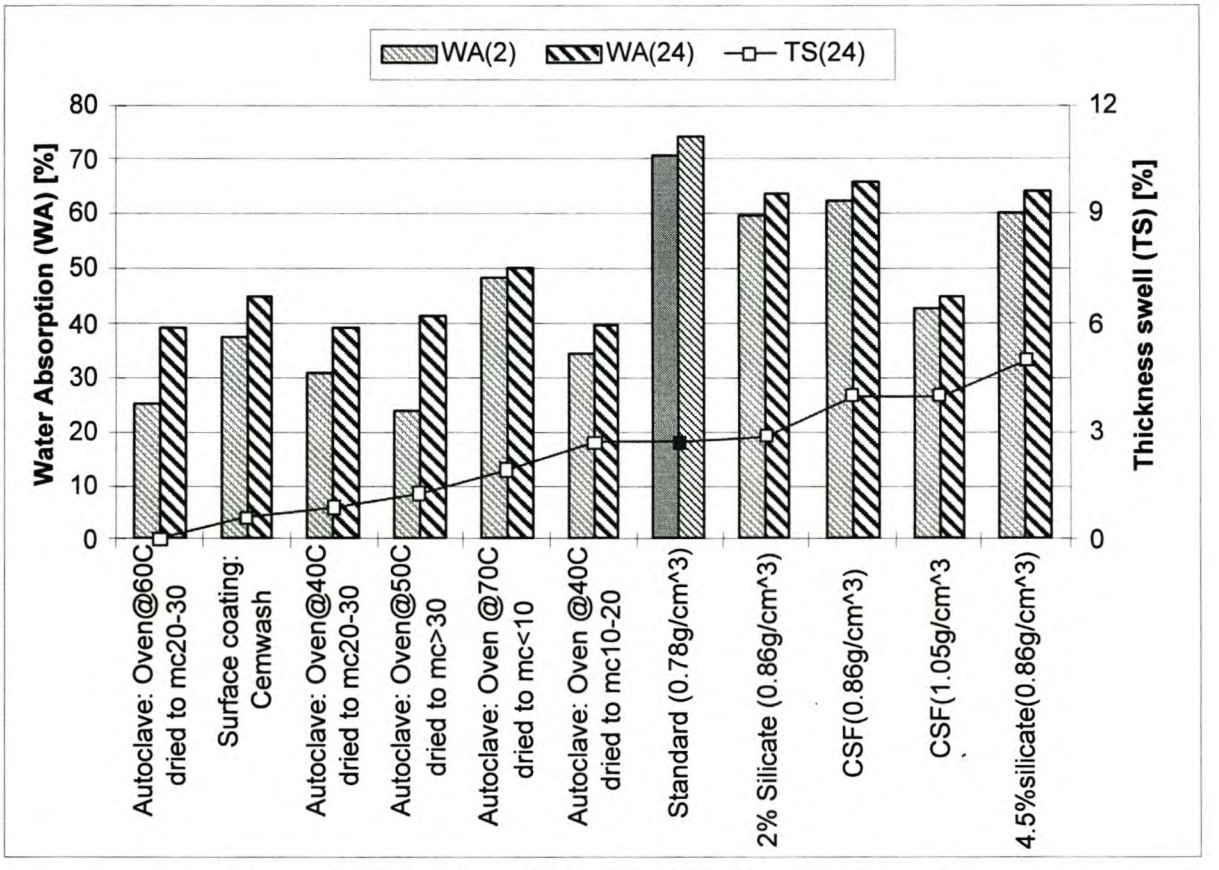

Figure 3.27. Sorption characteristics of improved panels and the standard Deviro panel

3.3 Manufacturing optimisation

3.3.1 Introduction

To further the commercial viability of the panel, enhancements that optimise the process are required. One such improvement is to recycle the process filtrate to reduce effluent disposal and fresh water consumption. Also, it is costly to store the de-inking sludge in a cold storage facility. Hence, it must be determined what the effect sludge aging has on the panel strength and how to preserve the sludge. Another improvement is embossing the panel to broaden the potential market.

3.3.2 Recycling the filtrate

Sankey diagrams are given in figure 3.28 and 3.29 to depict the water balance for a standard 0.75 g/cm^3 and 1.0 g/cm^3 panel. Should all the filtrate be recycled, the 0.75 g/cm^3 density panel requires a further 180 ml of fresh water, while the 1.0 g/cm^3 density panel will produce 300 ml of effluent when manufacturing one panel.

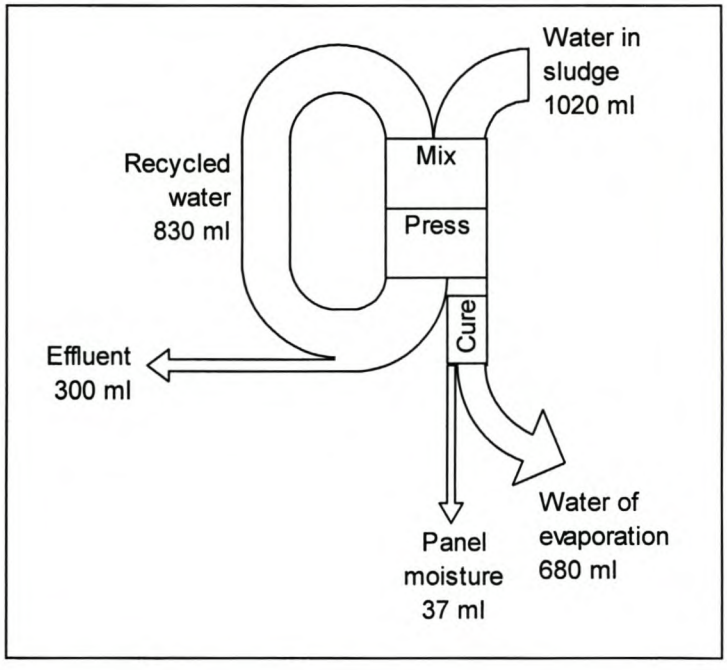

Figure 3.28. Sankey diagram for the water balance of the 1.0 g/cm^3 standard panel

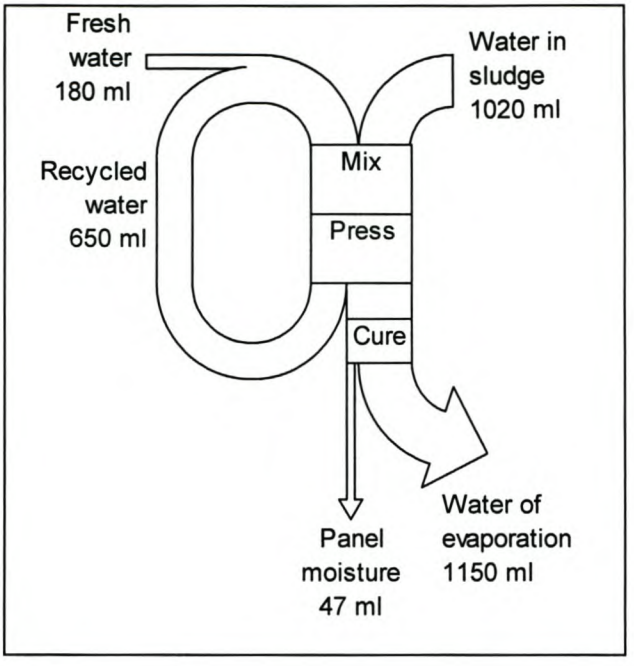

Figure 3.29. Sankey diagram for the water balance of the 0.75 g/cm^3 standard panel

During the laboratory preparation all the filtrate could not be collected. Hence, a net intake of water was required. To simulate the water recycling, standard panels were produced with fresh water, while the filtrates were collected in a container. This filtrate was used as dilution water called *once recycled dilution water* for the next set of panels. The filtrate of these panels was once again collected in another container and used as *twice recycled dilution water*.

The filtrates are evaluated in table 3.15. A sample of the cloudy filtrate was diluted to 10% to measure turbidity with a spectrophotometer. The remainder of the filtrate was filtered through a Whatmans 40 filter paper to measure pH and chemical oxygen demand (COD). Turbidity and COD load increased sharply after the first pressing emphasizing the importance of recycling the filtrate, rather than sending it to the sewer.

Table 3.15. Standard panel filtrate analysis

Water	pH	Turbidity [NTU]	COD [g/l]
Fresh water	8.35 – 9.42	0	78.8
Once recycled	11.70 – 12.03	109	3299
Twice recycled	11.70 – 12.08	146	3728
Third cycle	11.85 – 12.10	149	3805

Flexural strength evaluations were performed on these panels and are compared with the characteristics of the standard panel in table 3.16. Strength values are normalised to a panel density of 1 g/cm^3. Given a 95% confidence interval, no significant difference exists between these strength values. Hence, closing the water loop had no detrimental effect on panel strength properties.

Table 3.16. Flexural strength when using the recycled filtrate for dilution water

Dilution water	MOR @ ρ = 1g/cm^3 [MPa]		MOE @ ρ = 1g/cm^3 [MPa]	
	Average	Std deviation	Average	Std deviation
Fresh water	5.31	0.499	2200	216
Once recycled	5.35	0.438	2200	157
Twice recycled	5.21	0.497	2200	233

3.3.4 Sludge preservation with sodium silicate

Bacteriological decay occurred in relatively fresh sludge, and even though refrigeration reduced this decay, it was not completely eliminated.[1] Cold storage for shorter periods sufficiently limited this decay for the laboratory applications, but is not commercially feasible. Because sodium silicate coats the fibres, it was used to identify whether it would serve as a preservative. This, coupled with the strength improvements achieved with the addition of sodium silicate would support the justification for its addition.

Sludge samples, sufficient for one panel each, were weighed off from a fresh batch of de-inking sludge. Sodium silicate was mixed with the samples in the following quantities: 0%; 0.1%; 0.2%; 0.5%; 1.0%; 2.0% and 4.5%. The mixtures were sealed in airtight polyethylene bags and allowed to age. Panels were produced after 0; 1; 7; 21; 42 and 84 days to determine the degree of sludge aging at the different silicate

addition rates. Table 3.17 compares the flexural strength. The standard panel produced with fresh sludge and no (0%) silicate addition served as the standard and was given a strength of 100%, with all other results reported relative to this standard.

Table 3.17. Addition of sodium silicate to prevent sludge decay

	Sludge age [days]	Silicate addition [%]						
		0	0.1	0.2	0.5	1	2	4.5
MOR [% of std]	0	100	137.9	103.4	117.6	**139.6**	**132.9**	87.6
	1	80.1	129.4	98.6	128.3	141.6	155.0	73.5
	7	74.0	91.4	104.0	133.3	118.6	156.8	66.4
	21	102.8	69.4	101.3	106.3	99.2	134.8	69.8
	42	87.8	85.7	60.3	95.5	101.5	130.0	76.8
	84	44.6	50.9	82.0	67.2	**110.8**	**119.8**	65.0
MOE [% of std]	0	100	111.3	103.8	101.9	**120.8**	**129.9**	56.6
	1	81.1	101.9	98.1	135.8	117.0	130.2	50.9
	7	60.4	69.8	77.4	117.0	105.7	118.9	49.1
	21	77.4	67.9	84.9	90.6	96.2	117.0	60.4
	42	83.0	67.9	47.2	86.8	98.1	117.0	66.0
	84	52.8	39.6	77.4	62.3	**99.2**	**109.4**	60.4

At the optimum silicate addition levels of 1-2% the gain in flexural strength was not maintained. However the 1-2% silicate enhanced panels that were produced with sludge aged for 84 days (12 weeks), still exhibited greater strength than the standard panel manufactured with fresh sludge.

3.3.5 Embossing

The ease with which the slurry moulds, makes it suitable for relief embossing.[1] Embossed panels were produced by placing a polyurethane mould on top of the mat in the moulding frame during the pressing stage. A complex image was embossed to ensure that small imperfections were more easily identified. The standard panel was unable to mould the finer detail as seen in figure 3.30.

In an effort to reduce the density of such a panel, up to 7.5% Perlite was added. With the decrease in density, a concomitant improvement in the profile was recorded (refer to figure 3.31).

Figure 3.30. Embossed standard panel

Figure3.31. Embossed Perlite panel

3.4 Pilot Scale-up

3.4.1 Manufacturing process

The manufacturing time for a $1m^2$ panel is approximately 3 hours and labour intensive with two personnel required. Two fully cured standard panels are shown in figure 3.32.

The same high shear forces were not achieved in the industrial cement mixer as with the laboratory kneader resulting in the lumping of the raw materials not breaking up easily in the mixer.

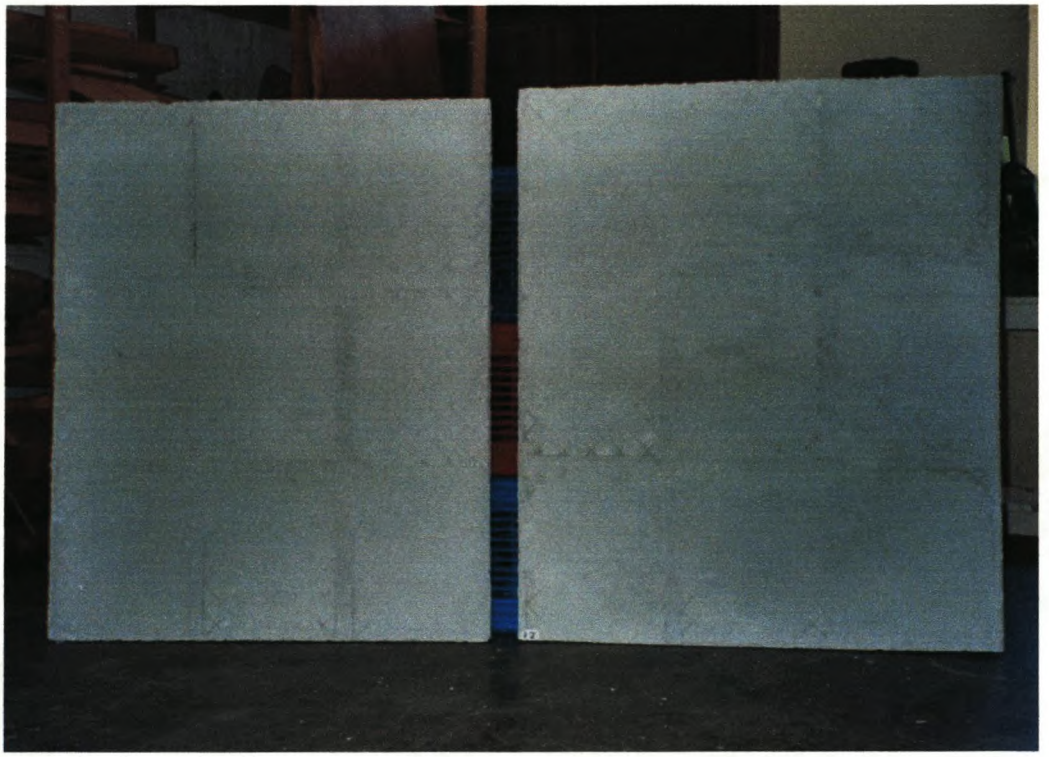

Figure 3.32. Fully cured large panels

The following panels were manufactured:

Low density ($\rho \approx 0.75$ g/cm^3) standard large panels

55% sludge; 30% cement; 15% fly ash

Silicate enhanced large panels ($\rho \approx 0.9$ g/cm^3)

54% sludge + 2% sodium silicate; 30% cement; 14% fly ash

54% sludge + 2% sodium silicate; 30% cement; 14% CSF

Perlite large panels ($\rho \approx 0.75$ g/cm^3)

54% sludge + 2% sodium silicate; 30% cement; 10% fly ash; 4% perlite

54% sludge + 2% sodium silicate; 30% cement; 10% CSF; 4% perlite

The above panel nomenclature will be used for comparison of results.

The addition of sodium silicate to the sludge, prior to mixing, made the slurry more malleable, causing less lumps to form. Therefore sodium silicate was used in all the enhanced large panels. The replacement of fly ash with perlite by mass, resulted in a higher panel volume and greater stresses during pressing. The manufacture of the first perlite panel was stopped after shearing the bolts that fixed the horizontal support beams to the press frame. After replacing these bolts with high tensile strength bolts, and replacing the 10% fly ash with CSF, the panel was successfully produced.

The press gradually deformed in all the horizontal I-beams after producing all these panels, due to the large bending moments.

3.4.2 Pilot plant panel characteristics

One of the standard panels was cut into 42 segments, each 150 x 150 mm, to evaluate the homogeneity of the panels and tested for mass, thickness, density and moisture. The outer 30-50 mm were cut away and discarded. The variation is tabulated in table 3.18 below and illustrated in figure 3.33 to figure 3.37.

The coefficient of variation for the large panel moisture content was the greatest at 24.1% versus 0.58% for the standard Deviro panel. This indicates that the press design did not ensure homogenous dewatering. When evaluating the moisture content profile of the fully cured panel, it appears that water was trapped in the middle of the panel. This was most probably due to the lack of dewatering on the top-side of the

press, trapping the water in the centre of the panel. Dewatering was also easier on the edges during pressing and curing.

The thickness and oven dry mass profiles decreased from front to back that meant the panel was pressed more on the backside, than on the front. This indicated that the press platen was not aligned with the moulding tray. In the light of the press manufacturing constraints, this was very probable. This thickness variation to the backside can be corrected by shimming the back spacers to ensure an even thickness. To correct the moisture variation would require some further engineering and design work, to improve on the press dewatering capabilities.

Due to these inhomogenities, the density also exhibited a high coefficient of variation of 2.34% versus 0.133% of the standard panel (refer to 3.1.3.1). The oven dry density in the panel centre should be lower than the edges due to the higher moisture content at the centre (refer to figure 3.2). From figure 3.33, it is evident that this was not the case. The density was lower at the edges and erratic in the centre. This is most probably due to the higher rate of evaporation at the edges, resulting in a lower density.

Table 3.18. Variation within a low density standard large panel

	Mass [g] (2 weeks)	Mass (O.D.) [g]	Thickness (O.D.) [cm]	Density [g/cm^3]	Moisture content [%]
Average	695.6	482.3	2.887	0.760	11.65
COV [%]	3.70	4.50	3.15	2.34	24.1

Drying shrinkage was measured as the average of the four edges and expressed in mm/m. The results in table 3.19 are lower than the 33mm/m measured by Crafford (1997) for the low density (0.6 g/cm^3) standard panels[1].

Table 3.19. Drying shrinkage of larger panels

Panel	Drying shrinkage [mm/m]
Low density standard large panel	29.63
Silicate enhanced large panel	27.65
Perlite large panel (Pozzalan = CSF)	24.40

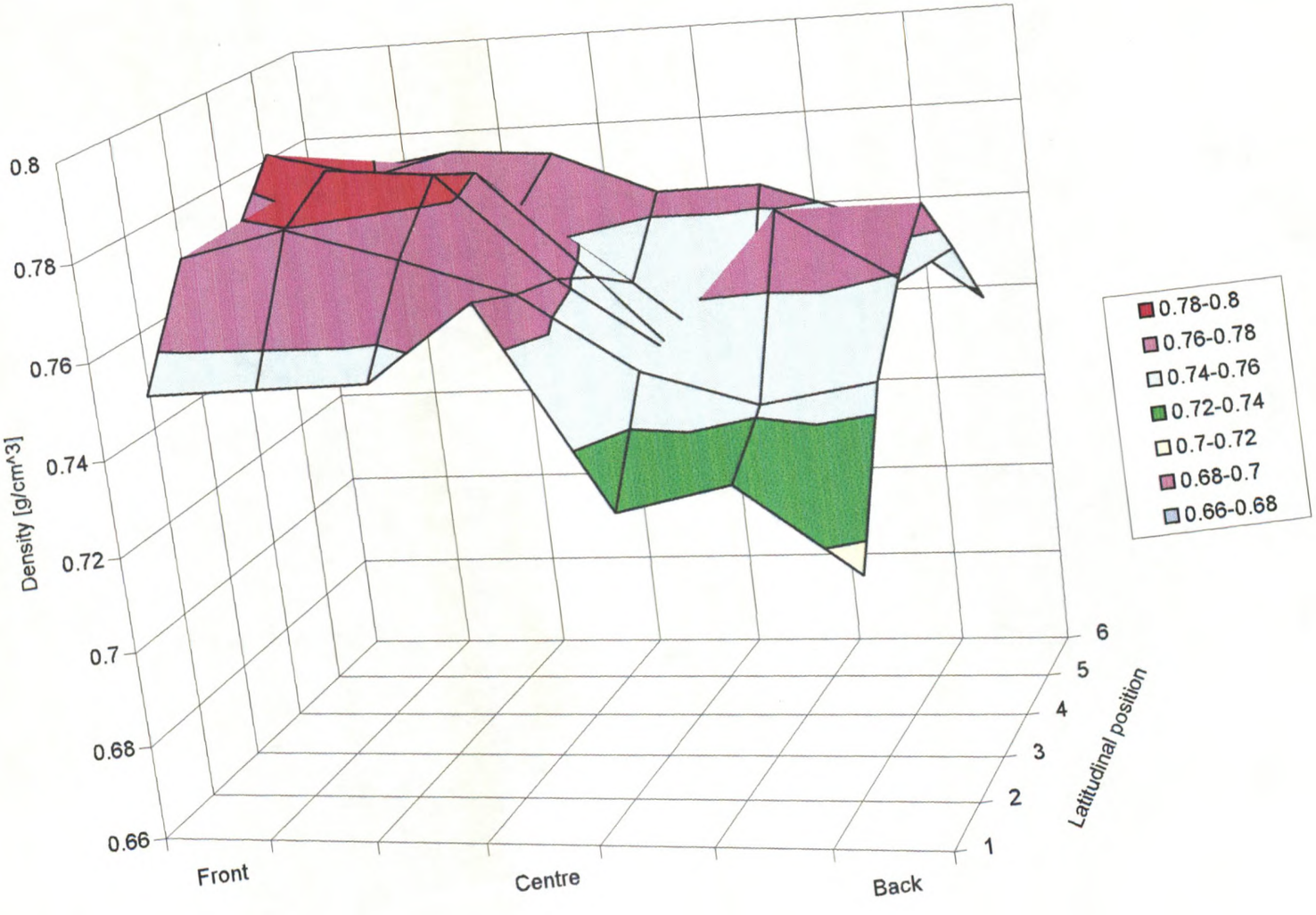

Figure 3.33 Oven dry density of fully cured panel

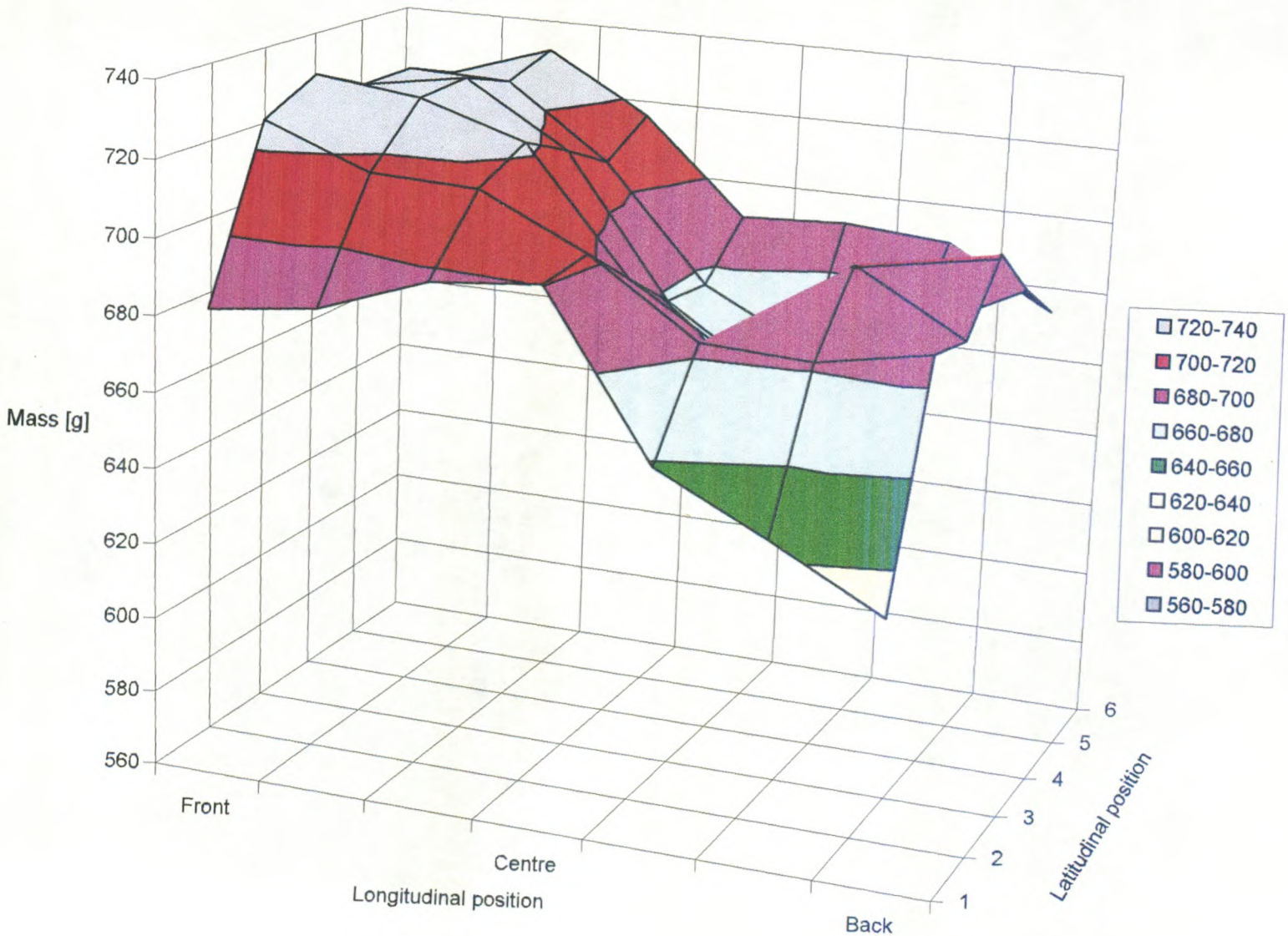

Figure 3.34. Mass after 2 weeks of curing

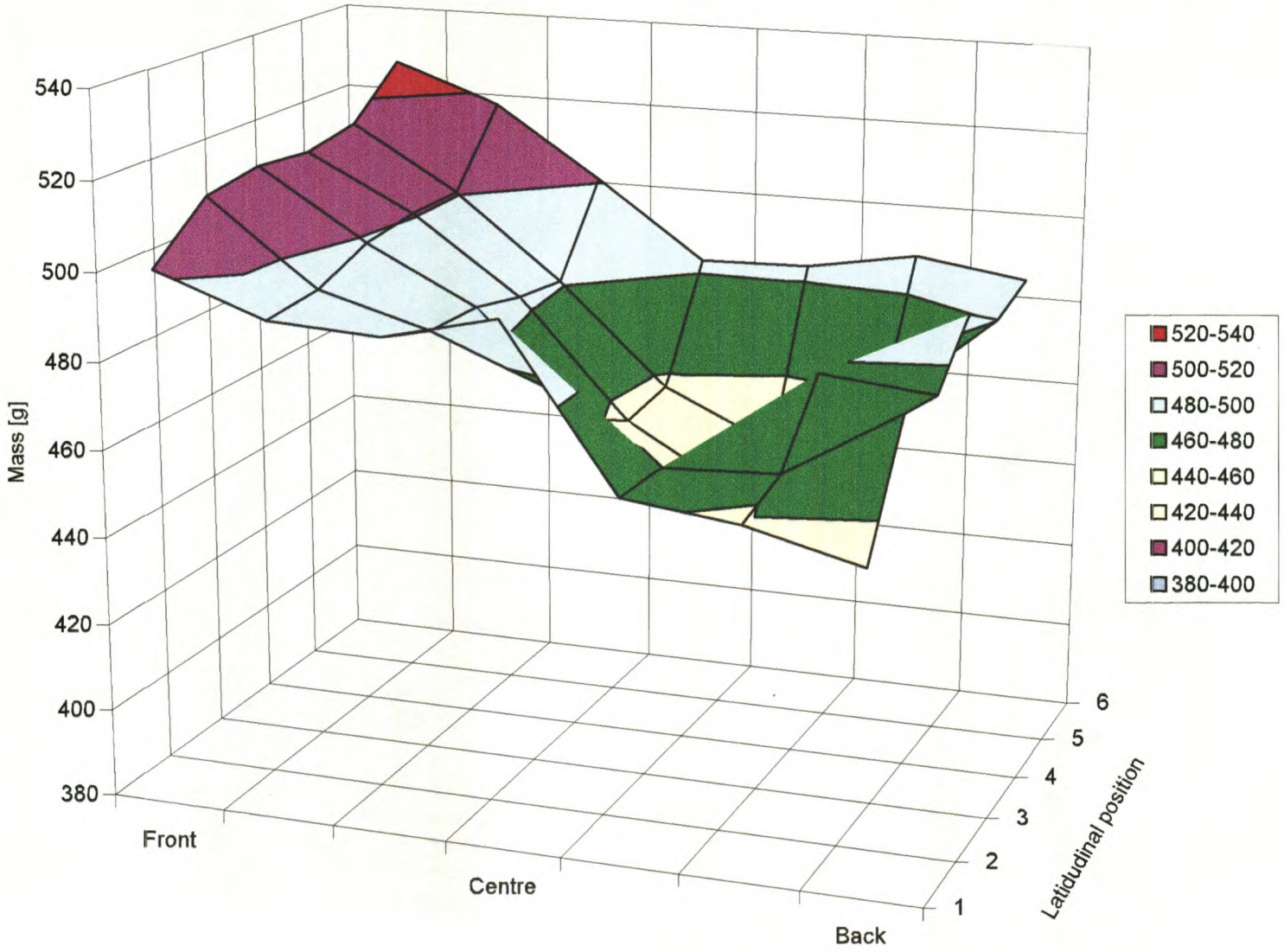

Figure 3.35. Oven dry mass of fully cured panel

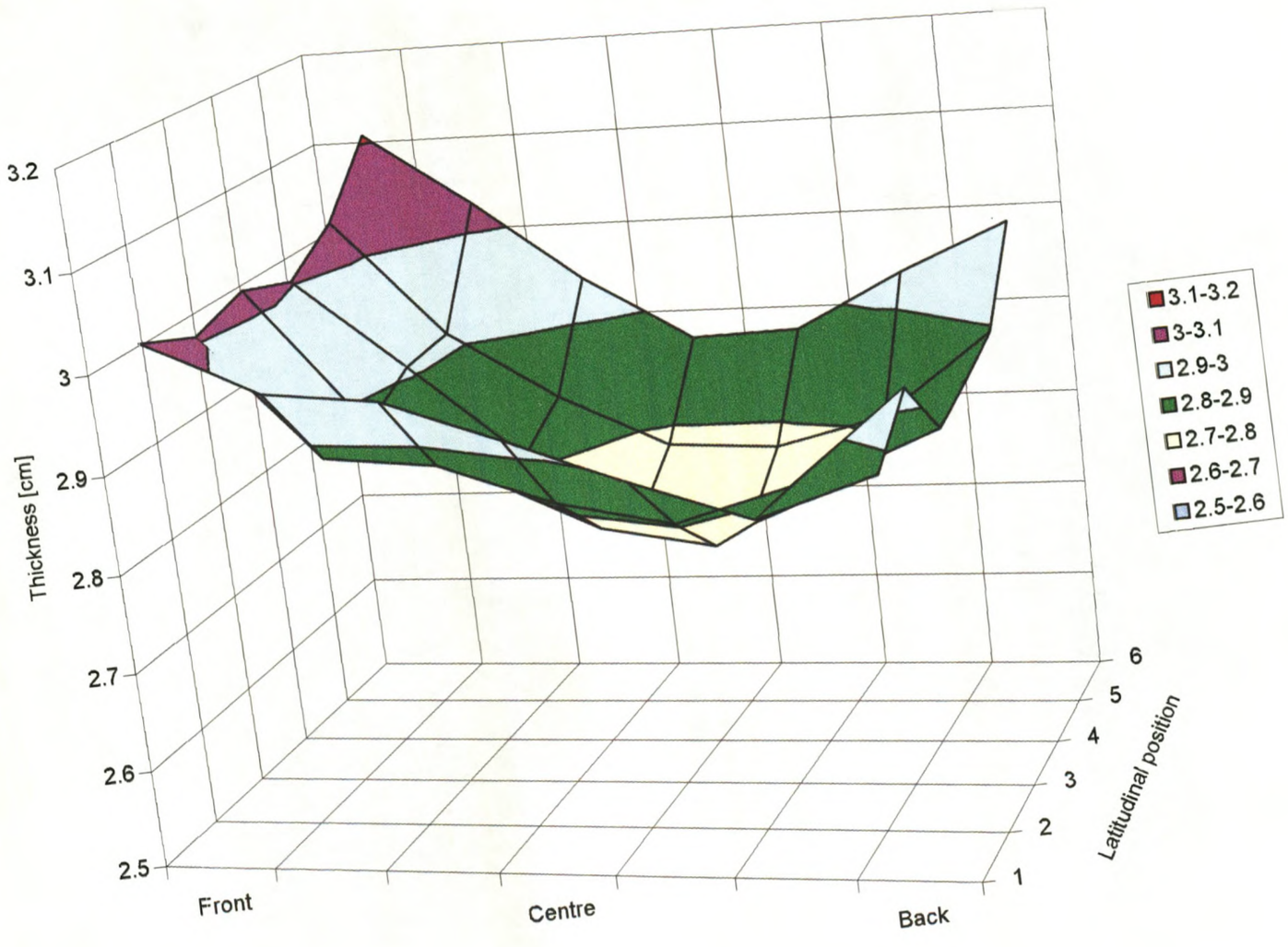

Figure 3.36. Thickness of fully cured panel

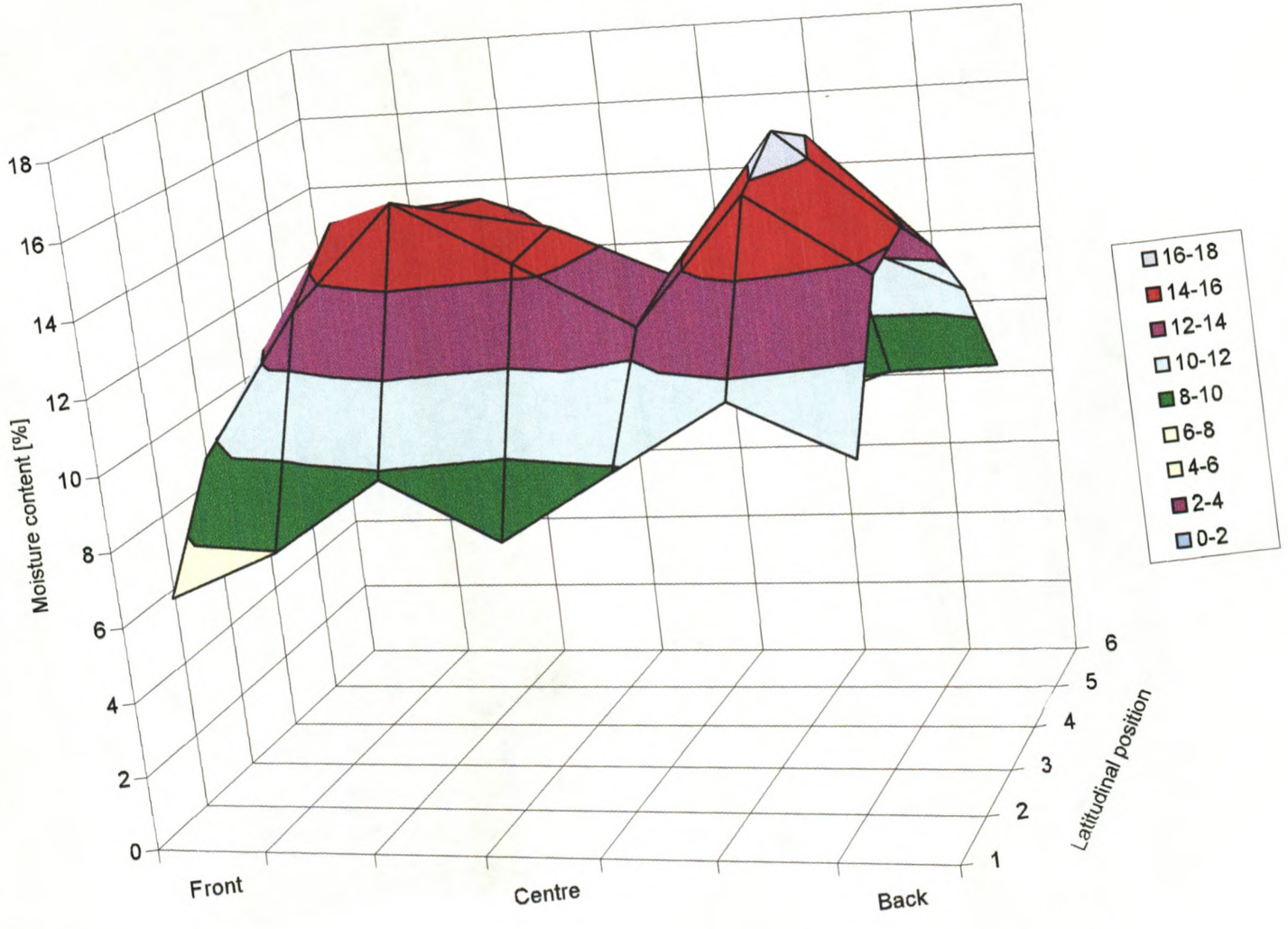

Figure 3.37. Moisture content of fully cured panel

3.5 SWOT analysis

To screen which potential applications may be considered, a strength, weakness, opportunities and threats (SWOT) analysis will be conducted on the market environment and panel characteristics.

3.5.1 Strengths

- The Deviro panel contains 55% de-inking sludge, thus more than half the raw material should be cost free during the early stage of the product life cycle. Therefore a pricing structure based on cost would make the composite more affordable than the competitors' products.
- Customers want a product that is not only functional, but is also value added. The ease at which the composite can be embossed during the manufacturing process lends itself to standard applications with additional decorative benefits.
- Due to its insulating properties, it is well suited for regions where thermal insulation plays an important role. The fire resistance is important for the low cost housing sector, where houses are densely located and fires can run rampant.
- The panel machines easily on traditional wood-working equipment making it well suited for industrial and *do-it-yourself* applications. The good screw holding and the ease to paint and shade makes it ideal for dry walls, skirting and cornices.
- Residual materials constitute more than half the composite compared to other less environmentally friendly composites, some of which still contain asbestos. Adding to this societal concept, the emphasis in more recent years is that of carbon saving, where this product has an advantage over similar composite.
- De-inking sludge produced is on the increase.

3.5.2 Opportunities

- The composites green tag carries weight in developed countries such as those in Europe and North America.
- The developments in the home improvement industry increases the market potential, with the decorative type value added market being new and expanding.

- Alternative opportunities may be low cost housing developments in developing countries due to the composite's fire resistance and insulation.
- Because of the association with a paper mill, the mill's distribution network may be available for transporting raw material and finished goods.
- Steam required for the autoclaving process could be sourced from the mill, due to the probable close proximity of the manufacturing facility to the paper mill.
- Should the product become established, products with similar applications, but using other residual raw materials could be realised.
- Flexible product opportunities exist from the variety of moulded forms.

3.5.3 Weaknesses

- Although de-inking sludge is a raw material cost saver, it consists of 4-60% water. This restricts the production facility to be located close to the paper mill.
- The sludge ages rapidly, which impacts on the quality of the finished product, reducing raw material holding time.
- The manufacturing process is time consuming with lengthy product curing times increasing work in process costs.
- The composite compares unfavourably against wood-fibre-cement composites with regards to strength and durability.
- The panel density is equal to or higher than commercially available fibre-inorganic composite, increasing handling costs.

3.5.4 Threats

- The market for modular panels (dry walls) already exists, making entry into these markets difficult. In addition to established competitors, the holding company of the paper mill may have a forest product division with competing products.
- After the initial *honeymoon* years, the paper mill may start charging for the de-inking sludge, causing the cost of the composite to significantly rise.
- The production process may be affected when the paper mill shuts for maintenance due to the dependence on the mill for the de-inking sludge.

CHAPTER 4 – CONCLUSION

4.1 Summary

The flexural strength and dimensional stability of the Deviro panel compared less favourably against wood and wood-fibre inorganic composites due to the high fibre content. It however compared very favourably to resin bonded wood fibre composites.

All physical properties were strongly dependant on density, with flexural strength linearly proportional to density. The less dense panel was more dimensionally stable, while absorbing moisture more readily. A denser product would however increase the cost of the product and reduce panel handling.

The greatest enhancements were realised when **autoclaving** the Deviro panel. To optimise properties, the fly ash was replaced with CSF to achieve a $CaO:SiO_2$ ratio of 1. Panel dehydration was accelerated to the desired moisture content. This ensured that the secondary hydration period coincided with the time when the panel was cured in the autoclave. The moisture content was critical. The greater the amount of water removed during pressing, the less water had to be evaporated. This resulted in greater strength improvements, but at the expense of an increase in density. A moisture content exceeding 30% from the oven to the autoclave resulted in blow-out, while a too low moisture caused insufficient hydration water to be available to promote cement curing. An oven temperature exceeding 60°C dehydrated the panel too quickly causing the panel to become brittle. From table 4.1, it can be noted that the autoclaved panels compare well against commercially available wood and wood-fibre inorganic composites.

Table 4.1. Comparison between autoclaved panel and wood and wood-fibre inorganic composites

Physical property	**Autoclave sludge panel**	Gypsum plaster board	Gypsum fibre board	Gypsum particle board	Cement fibre board	Cement particle board
Density [g/cm^3]	**1.0 - 1.16**	0.8 - 0.9	1.1 - 1.3	1.1 - 1.3	1.3-1.5	1.1 - 1.3
MOR [MPa]	**8.2 - 11.2**	3.0 - 3.8	5.0 - 7.5	6.0 -11.5	11.5 - 23	9.5 -15.5
MOE [GPa]	**3.9 - 5.8**	2.0 - 4.0	2.5 - 4.0	2.0 – 3.5	5.0-15	3.0 - 6.0
WA_{24} [%]	**39.1- 41.3**	54.4	-	-	25.1	20.1
TS_{24} [%]	**0.1 - 2.0**	4.8	-	-	~ 0	~ 0
Aged MOR [%]	**71.5**	Panel failure	-	-	91.9	-
Aged MOE [%]	**89.4**	Panel failure	-	-	88.2	-

The addition of **sodium silicate** increased flexural strength and reduced panel density, with best results achieved at a 2% addition. Unexpectedly, the addition of sodium silicate made the panel less dimensionally stable. Autoclaving silicate enhanced panels and substituting fly ash with CSF, did not improve physical properties above the standard autoclaved panels. The addition of sodium silicate to fresh sludge, limited sludge decay somewhat.

Perlite reduced the panel density, while limiting the concomitant reduction in flexural strength. An empirical formula was established to determine the panel density at various Perlite addition levels and press loadings. Perlite improved the quality of embossed panels, improving such market opportunities.

The replacement of fly ash with the more reactive **CSF** without autoclaving the panel, showed no improvement in strength properties and dimensional stability. Hence the reactivity of the pozzalan served little or no function in promoting the curing characteristics of the sludge-cement composite under ambient curing conditions and at the high fibre addition rates.

Applying a cement based **surface coating** to the panel made the composite suitable for outdoor applications. The coating applied easily to the panel surface, but was susceptible to deflaking when exposed to an abrasive/ shear force.

The enhanced panels generally retained their flexural strength when exposed to accelerated weathering treatments. The surface coating ensured that the panel strength was nearly fully retained, making such products suitable for outdoor applications.

The $1m^2$ panels manufactured in the pilot plant press formed well. Analysis of the larger panel indicated that similar hydration was achieved on a larger scale.

4.2 Commercial evaluation

Although a product idea may be good, a number of factors cause products to fail. It has been reported that a third of all new industrial projects fail at the launch and that only 40% of all new products will exist 5 years later.[96] Most often new products do not offer a unique selling proposition (USP) or the competition of other products is underestimated.[97] An effective strategy based on a new-product development process is required to reduce the odds for the Deviro panel to suffer an equal fate.

Based on the SWOT analysis (refer 3.5) target markets and a product mix is established. By autoclaving the standard panel, similar applications covered by gypsum based products can directly be marketed, such as serving as substrate for interior walls. Such products would be pre-cast, *ready-to-assemble* dry walls and wall dividers of various dimensions, which dove-tail within each other, suitable for home owners and corporate clients. The fire resistant properties are beneficial for such applications. Surface coating the composite with a cement-based coating can produce more durable products that may be applied in exterior environments. This includes modular panel sidings and moulded corrugated roofing products. Embossed skirting board and cornice products are value added products that may realise great benefits. Added to this product line would be picture frames, internal doors and door panes, decorative tiles and paving panels from autoclaved, embossed panels.

These product ideas must be converted into product concepts through a market research process. This requires descriptive research that should establish market potential and attitudes.[96] The marketing strategy that follows must focus on the target consumer, which are the homeowner, building contractor and corporate client. The customer must have the social awareness to preferentially purchase a product that is environmentally friendly. It is therefore expected that the customer should be from a developed country where building developments are popular. Hence, the marketing management philosophy must be based on a societal marketing concept, focusing on the customers' needs, profits and the society welfare.

When a market segment has been successfully identified, funding will be required to expand the laboratory manufacturing process to an industrial pilot scale plant. This would include a mixer; press; drying kiln and an autoclave. Further developmental work is required to capture the target market(s). This may include:

- The ability of the product to be laminated or glued
- Whether embossed images do not deteriorate during the subsequent drying and autoclaving treatments
- All physical properties meet the requirements for the target market

When reviewing this strategy, it is important to note that the Deviro panel and enhanced Deviro panels are best classified as original and unique, drawing largely from residue materials to produce a value added product. Therefore the USP of the product line should be based on its environmental benefits, with the critical success factor initially being the product pricing. The customer does not want to pay more for a higher quality product, but instead be penny-wise and environmentally conscious at the same time.

REFERENCES

1. Crafford, J.G (1997): **"The sludge panel" A wood fibre-cement composite from paper de-inking sludge.** M.Sc. Thesis. University of Stellenbosch, Department of Wood Science.

2. Dowe, S. (1993): **Solid waste solutions.** Papermaker, April 1993, p.36-38.

3. Hasbach, A.C. (1991) **Putting sludge to work.** Pollution Engineering, December 1991, p. 63-69.

4. Russel, C.; Odendahl, S. (1996): **Environmental considerations for landfill development in the pulp and paper industry.** Pulp & Paper Canada, Vol.97, No.1, p.51-56.

5. Wiegand, P.S.; Unwin, J.P. (1994**): Alternative management of pulp and paper industry solid wastes.** Tappi Journal, Vol.77, No.4, p.91-97.

6. Ysbrandy, R.E.; Gerischer, G.F.R. (1995): **SA Provisional Patent # 95/9594: Industrial paper-mill solid waste utilisation.**

7. Ferguson, L.D. (1992): **De-inking chemistry: part1.** Tappi Journal, Vol.75, No.7, p.75-82.

8. Srinath, A.; Szewczak, J.T.; Bowen, I.J. (1991): **A current review of ink-removal techniques in current de-inking technology.** Tappi Journal, Vol.74, No.7, p.85-93.

9. Carr, W.F. (1991): **New trends in de-inking technology.** Tappi Journal Vol.74, No.2, p.127-132.

10. Olson, C.R.; Richmann, S.K.; Sutman, F.J.; Letcher, M.B. (1993): **De-inking of laser-printing stock using chemical densification and forward cleaning.** Tappi Journal, Vol.76, No.1, p.137-144.

11. Ferguson, L.D. (1992): **De-inking chemistry: part2.**Tappi Journal, Vol.75, No.8, p.49-57.

12. Britz, H. (1997): **Flotation de-inking – a key technology for brightness and cleanliness.** Voith Sulzer Paper Technology.

13. Sutman, F.J.; Letscher, M.B.K.; Dexter, R.J. (1996): **Chemimechanical de-inking of office waste: Effects of lower-grade furnishes on de-inked pulp quality and process design.** Tappi Journal, Vol.79, No.3, p. 177-188.

14. Douglas, M.A.; Latva-Somppi, J.; Razbin, V.V.; Friedrich, F.D.; Tran, H.N. (1994): **Combustion of paper de-inking solids in a pilot scale fluidised bed.** Tappi Journal, Vol.77, No.5, p.109-119.

15. Cerff, C.B. (1996): **Pulp and paper study tour – June/July 1996.** Unpublished Report. University of Stellenbosch, Department of Wood Science.

16. Mabee, W. (1996): **Characterization and recycling of papermill sludges.** Annual Report 1996, p.95.

17. Ettala, M. (1993): **Quality of de-inking sludge.** Journal of Environmental Science and Health, A28(4), p.923-932.

18. Anon (1998): **The fibre recovery system.** TAU Environmental Consultant and Research GMBH.

19. Webb, L. (1994): **Sludge disposal: The unregulated loophole.** Pulp and Paper International, October 1994, p.18-23.

20. Latva-Somppi, J.; Tran, H.N.; Barham, D.; Douglas, M.A. (1994): **Characterisation of de-inking sludge and its ashed residues.** Pulp & Paper Canada, 95:10, p. 31-35.

21. Raitio, L. (1992): **The properties of de-inking sludge.** Paperi ja Puu – Paper & Timber, Vol.74 No.2, p.132-138.

22. Nickull, O.; Lehtonen, O.; Mullen, J. (1991): **Burning mill sludge in a fluidised-bed incinerator and waste-heat-recovery system.** Tappi Journal, Vol.74, No.3, p. 119-122.

23. Energy Products of Idaho (1998): **No.10 paper sludge fired boiler project.** Fort James Company. Available from : http://www.energyproducts.com [Accessed June 1999]

24. Dorica, J.; Simandl, J. (1995): **Separation of fibre and ash in de-inking effluents: A case study.** Tappi Journal Vol.78, No.5, p.109-116.

25. Swann, C.E. (1993): **Waste to energy.** Papermaker, April 1993, p.40-41

26. Fierro, A.; Norrie, J.; Gosselin, A.; Beauchamp, C.J. (1997): **De-inking sludge influences biomass, nitrogen and phosphorus status of several grass and legume species.** Canadian Journal of Soil Science, Vol.77, No.4, p. 693-702.

27. Bouranis, D.L.; Vlyssides, A.G.; Drosopoulos, J.B.; Economides D.G.; Mourafeti, B.; Drissis, D.G. (1997): **Physicochemical characteristics of a new organic soil conditioner from composted sludges from a pulp de-inking process**. Communications in Soil Science and Plant Analysis, No.28, p.17-18.

28. Brouillette, M.; Trepanier, L.; Gallichand, J.; Beauchamp, C. (1996): **Composting paper mill de-inking sludge with force aeration.** Canadian Agricultural Engineering. Vol.38, No.2, p.115-122.

29. Neville, A.M. (1997): **Properties of concrete.** Fourth Edition, John Wiley & Sons, Inc.

30. Soroka, I. (1979): **Portland cement paste and concrete.** The Macmillan press limited. London.

31. Ramachandran, V.S. (1984): **Concrete admixtures handbook. Properties, science and technology**. Noyes Publications, Park Ridge, New Jersey, USA.

32. Yan Fu; Ping Gu; Ping Xie; Beaudoin, J.J. (1995): **A kinetic study of delayed ettringite formation in hydrated Portland cement paste**. Cement and Concrete Research, Vol.25, No.1, pp.63-70, 1995.

33. Simatupang, M. et al (1990): **Technologies for rapid production of mineral bonded wood composite boards**. Inorganic wood and fibre composite materials. Proceedings of the 2nd international inorganic bonded wood and fibre composite materials conference, 15-17 October 1990. University of Idaho. Forest Products Research Society.

34. Tazawa, E.; Miyazawa, S.; Kasai, T. (1995): **Chemical shrinkage and autogenous shrinkage of hydrated cement paste**. Cement and Concrete Research, Vol.25, No.2, pp.288-292, 1995.

35. Nixon, P.J. (1986): **Changes in Portland cement properties and their effects on concrete**. Building Rresearch Establishment Information paper 3/86, March 1986.

36. Kirkbride, T. (1971): **Review of accelerated curing procedures. Reprinted form: Precast concrete.** February 1971 for the Cement and Concrete Association, Wexham, Springs, Slough Sl3 6PL

37. Addis, B.J.(ed.) (1994): **Fulton's Concrete technology**. Portland Cement Institute, Midrand, South Africa.

38. Maldas, D.C.; Kokta, B.V. (1992): **Process for the manufacture of precoated cellulose fibre characterised by mixtures of thermoplastics/ silicate/ anhydride/ isocyanate and composites made from coated fibre and polystyrene.** Canadian Patent, No.2029726.

39. ...(2000): **Eco-Hard-N-Seal™**. www.thomasregister.com/olc/tennant/tcohseal.htm [Accessed February 2001]

40. ... (2000): **Vulkem 2102. Silicate sealer, hardener and dustproofer.** Available from: www.tremcosealants.com/Newfiles/vukem2102.htm [Accessed February 2001]

41. MA, L.; Pulido, O.R.; Sasaki, H.; Kawai, S.; Ye, L.; Xue-Jun Yu (1996): **Strength and dimensional stability of cement-bonded composites manufactured by rapid curing methods with sodium silicate.** Proceedings from the 3rd Pacific Rim bio-based composite symposium, Kyoto, Japan, pp.484-489.

42. Nagadomi, W.; Kuroki, K.; Kawai, S.; Sasaki, H. (1996): **Rapid curing of cement-bonded particleboard with silica fume I. Effects of an additive for cement hydration during steam injection pressing.** Mokuzai Gakkaishi Vol42, No.11, pp.1090-1097.

43. Nagadomi, W.; Kuroki, K.; Kawai, S.; Sasaki, H. (1996): **Rapid curing of cement-bonded particleboard with silica fume II. Effects of autoclave curing on cement hydration.** Mokuzai Gakkaishi Vol42, No.12, pp.1202-1210.

44. Perlite Mining Co. (Pty) Ltd. (1999): **Pratliperl Ultra lightweight insulating and fibre proofing mixes.** Technical information brochure

45. D Etherington & Roberts. (1999): **Dictionary – Sodium Silicate**. Available from: http://171.64.128.118.don.dt.dt3206html [Accessed November 2000]

46. LA & HA Campbell (1999): **Silicates**. Available from: http://chemistry.co.nz/deterg_inorganic.htm [Accessed November 2000]

47. ... **Sodium Silicate**. (1993): The Columbia Encyclopaedia, 5th Ed. Columbia University Press.

48. Lee, A.W.C. (1984): **Physical and mechanical properties of cement bonded southern pine excelsior board**. Forest Products Journal, Vol.34, No.4, pp.30-34, 1984.

49. Fuwape, J.A.; Oyagade, A.O. (1993): **Bending strength and dimensional stability of tropical wood-cement particleboard**. Bioresource Technology, Vol.44, Part1, pp.77-79, 1993.

50. Parameswaran, N.; Broker, F.W. (1979): **Microphological investigations on wood-cement composites after long-term use**. Holzforschung, Vol.33, pp.97-102, 1979.

51. SA Bureau of Standards: SABS Standard method 1015 **Modulus of elasticity and modulus of rupture in static bending of particle board**

52. SA Bureau of Standards: SABS Standard method 1011 **Cutting and marking of test specimens of particle boards**

53. SA Bureau of Standards: SABS Standard method 1012

54. Rypstra, T. (1995): **Analytical techniques for the evaluation of wood and wood finishes during weathering**. Thesis. University of Stellenbosch, Department of Wood Science. 1995

55. American Society for Testing and Materials. (1987) **Standard methods of evaluating the properties of wood based fibre and particle panel materials**. ASTM designation D1037. Annual book of ASTM Standards. Vol.04.09.

56. Deppe, H.J. (1981) **Long-term comparison tests between natural and accelerated weathering exposure of coated and uncoated wood based materials**. Proceedings of the 15th WSU International Symposium on particleboard, Washington State University, Washington, p.79-100.

57. Kajita, H.; Mukudai, J.; Yano, H. (1991) **Durability evaluation of particleboards by accelerated aging tests**. Wood Science and Technology No.25, p.239-249.

58. River, B.H. (1994) **Outdoor aging of wood-based panels and correlation with laboratory aging**. Forest Products Journal, Vol.44, No.11/12, p.55-65

59. Marikunte, S.; Soroushian, P. (1994) **Statistical evaluation of long-term durability characteristics of cellulose fibre reinforced cement composites**. ACI Materials Journal. Nov./Dec.1994, p.607-616.

60. National Starch Chemicals (Pty) Ltd.: **Sodium silicate in the building industry No.1**. Technical information brochure

61. Soriano, F.P.; Eusebio, D.A.; Cabangon, R.J.; Alcachupas, P.L. (1997): **The effect of wood/cement ratio and accelerators on the properties of wood wool cement boards made from *acacia mangium*.** FPRDI Journal, Vol.23, No.1, pp.67-74.

62. Geimer, R.L.; de Souza, M.R.; Moslemi, A.A. (1996): **Accelerated ageing of low-density cement-bonded wood composites made conventionally and with carbon dioxide injection.** Drvna Industria, Vol.47, No.2, pp.55-62

63. Mel'-nikova, L.V.; Bulaeva, M.V. (1996); **Effect of lignosulfonate on the properties of cement / wood wool boards.** Derevoobrabatyvayuschaya-Promyshlennost, No.5, pp.6-7

64. Ysbrandy, R.E. **Inorganic wood fibre reinforced composites**. University of Stellenbosch. Unpublished

65. Sanderman, W,; Brendel, M. (1956): **Die "zementvergiftende" Wirkung von Holzinhaltsstoffen und ihre Abhänggigkeit von der chemischen Konstitution**. Holz als Roh- und Werkstoff Vol.14, No.8; p.307-313.

66. Crafford, J.G. (1996): **The use of binders in wood-based composites**. Unpublished report. University of Stellenbosch.

67. Moslemi, A.A. (1991): **Wood-cement composites: species and heartwood-sapwood effects on hydration and tensile strength**. Forest Products Journal Vol.41, No.3, p.9-14.

68. Couts, R.S.P. (1989): **Wood fibre reinforced cement composites**. From: Concrete Technology and Design. Vo.5, Natural Fibre Reinforced Cement and Concrete, R.N. Swamy (ed). Blackie, Glasgow & London

69. Sattler, H.; Roffael, E. (1991): **Germanite: a new fibre-reinforced composite for structural applications**. From: Inorganic bonded wood and fibre composite materials. Proceedings of the 2nd international inorganic bonded wood and fibre composite materials conference held 15-17 October 1990. University of Idaho. A.Moslemi (ed). Forest Products Research Society.

70. Soroshian, P.; Arola, R.A.; Shah, Z. (1992): **Recycling of wood and paper in cementitious materials**. Material Research Society Proceedings, Vol.266, p.165-175. Material Research Society

71. Davis, D.E. (1987): **Fly ash utilisation in cement bonded products. A general overview**. Ash – A valuable resource Vol.2. Concrete. CSIR Conference Centre, Pretoria, RSA. 2-6 February 1987. Article 2i.

72. Krüger, J.E. (1987): **Research at the NBRI on the utilisation of fly ash: An overview**. A valuable resource Vol.2. Concrete. CSIR Conference Centre, Pretoria, RSA. 2-6 February 1987. Article 2ii.

73. Loedolff, G.F. (1987): **Partial replacement of cement with fly ash – Optimum blends**. A valuable resource Vol.2. Concrete. CSIR Conference Centre, Pretoria, RSA. 2-6 February 1987. Article 5iii.

74. Miller, D.P.; Moslemi, A.A.; Short, P.H. (1989): **The use of fly ash in wood-cement composites**. Forest Products Journal Vol.39, No.9, p.34-38.

75. Fraay, A.L.A.; Bijen, J.M.; de Haan, Y.M. (1989): **The reaction of fly ash in concrete. A critical examination**. Cement and Concrete Research. Vol.19, p.235-246.

76. Halmagiu, M.; Halmagiu, A; Fliss, L. (1987): **Partial replacement of cement with fly ash – Optimum blends**. A valuable resource Vol.2. Concrete. CSIR Conference Centre, Pretoria, RSA. 2-6 February 1987. p.303-311

77. Molhotra, V.M. Carette, G.G. (1982): **Silica fume. A pozzalan of new interest for use in some concretes**. Concrete Construction. May 1982, p.443-446.

78. Levitt, M. (1993): **Microsilica in concrete. Report of a Working Party**. Concrete Society Technical Report No.41. The Concrete Society

79. Zhang, M-H.; Gjorv, O.E. (1991): **Effect of silica fume on cement hydration in low porosity cement pastes**. Cement and Concrete Research. Vol.21, No.5, p.800-808.

80. Bolen, W.P. (1992): **Perlite**. Ceramic Bulletin. Vol.71, No.5, 1992, p.812/3

81. Pratley Perlite Mining Co.(Pty)Ltd (1998): **Pratiperl ultralightweight insulating and fireproofing mixes**. Technical report.

82. Cemcrete (Pty) Ltd. (1998): **Cemcrete 1998**. Technical information brochure.

83. Taylor, H.F.W. (1887): **Cement chemistry**. Second edition, Tomas Telford

84. Hewlett, P.C. (1988): **Lea's chemistry of cement and concrete**. Fourth edition, John Wiley & Sons Inc.

85. Siemplekamp GmbH & Co.: **Plants for the fibrecement industry**. Technical information brochure. 1994.

86. Porter, K. (1998): **Fiber-cement plant is first for ABTco**. Wood technology, March 1998, pp.52-54

87. Sorfa, P. (1984): **Properties of wood-cement composites**. Journal of applied polymer science: Applied polymer symposium. 40, pp.209-216, 1984

88. Eltomation: **Wood wool cement board properties, application and production technology**. Technical information on wood wool cement board.

89. Dinwoodie, J.M. (1983): **Wood cement particle board – a technical assessment**. Building research establishment information paper. IP4/83. April 1983.

90. Wolfe, R.W.; Gjinolli, A. (1997): **Durability and strength of cement bonded wood particle composites made from construction waste**. Forest Products Journal, Vol.49, No.2, pp.25-31.

91. Soroushian, P.; Shan, Z.; Jong-Pil Won (1995): **Optimisation of wastepaper fibre-cement composites**. ACI materials Journal. January-February 1995.

92. Chow, P. (1979): **Phenolic adhesive bonded medium density fibreboard from Quercus Rubra L. bark and sawdust**. Wood and Fiber, 11(2), pp.92-98, 1979.

93. Moslemi, A.A. (1990): **Mineral bonded wood composites: Emerging technologies**. International Union of Forest Research Organisations. 19th World congress, Montreal, Canada, 1990.

94. Lin, X.; Silsbee, M.R.; Roy,D.M.; Kessler, K.; Blankenhorn, P.R. (1994): **Approaches to improve the properties of wood fibre reinforced cementituous composites**. Cement and Concrete Research, Vol.24, No.8, pp.1558-1566, 1994.

95. Lempfer, K.; Hilbert, T.; Gunzerodt, H. (1990): **Development of gypsum-bonded particleboard manufacture in Europe**. Forest Product Journal, Vol.40, No.6, pp.37-40, 1990.

96. Armstrong, G.; Kotler, P. (2000): **Marketing – An introduction**. New York, Prentice-Hall Inc.

97. Perrault Jr, W.D.; McCarthy. E.J. (1999): **Basic marketing – A global managerial approach**. New York, McGraw-Hill.

APPENDIX A – DE-INKING

A.1 Introduction

The principal objective of a de-inking process is to remove printing ink from the secondary fibre in order to achieve a uniform colour shade of the produced paper. Important parameters are ash content of the de-inked pulp, suspended solids and chemicals in the white water, water hardness, availability of fresh water and water and solid waste discharge.[7]

De-inked pulp can be a cost-effective component of a paper furnish. These fibres have been successfully used in tissue, newsprint and printing paper manufacturing. It has found only limited application in the production of fine paper grades, mainly because non-dispersed ink particles remaining in de-inked fibre appear as specks in the finished paper.[8]

The suitability of de-inked fibre is therefore largely dependent on:

- Quality of the de-inked fibre, which is a function of the type of inks and contaminants contained in the waste paper, especially with the introduction of non-impact printing techniques;
- End-product quality requirements, which will determine whether de-inked fibre can be incorporated into the furnish and to what extent;
- Cost;
- Environmental regulations.

A.2 Printing Inks

A.2.1 Introduction

Ink characteristics and their setting properties have a direct bearing on the efficiency of de-inking. This determines how intimately the ink is attached to the fibre and, consequently, how difficult the ink is to remove.

Traditionally printing inks have two basic ingredients, a pigment or dye and a vehicle.[8] The pigment provides colour and opacity to ensure contrast of the printing image. The vehicle serves as a carrier medium and helps to transfer and bind the pigment or dye to the sheet. Some modern inks, such as those associated with xerographic and laser printing (q.v. A.2.3.5 & A.2.3.7), consist of fine particles fixed by fusion.[7,8,9,10]

Printing inks can contain several other components including binders, solvents, dryers, wetting agents and waxes. The makeup of the ink is determined by the type of paper on which it is applied, the printing and drying process and the end use of the paper.

A.2.2 Printing Process

A.2.2.1 Letterpress

Letterpress was typically used in printing newsprint, magazines and kraft bags. The ink is applied to a raised surface on a printing plate, and is transferred to the paper when the plate presses against the paper web. The inks can be dried by absorption, evaporation or precipitation, while most sheet-fed letter press inks dry by oxidation.[8]

A.2.2.2 Lithography

The printing plate consists of an image area, which is receptive to oil-based inks and a non-image area, which is water receptive. This allows the print and non-image areas to be on the same level plate surface. The image is firstly transferred onto a rubber-blanket covered roll. The blanket in turn imparts the image to the paper sheet. Lithography is used for printing matt and glossy magazines, newspapers, books, art and photographic reproductions.

Lithographic inks are based on water-resistant vehicles and pigments that do not bleed in water or alcohol. The vehicle is conventionally a linseed oil, but modern formulations use an alkyd resin with a

drying oil, which polymerises to form a tough, cross-linked film. Heat-set inks are often based on hydrocarbon resins that dry by evaporation. Colour printing in newspapers use UV inks that contain a mixture of acrylic monomers and pre-polymers that polymerise to a strong film.

A.2.2.3 Gravure

The gravure printing cylinder has a recessed image-forming area, which is immersed in an ink bath. The excess ink is removed by a doctor blade before the paper is pressed against the ink-filled recesses of the impression cylinder. Rotogravure is used in printing colour newsprint supplements, magazines of large issues and various wrappers.

The inks are fast-drying by evaporation of the ink solvent. The inks are usually based on polyamides or polyacrylate resins in aromatic hydrocarbon or ester solvents. Some are water-based with a low alcohol content.

A.2.2.4 Flexography

This is a combination of the letterpress and gravure printing processes. The rubber based printing stereo has a raised printing image clamped around the printing cylinder. This process is mostly used for printing corrugated packaging materials.[8]

The inks are fast-drying. The pigment is either based in an alcohol-ester mixture, where drying is by evaporation or in a water-based vehicle, which dries by both evaporation and absorption.

A.2.2.5 Xerography

The xerographic process, is an indirect, non-impact printing method where a latent image is formed on an electrostatically charged photoconductive metal drum. Light exposure discharges the drum. Ink powder (toner and carrier) is cascaded over the image surface, adhering to the unexposed areas. The ink releases to a statically charged paper. The paper is then heated, allowing the toner to be thermally fused.

The toners are coloured pigments such as carbon black, in a thermoplastic resin binder. A small percentage of zinc stearate, which serves as a dry lubricant, is sometimes present in the toner. Liquid toners are suspensions of toner particles in an insulating liquid, while resins and oils may be added as charge-control agents.

A.2.2.6 Ink-jet Printing

Ink-jet printing involves the translation of a digital image into a printed image by the controlled projection of ink droplets onto the paper. The ink typically consist of soluble dyes in a water or alcohol-water base containing glycols, polyethers and wetting agents.

A.2.2.7 Laser Printing

A computer-directed laser beam forms a latent image on a charged drum by neutralising the charge on the non-image areas. Toner particles applied to the drum, adhere to the charged image areas. The image, which has formed, is then transferred to the paper where the toner particles are fused by heat and pressure. The ink used in this process is similar to xerographic ink.

A.3 De-inking Principles

A.3.1 Introduction

The type of ink contained in the waste paper will determine the equipment and chemicals used in the de-inking process. Some inks are more amenable to being broken down during pulping and are more easily removed.

The size of the ink particle to be removed, is of primary importance. Large ink particles are removed by screens and centrifugal cleaners. The smallest ink particles can be removed by washing. Flotation

removes particles that are too small to be removed by screens and cleaners, but are too big to be removed by washing. The optimum size ranges for the different unit operations are illustrated in figure A.1.

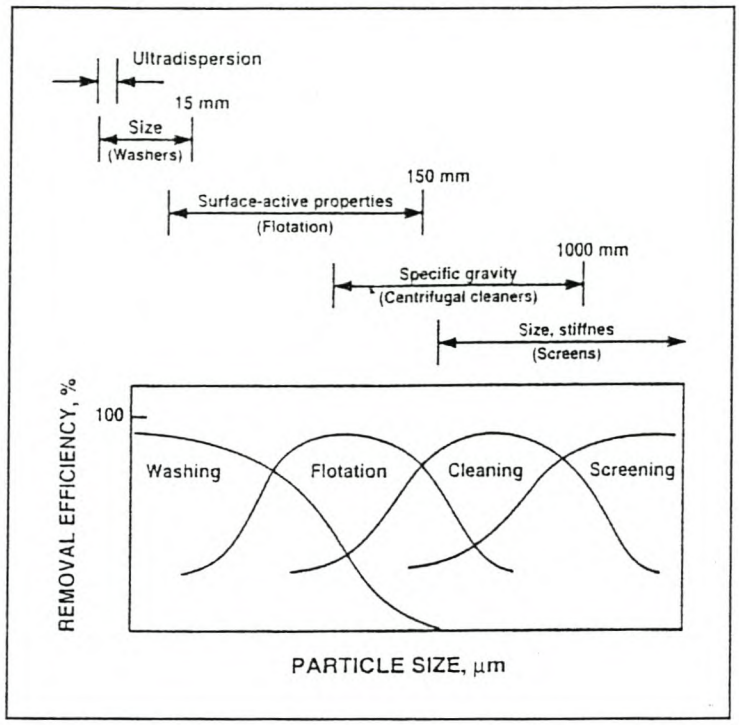

Figure A.1 Removal efficiencies of de-inking removal units vs. ink particle size[8,11]

A.3.2 Pulper

In a de-inking operation, the pulper serves to slush the paper in water and to detach the ink particles from the fibres, while keeping contraries large enough to be removed by the cleaners and screens. Caustic soda and silicates are added at the pulper to assist with the removal of ink and stickies, and make them accessible for flotation de-inking.

A.3.3 Wash De-inking

The objective in wash de-inking is to keep the ink particles finely dispersed with the aid of dispersants such that they can be removed through screens or washer screen wires (e.g. Vario Split). Washing also requires the ink particles to be rendered hydrophilic so that they remain in aqueous solution and will also drain easily.[7,8] Non-ionic surfactants are used for this purpose. The mechanism involved in wash de-inking is outlined in figure A.2.

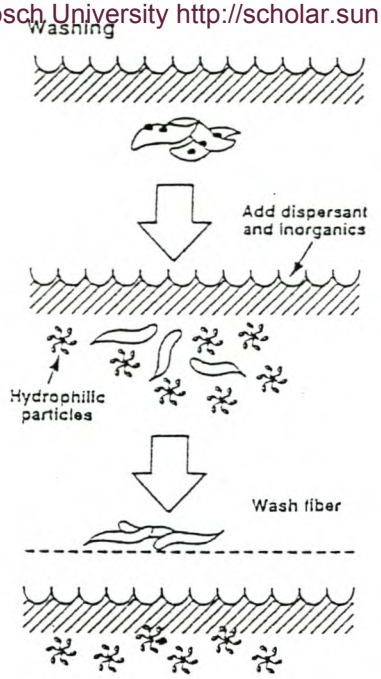

Figure A.2 Mechanism of wash de-inking[8,11]

A.3.4 Flotation De-inking

Flotation de-inking is a selective process, based on the different wettabilities of solids.[12] Hydrophobic solids with a 5 – 500 micron diameter, adhere to rising air bubbles entering the de-inking cell. These bubbles are transported by flotation to the surface, where they become part of the foam layer. This surface layer of froth is then drawn off. Thus substances such as inks, stickies, plastics, NCR (no carbon required) capsules and fillers can be separated from the furnish in this manner. Figure A.3 illustrates the mechanism involved in flotation de-inking.

For effective flotation, the ink particles must therefore be made hydrophobic and must be maintained within an optimum size range. The other aspect affecting selectivity is the hydrodynamics of the flotation cell.

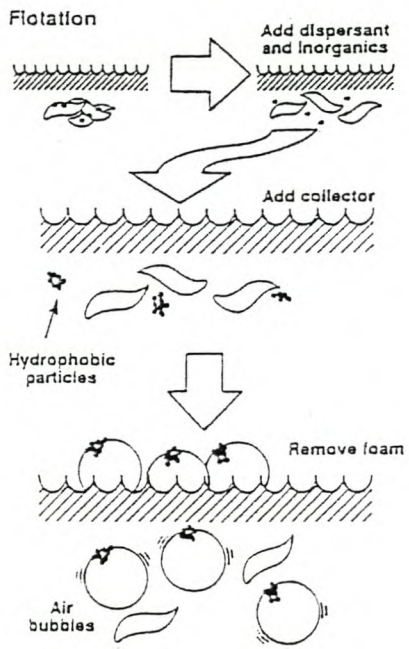

Figure A.3 Mechanism of flotation de-inking[8,11]

A.3.5 Forward Cleaning and Screening

The larger contraries are removed during the screening stage. The cleaners remove particles which otherwise pass through the screens. Under appropriate pulping conditions, stickies mingle with ink particles and can be removed through cleaning and screening.[13] Toners and inks and substantial portions of filler and dirt can be chemically agglomerated and be subsequently removed by the screens and cleaners.[8,9]

A.3.6 Cold Dispersion

Ink particles can be separated from the fibres by incorporating a cold dispersion stage ahead of flotation and washing. The dispersion unit is a non-pressurised high-shear dispersion device. High shear is imparted to the fibres, detaching the ink particles, without causing fibre damage.

A.4 De-inking Chemicals

A.4.1 Introduction

Chemistry is involved in many of the key processes in a de-inking mill: pulping, flotation, washing, deposit control and water clarification. De-inking chemicals are required to ensure the efficient performance of these processes.

A.4.2 Sodium Hydroxide (NaOH)

Sodium hydroxide is added at the pulper to increase pH to the alkaline region. The alkaline environment makes the fibres more flexible by "swelling" them. This opens the pores of the fibres and thus enhances the de-inking process.[8] Additionally, sodium hydroxide breaks down oil-based vehicles carrying ink pigments. The vehicle is saponified and broken down to form a soap and an alcohol:[8]

(A.1)

Ester (Vegetable oil) Alkali Soap (Sodium salt) Glycerol

The addition of sodium hydroxide to a wood containing furnish will cause the pulp to yellow and darken, a phenomenon referred to as "alkali darkening". In such cases, a careful balance should exist between having sufficient alkalinity for good saponification and hydrolysis of the resins, while minimising the formation of chromophores in lignin. A pulper pH slightly greater than 10 has been reported to provide optimum brightness results.[7] Alkali darkening is not a concern for wood-free furnishes, allowing higher pH's (11.0) to be used.

A.4.3 Hydrogen Peroxide

Hydrogen peroxide (H_2O_2) is used in the pulper to offset the formation of chromophores generated as a result of the alkaline pH. It however does not serve as an efficient bleaching agent in the pulper, because of the high ink and contraries load, which reduces bleaching efficiency. It is therefore additionally used as a post-bleaching agent. The furnish will determine the balance between how much peroxide is added at the pulper versus how much is used in the bleaching stage.

The peroxide reaction with sodium hydroxide is given in equation A.2:

$$H_2O_2 + NaOH \rightleftharpoons HOO^- + Na^+ + H_2O, \qquad (A.2)$$

where $10.0<pH<11.5$ and temperature = 40-80°C.

To optimise the use of the peroxide, it is important to maximise the amount of perhydroxyl ions (HOO^-), because this anion is the active bleaching agent.[7] This can be achieved by increasing the caustic level to raise the pH, raising the temperature and reducing the competing side reactions, which decompose peroxide. Peroxide can decompose in the presence of heavy metal ions such as Mn^{2+}, $Cu^{2+}$and Fe^{2+}, as shown in equation A.3, or enzymes such as catylase.

$$M^{2+} + H_2O_2 \xrightarrow{pH,\ temp.} \tfrac{1}{2}\,O_2 + H_2O, \qquad M = metal \qquad (A.3)$$

These decomposition products and conditions are believed to contribute to a further loss in brightness in wood-containing furnishes.[3] The peroxide decomposing reactions can be reduced by the addition of stabilising agents such as chelants (q.v. A.4.4) and sodium silicate (q.v. A.4.5).

A.4.4 Chelating Agent

Chelants such as DTPA (diethylene-triamine-penta-acetic acid) and EDTA (ethylene-diamine-tetra-acetic acid) are employed to sequester heavy metal ions. The soluble complexes formed, prevent the metal ions from decomposing hydrogen peroxide.

A.4.5 Sodium Silicate

Sodium silicate (Na_2SiO_3) assists in de-inking in the pulper by dispersing the ink and preventing the ink from redepositing on the fibre. Additionally, it serves as a source of alkalinity, derived from free hydroxyl groups, while buffering the pH at 11.3. The equilibrium reaction can be written as follows:

$$Na_2SiO_3 + H_2O \rightleftharpoons 2Na^+ + OH^- + HSiO_3 \qquad \text{(A.4)}$$

Sodium silicate is used in conjunction with hydrogen peroxide to reduce peroxide decomposition by stabilising operating conditions.[7,8] Silicates are believed to form colloidal structures with the heavy metal ions.[7]

Problems associated with the use of silicates include scaling and fouling of equipment, wires and felts; coating of fibres; harshness in paper; difficult handling in cold conditions; and high temperature breakdown which causes fouling in refiner-type disperger plates.

A.4.6 Agglomerating Chemical [7,8,10]

Agglomerating chemicals are used for de-inking fused-toner papers (q.v. A.2.3.5 & A.2.3.7), by adding the chemical at the pulper at temperatures between 60-70°C, with long mixing times of 40-60 minutes.

Upon repulping, the electrostatic toners generally form large, flat plate-like structures that are too large to be removed by washing or flotation and are too small to be removed by the cleaners and screens. The surfaces of these toner flakes are chemically modified so that the repulsive forces between the particles are reduced. Additionally, the glass transition temperature (temperature at which resins begin to flow) is lowered such that at 60°C, the toner particles become plastic and agglomerate. The softer particles grow into larger spherical particles, which can then be removed by slotted pressure screens and forward centrifugal cleaners.

A.4.7 Surfactants

Surfactants are surface active agents, used as dispersants, collectors, wetting agents, displectors and anti-redeposition aids. Surfactants have a hydrophilic and hydrophobic component. When introduced into the pulper or just prior to flotation, the hydrophobic end will associate with the ink, oil or dirt, while the hydrophilic end remains in solution.

A.4.7.1 Dispersants

The function of dispersants is to keep the ink and dirt particles that have been released during pulping, in suspension so that they can be removed during washing or thickening. Surfactants such as nonylphenol ethoxylate and linear ethoxylated alcohols are the most commonly used wash de-inking dispersants. The structure for these wash de-inking surfactants are shown in figure A.4.

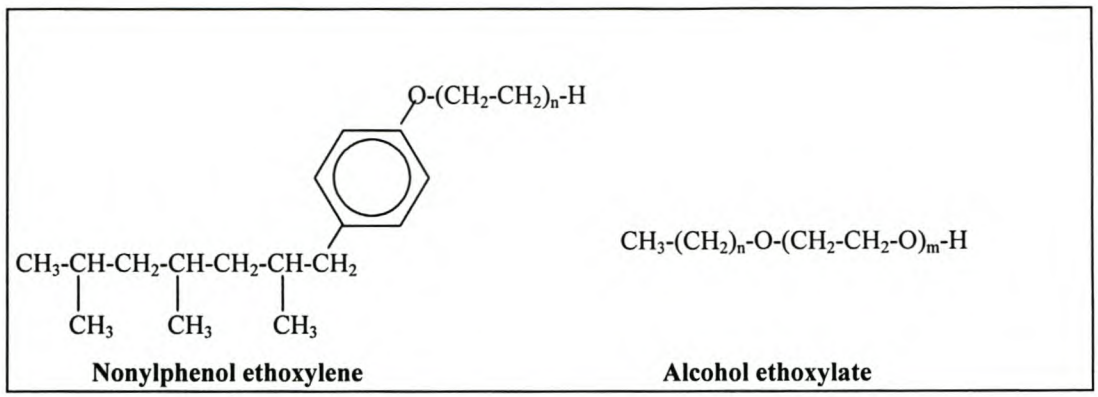

Figure A.4 Wash de-inking surfactants [8,11]

Dispersants for short sequence de-inking are often blends of ethylene oxide/ propylene oxide (Eo/Po) copolymers and glycols and fatty acid alcohol alkoxylates.

A.4.7.2 Collector Chemicals

Collector chemicals are used in flotation de-inking and can be added at the pulper or just prior to the de-inking cells.[6] These chemicals are designed to bring together the ink particles that have been released in the pulper, so that they can be removed by froth flotation. Collectors are fatty acid soaps (shown in figure A.5), Eo/Po copolymers or blends such as ethoxylated fatty acids.

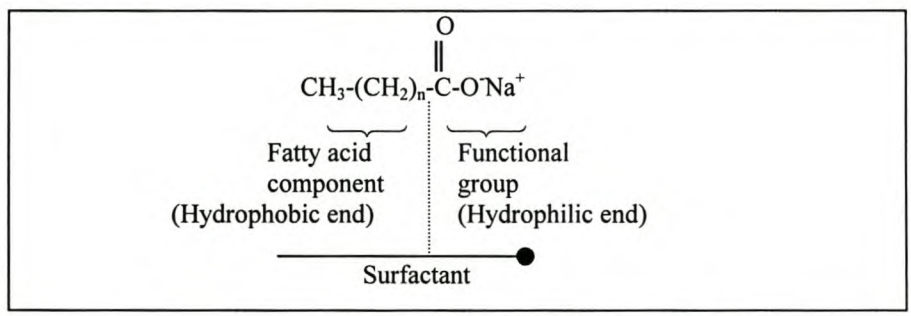

Figure A.5 Soap as a collector chemical

When using the fatty acid soaps, the calcium salt of the fatty acid must be formed before it can function as a collector. Calcium ions must therefore be added to achieve the required water hardness levels. Process interference, stock loss, scaling and other deposits associated with calcium is a concern with such systems.[11]

A.4.7.3 Displectors

Displectors are surfactants that are a combination of dispersants and collectors, which are designed to assist in de-inking plants that have both flotation and washing/ thickening stages.

A.5 Ink Removal Strategies

A.5.1 Letterpress Inks

The hydrocarbon vehicles in letterpress newsprint inks are readily dispersed with the addition of a surfactant such that the pigment is released and is easily removed by a washing stage.

A.5.2 Lithograhic Inks

Offset lithographic inks are similar to letterpress inks, except that they contain considerably more pigment and up to 50% hydrocarbon resin binder, which impedes ink dispersion. The addition of

silicates with a surfactant is required for effective dispersion for washing. An alternative is to use cold dispersion units to disperse the offset inks.

A.5.3 Flexographic Inks

The water-based pigments of flexographic inks are not effectively collected by conventional calcium-ion/fatty acid collector systems, because the ink particle can not be rendered sufficiently water-repellent. The addition of displectors for flotation and subsequent washing de-inking is required.

A.5.4 UV-cured and Cold Set Inks

UV-cured and cold set inks are firmly bonded to the fibres by resin binders, such that they are not easily separated from the fibres and are resistant to being broken down. After pulping, these inks are large, thin, film-like particles, with a density slightly greater than 1. Therefore, cleaners and screens do not easily remove the particles. These inks can not be removed by washing, because they are difficult to saponify and disperse. The tough cross-linked surfaces of these films also make the particles resistant to attachment by collector chemicals, thus reducing the efficiency of flotation de-inking. Cold dispersion is claimed to be extremely successful in removing UV-cured particles from the fibres.[11]

A.5.5 Xerographic and Laser-Printed Inks

Upon repulping, the electrostatic toners contained within these furnish types, form large, flat plate-like structures that are too large to be removed by washing or flotation and are too small to be removed by the cleaners and screens. These inks are also very difficult to disperse. Therefore, conventional de-inking processes of washing and flotation fail to effectively reclaim speck-free fibres.

High consistency pulping followed by flotation is more effective in removing toners. A dispersion stage before the flotation stage will further assist in reducing ink particles to the optimal size. Dispersion is effective in freeing the ink from the fibres through a kneading and flexing action on the fibres.

The flat, plate-like toner particles can also be agglomerated into larger, spherical particles that can be removed in slotted pressure screens and forward centrifugal cleaners.

APPENDIX B

A representation of the data matrix, as downloaded from the computerised Instron testing apparatus.

Comp: L vs D
Dimensions

Thickness (mm)	Width (mm)
t_1	b_1

Integration Results

Force(N)	Deviation(mm)
0	0
F_{11}	s_{11}
...	...
F_{1i}	s_{1i}
...	...
F_{1n}	s_{1n}

Dimensions

Thickness (mm)	Width (mm)
t_2	b_2

Integration Results

Force(N)	Deviation(mm)
0	0
F_{21}	s_{21}
...	...
F_{2i}	s_{2i}
..	..,
F_{2n}	s_{2n}

Dimensions

Thickness (mm)	Width (mm)
t_m	b_m

Integration Results

Force(N)	Deviation(mm)
0	0
F_{m1}	s_{m1}
...	...
F_{mn}	s_{mn}

, with t_i = test specimen thickness, mm

t_i = test specimen width, mm

F_i = load on test specimen i at time j, N

s_i = deflection of test specimen i at time j, mm

Visual Basic 5.0 code developed to process the data matrix downloaded from the Instron testing apparatus.

```
Option Explicit

Dim counter As Integer
Dim data As Object
Dim chartNo As Integer
Dim leftChart As Boolean
Dim devStart As Single
Dim maxForce As Single
Dim MOE, MOR As Single
Dim workToFail As Single
Dim b, t As Single
Dim rSqr As Single

Sub ChartIt()
   Dim chartObj As String
   Dim chartName As String
   Dim pos As Double
   Dim infoRow As Integer

   chartNo = chartNo + 1
   chartName = "FilenameNo" & chartNo
   leftChart = Not leftChart
   Charts.Add
   ActiveChart.ChartType = xlXYScatterSmoothNoMarkers
   ActiveChart.SetSourceData Source:=data, PlotBy:=xlColumns
   ActiveChart.Location _
      Where:=xlLocationAsObject, Name:="Graphs"
   With ActiveChart
      .HasTitle = True
      .ChartTitle.Characters.Text = chartName
      With .Axes(xlCategory, xlPrimary)
         .HasTitle = True
         .AxisTitle.Characters.Text = "Deviation [mm]"
         .CategoryType = xlAutomatic
      End With
      .Axes(xlValue, xlPrimary).HasTitle = True
      .Axes(xlValue, xlPrimary).AxisTitle.Characters.Text _
         = "Force [N]"
      .HasAxis(xlCategory, xlPrimary) = True
      .HasAxis(xlValue, xlPrimary) = True
      With .Axes(xlCategory)
         .HasMajorGridlines = False
         .HasMinorGridlines = False
         .MinimumScale = 0
      End With
      With .Axes(xlValue)
         .HasMajorGridlines = True
         .HasMinorGridlines = False
         .MinimumScale = 0
         .MaximumScale = 400
      End With
```

```
        .HasLegend = False
        .ApplyDataLabels Type:=xlDataLabelsShowNone, _
          LegendKey:=False
    End With
    chartObj = "Chart " & chartNo
    pos = -30 + ((chartNo - 1) \ 2) * 229.5
    If leftChart Then
      ActiveSheet.Shapes(chartObj).IncrementLeft -111.75
    Else
      ActiveSheet.Shapes(chartObj).IncrementLeft 128.25
    End If
    ActiveSheet.Shapes(chartObj).IncrementTop pos
    ActiveSheet.Shapes(chartObj).ScaleWidth 0.7, _
      msoFalse, msoScaleFromTopLeft
    ActiveSheet.Shapes(chartObj).ScaleHeight 1.4, _
      msoFalse, msoScaleFromTopLeft
    ActiveChart.PlotArea.Select
    With Selection.Border
      .ColorIndex = 16
      .Weight = xlThin
      .LineStyle = xlContinuous
    End With
    Selection.Interior.ColorIndex = xlNone
    ActiveChart.Axes(xlValue).Select
    Selection.TickLabels.NumberFormat = "0"
    ActiveChart.Axes(xlCategory).Select
    Selection.TickLabels.NumberFormat = "0.0"
    ActiveWindow.Visible = False
    Windows("Filename.XLS").Activate
    infoRow = ((chartNo - 1) \ 2) * 18 + 2
    If leftChart Then
      Cells(infoRow, 1).Formula = "WorkToFail"
      Cells(infoRow, 2).Formula = workToFail
      Cells(infoRow, 3).Formula = "MOR"
      Cells(infoRow, 4).Formula = MOR
      Cells(infoRow, 5).Formula = "MOE"
      Cells(infoRow, 6).Formula = MOE
      Cells(infoRow + 1, 6).Formula = "rSqr"
      Cells(infoRow + 2, 6).Formula = rSqr
    Else
      Cells(infoRow, 7).Formula = "WorkToFail"
      Cells(infoRow, 8).Formula = workToFail
      Cells(infoRow, 9).Formula = "MOR"
      Cells(infoRow, 10).Formula = MOR
      Cells(infoRow, 11).Formula = "MOE"
      Cells(infoRow, 12).Formula = MOE
      Cells(infoRow + 1, 12).Formula = "rSqr"
      Cells(infoRow + 2, 12).Formula = rSqr
    End If
End Sub

Sub Calc()
    Dim dev(79) As Single
    Dim force(79) As Single
    Dim devAve As Single
    Dim forceAve As Single
    Dim devErr As Single
    Dim forceErr As Single
    Dim sumDevSqrErr As Single
    Dim sumForceSqrErr As Single
```

```
Dim sumDevForceErr As Single
Dim graphCount As Single
Dim i As Integer
Dim section As Single
Dim bTemp As Single
Dim bRgrsn As Single
Dim integral As Single
Dim rSqrTemp As Single

maxForce = 0
integral = 0
graphCount = 0
dev(0) = -1
force(0) = 0
rSqr = 0
Do While ActiveCell.Value > 0
   graphCount = graphCount + 1
   ActiveCell.Formula = ActiveCell.Value - devStart
   section = graphCount \ 80
   i = graphCount - section * 80
   dev(i) = ActiveCell.Value
   force(i) = ActiveCell.Offset(0, 1).Value
   If i = 0 Then
      integral = integral + _
      (1 / 2) * (force(i) + force(79)) * (dev(i) - dev(79))
   Else
      integral = integral + _
      (1 / 2) * (force(i) + force(i - 1)) * (dev(i) - dev(i - 1))
   End If
   If graphCount >= 80 Then
      i = 0
      devAve = 0
      forceAve = 0
      Do While i < 80
         devAve = devAve + dev(i)
         forceAve = forceAve + force(i)
         i = i + 1
      Loop
      devAve = devAve / 80
      forceAve = forceAve / 80
      i = 0
      sumDevForceErr = 0
      sumDevSqrErr = 0
      sumForceSqrErr = 0
      Do While i < 80
         devErr = dev(i) - devAve
         forceErr = force(i) - forceAve
         sumDevSqrErr = sumDevSqrErr + devErr * devErr
         sumForceSqrErr = sumForceSqrErr + forceErr * forceErr
         sumDevForceErr = sumDevForceErr + devErr * forceErr
         i = i + 1
      Loop
      bTemp = sumDevForceErr / sumDevSqrErr
      rSqrTemp = (sumDevForceErr * sumDevForceErr) _
         / (sumDevSqrErr * sumForceSqrErr)
      If rSqrTemp > rSqr Then
         bRgrsn = bTemp
         rSqr = rSqrTemp
      End If
   End If
```

```
        If ActiveCell.Offset(0, 1).Value > maxForce Then
            maxForce = ActiveCell.Offset(0, 1).Value
            workToFail = integral / 1000
        End If
        ActiveCell.Offset(1, 0).Activate
    Loop
    MOE = ((140) ^ 3) * bRgrsn / (4 * b * t ^ 3)
    MOR = 1.5 * maxForce * 140 / (b * t ^ 2)
    counter = counter + graphCount
End Sub

Sub SetUp()
    Do While ActiveCell.Offset(1, 1).Value < 10
        ActiveCell.Offset(1, 0).Range("A1:B1").Delete Shift:=xlUp
    Loop
    'Eliminate first near-zero values
    devStart = ActiveCell.Offset(1, 0).Value
    Selection.Range("A1:B1").Insert Shift:=xlDown
    'Isolate upper boundry
    ActiveCell.Offset(2, 0).Activate    'Goto 1st cell of dataTable
    Calc
    ActiveCell.Offset(-1, 0).Activate
    Selection.Offset(1, 0).Range("A1:B1").Insert Shift:=xlDown
    'Isolate lower boundry
End Sub

Sub Initiate()
    Dim col As Object

    Columns("A:A").Select
    Selection.Cut Destination:=Columns("C:C")
    Columns("A:A").Select
    Selection.Delete Shift:=xlToLeft
    Columns("A:B").Select
    Selection.NumberFormat = "0.000"
    counter = 0
    chartNo = 0
    leftChart = False
    Sheets.Add
    Sheets("Sheet1").Select
    Sheets("Sheet1").Name = "Graphs"
    For Each col In Worksheets("Graphs").Columns
        If col.Column Mod 2 = 0 Then
            col.ColumnWidth = 9
            col.HorizontalAlignment = xlRight
        Else
            col.ColumnWidth = 4
        End If
    Next col
    Columns("A:M").Select
    Selection.NumberFormat = "0.000"
End Sub

Sub ARun()
    Initiate
    Do
        counter = counter + 1
        Windows("Filename.XLS").Activate
        Sheets("Filename").Select
        Cells(counter, 1).Select
```

```
        If ActiveCell.Value = "Breadth (mm)" Then
            b = ActiveCell.Offset(1, 0).Value
            t = ActiveCell.Offset(1, 1).Value
        ElseIf ActiveCell.Value = "Deviation(mm)" Then
            SetUp
            Set data = ActiveCell.CurrentRegion
            ChartIt
        End If
    Loop Until counter > LASTCELL
End Sub
```

A typical example of the results generated from each static bending test, after data processing.

Work To Fail	0.084 MOR	5.483 MOE	3456.20

rSqr
0.998

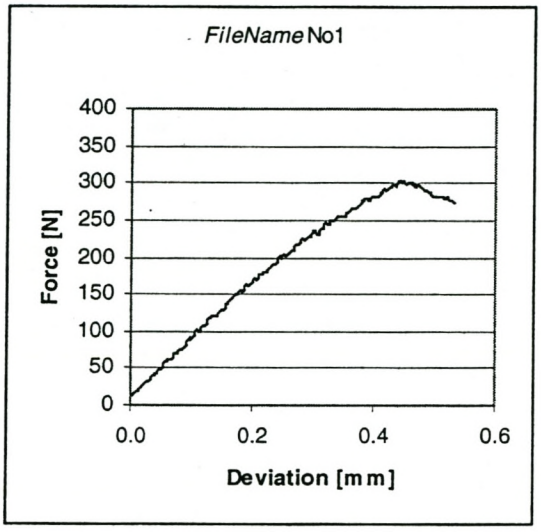

APPENDIX C – PSYCHOMETRIC CHART

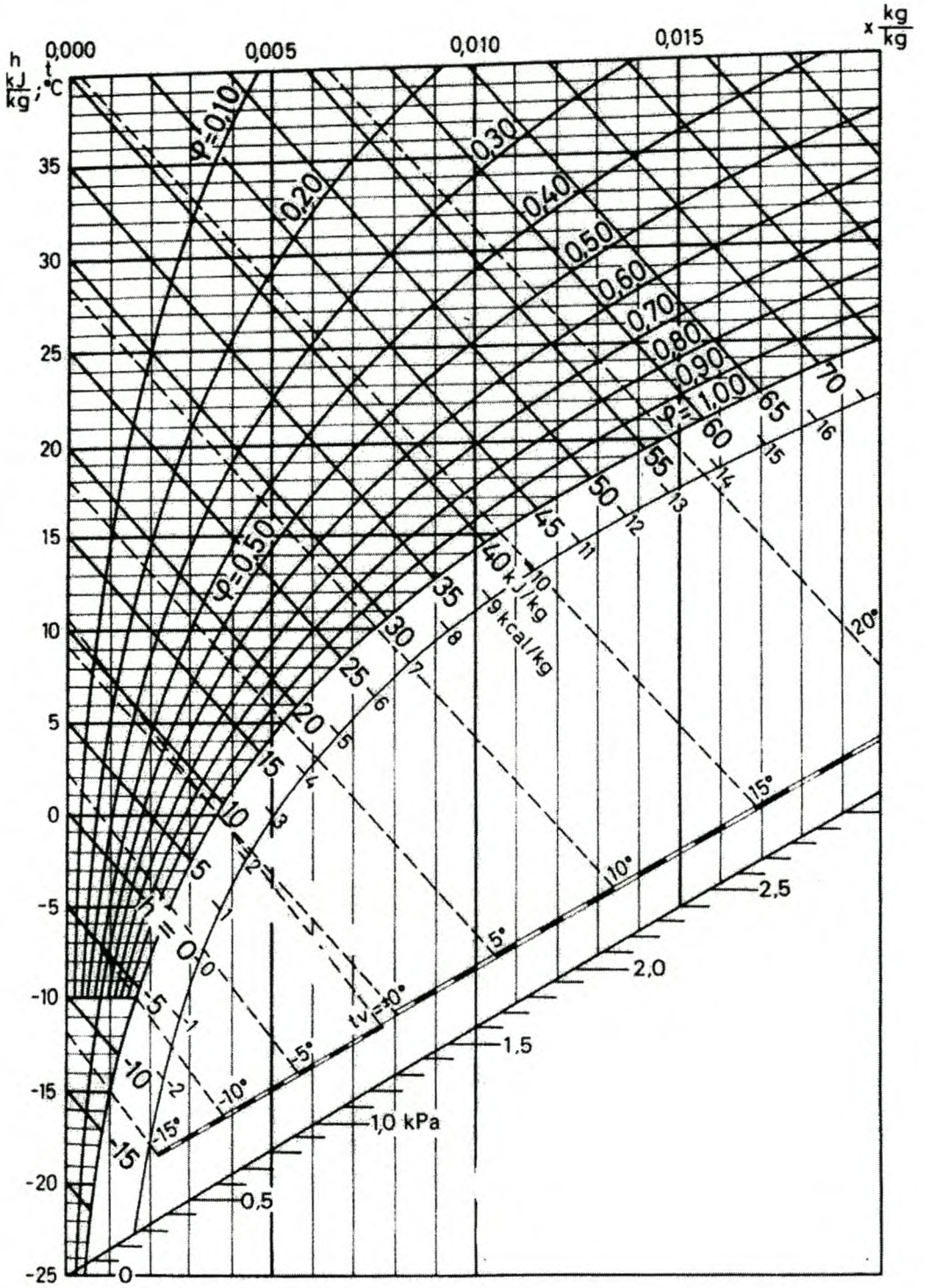

APPENDIX D – DERIVATION OF MOR & MOE CALCULATION NORMALISED TO DENSITY = 1 g/cm^3

To compare static bending results of panels with different oven dry densities, equations 3.3 & 3.4 were derived from equations 3.1 & 3.2.

If MOR = 8.85*ρ - 3.54 (3.1)

Then for MOR' at ρ = 1,

$$\frac{MOR'-MOR}{1-\rho} = 8.85$$

MOR' = 8.85*(1- ρ) + MOR (3.3)

& from MOE = 5047*ρ - 2848, (3.2)

MOE' = 5047*(1- ρ) + MOE (3.4)

With MOR' = Modulus of rupture corrected to a density of 1 g.cm^{-3}, MPa

MOE' = Modulus of elasticity corrected to a density of 1 g.cm^{-3}, MPa

MOR = Modulus of rupture, MPa

MOE = Modulus of elasticity, MPa

ρ = Oven dry density, g.cm^{-3}